'4

Assessment of and Improvements to a Stereophotogrammetric Patient Positioning System for Proton Therapy

by

Jan K Hough BSc (Hons) [UCT]

Department of Medical Physics
University of Cape Town.

Submitted to the University of Cape Town in fulfilment of the degree of Master of Philosophy

December 1999

Abstract

This thesis describes the construction and use of the facemask at the National Accelerator Centre (NAC) as used to both immobilise and position patients for precision proton radiotherapy. The precision achieved using the stereophotogrammetric (SPG) positioning system is measured, and the shortcomings and errors in using the facemask by the SPG system are measured and analysed. The implementation of improvements made to the SPG system is reported upon, and alternative means of both supporting the fiducial markers and immobilising the patient are investigated and evaluated.

The accuracy of positioning a facemask using the SPG system is 1.4 mm and of positioning a newly designed frame is 1.6 mm. These measurements were made without using a patient. It is estimated that the total uncertainty of positioning a patient's tumour at the isocentre is 1.6 (1SD) mm using the facemask and it is estimated that the precision using the frame will be less than this value. The largest component of this error (1.39 mm) is due to the error in obtaining the CT scanner co-ordinates. These results are comparable to those obtained by other investigators. The movement of patient bony landmarks within the facemask was measured to be 1.0 ± 0.8 mm.

Three main recommendations are that the CT scanner co-ordinating procedure be improved, the SPG computer program be rewritten in parts to achieve greater speed and accuracy, and that the new frame be used. The frame is easier to manufacture than the facemask and allows real time monitoring of the position of the patient's head by the SPG system thus allowing faster throughput of patients and better positioning quality control.

Acknowledgements

I wish to thank Prof. C L Vaughan, Department of Biomedical Engineering, University of Cape Town, for his willingness to take on a 'mature' working student from another department, and for his always-friendly guidance throughout the course of this project.

To Dr. D T L Jones, Head: Division of Medical Radiation, National Accelerator Centre, for his initial support of my project, and whose professionalism and infinite patience are an inspiration.

I am indebted to Prof. Laurie Adams of the MRC/UCT Biostereometrics Group, Department of Biomedical Engineering, University of Cape Town, whose enthusiasm, knowledge and encouragement were highly appreciated.

Thanks also to my colleagues at the National Accelerator Centre, Nick Schreuder, Jeni Wilson and Evan de Kock, with whom numerous enthusiastic discussions helped this thesis along.

Table of Contents

List of Figures

List of Tables

List of Graphs

Glossary

99% confidence interval	This is the range within which a reading will fall in a repeat measurement 99% of the time. The underlying distribution is assumed to be normal.
accuracy	The mean of the probability distribution of positioning errors (see 2.5.2 below). Also called the systematic error
calibration frame	A control frame used to calibrate the cameras of the SPG system (see below).
fiducial markers	The reference markers, located on an immobilisation device, and used by the SPG system cameras to locate the device.
isocentre	A point in the NAC proton treatment vault through which the proton beam vector passes and to which the SPG system positions the tumour reference point.
metrograph	see reflex metrograph
NAC	National Accelerator Centre, Faure, South Africa
patient positioning (system)	Often referred to as patient localisation (system) in the literature. The term is used in two ways in this thesis. One meaning is inclusive of the patient immobilisation (system), and the other is as a component of the overall positioning procedure, separate from the system used simply to immobilise the patient.
precision	The standard deviation of the distribution of positioning errors (see 2.5.2 below).
precision vector	A combination in quadrature of the precisions of each axis. See standard deviation vector below.
room co-ordinate system	The co-ordinate system used by the SPG system to specify the positions of the cameras, the proton treatment beam vector and the isocentre. These are located in the treatment vault at the NAC.
reflex metrograph	This instrument enables one to measure three-dimensional co-ordinates of an object. A pointer is observed through a special arrangement of glass plates, which allows the image to be seen

	unrefracted. The pointer is moved until it coincides with a reflected image of the object, and the co-ordinates of the pointer are recorded (Scott, 1981).
SPG system	The Stereo PhotoGrammetric system used at NAC to position patients in the proton treatment room. The system makes use of real-time digital stereophotogrammetry techniques commonly used in land surveying, and is described in section 1.3.2 (page 8).
standard deviation	Throughout this thesis the effect of random errors in positioning was minimised by repeating all measurements several times. When it is useful to gain an impression of the variability of an individual reading (made from the population of all possible readings), the standard deviation of the sample of readings is calculated.
standard deviation vector	Most positioning measurements made in this thesis are in three-dimensional Cartesian co-ordinate space. The standard deviation is calculated as explained above for each axis separately. In order to obtain one value that can be conveniently used for comparing different positioning systems, it is convenient to combine these standard deviations in quadrature. This is a meaningful value provided the data for each axis are independent of one another. This is usually the case.
standard error of the mean	When the mean value calculated from a sample of readings is of interest, the standard error of the mean (SE = □/□N) is calculated in order to give an idea of the variability of the mean value.
tumour reference point	A point obtained by the treatment planning system, usually located centrally in a tumour, through which the central axis of a planned proton treatment beam passes.

1 Introduction

1.1 Background

A 200 MeV proton beam radiotherapy treatment facility has been developed at the National Accelerator Centre (NAC), situated in Faure, South Africa (Jones, 1995). Unlike photons whose absorption in matter decays exponentially, protons have a depth-dose curve characterised by a relatively low entrance dose plateau region, followed by a sharp dose peak (the Bragg peak) near the end of the range. A well-defined range beyond which there is no irradiation depends on their initial energy and on the integrated stopping powers of the tissues traversed by the beam. Effective use for radiotherapy depends on a CT scanner with which the electron density and position of all tissue traversed can be determined. The stopping point of the particles can then be predicted and a treatment beam can be designed so that no dose is deposited beyond the tumour. The proton beam is conformed to the tumour by spreading the Bragg peak with a 'propeller' made up of different thicknesses of acrylic and which is rotated in the proton beam (Jones, 1995), and by using custom-made collimators. A further advantage is that because protons scatter very little, the typical beam penumbrae are smaller than in photon beams. Sites particularly suitable for proton treatments are those whose treatment can exploit these improved spatial accuracy properties to confine the dose to the treatment site. These are typically within the head and neck region and are often close to sensitive structures.

To take most advantage of the dose-confining feature of protons it is vital to position the patient in the beam with high precision and accuracy. The advantage offered by protons would be entirely lost if precision and accuracy were not optimal. In fact, often the close proximity of critical structures to the irradiated target volume is the reason that protons would be chosen as the preferred modality of treatment, but the consequences of inadequate positioning are worse than in conventional radiotherapy. Patients treated at the NAC have complex treatment plans mainly for irradiation of relatively small tumours. The beams are usually non-coplanar (more than two beams whose central axes do not lie in a single plane). In traditional radiotherapy the treatment gantry is moveable and when combined with the rotation of the patient support couch on an axis orthogonal to the gantry rotation axis, allows non-coplanar treatments to be set up with relative ease. Due mainly to cost constraints at the time the beam was originally developed, a fixed horizontal proton beam is used at NAC.

The currently used operational system was designed by G. van der Vlugt of the Department of Surveying and Geodetic Engineering, UCT, in conjunction with the Medical Radiation Group of the NAC (van der Vlugt, 1991). This stereophotogrammetric (SPG) system has also been described in the literature by van der Vlugt and Rüther (1992), Levin *et al.* (1993), Jones *et al.* (1995) and Schreuder *et al.*, 1997. A specially designed treatment chair with 5 degrees of freedom is used for patient support. It is extremely difficult in practice to position non-coplanar beams with the required accuracy using manual control and the conventionally used treatment room lasers for reference. A computer interface between the SPG system and the patient treatment chair was thus developed (Bennett *et al.*, 1994).

The method currently used to immobilise patients and a detailed description of the patient positioning procedure is given in the next two sections. On average about 60 patients have been treated per year since late 1993 using the SPG system. This seems to be keeping up with the perceived maximum patient load. However, it may well turn out that increasing the ease of proton treatments may lead to improved patient numbers. Being a multidisciplinary facility (Jones *et al.*, 1999) the beam is only available for proton therapy for limited periods.

Concerning future plans at the NAC, most of the patients have been immobilised with the head mask and positioned and monitored in the proton beam using the SPG system. However additional protocols are being developed for prostate and gynaecological treatments with the patients lying down. These require less precision and allow the possibility of patient positioning by the more conventional means of utilising the treatment room positioning lasers. In this case, the beam arrangements are usually co-planar, meaning that the central axes of the beams comprising the full treatment of a lesion lie in a single plane.

In addition, a second proton treatment vault is planned which will have both a horizontal and a 30° off-vertical spot scanning beam delivery system which will provide the capability of intensity modulated radiotherapy.

1.2 Patient immobilisation

The principles involved with immobilisation in general, and at NAC in particular are discussed below, and a detailed description of the currently used facemask patient immobilisation method follows. Thereafter the problems experienced with the facemask are discussed.

1.2.1 General conditions for a satisfactory patient immobilisation system

In order to irradiate an intracranial tumour successfully, two separate physical aspects of radiation treatment need to be achieved. Firstly, the head must be positioned using a positioning device so that the tumour is correctly located in the radiation beam. Secondly, the patient's head needs to be rigidly immobilised during the course of the treatment session.

A satisfactory method of restraining the patient is required for both successful CT scanning of the patient, and successful radiation treatment. The immobilisation system provides the interface between the patient's body (an organic structure) and the CT scanner and treatment room geometries. As such it requires firstly, a sufficiently adjustable yet rigid means of attachment to the CT scanner and treatment room mechanics, and secondly, reproducible registration on the patient's body to within a small tolerance.

As methods of diagnosis have become more sophisticated over time, they have been accompanied by an increase in spatial accuracy of locating relevant structures in the body. The physical characteristics of a proton therapy beam enable optimum use to be made of this gain in accuracy. Therefore, particularly in proton therapy there is a strong need for the patient to be accurately and reproducibly positioned within the immobilisation device, and an accuracy of less than 1 mm should be achievable. Rigid and accurate positioning for stereotactic intracranial radiosurgical procedures has traditionally been achieved using a frame screwed into the skull. For fractionated radiotherapy in which the total radiation dose is delivered over several occasions, the immobilisation system needs to be easily and reproducibly removed and replaced for each radiation fraction. Such a system, usually called 'relocatable', is required for the NAC proton beam which has been used mainly for stereotactic radiosurgical procedures delivered in a few fractions.

In a practical clinical setting, convenience of use, time and expense of construction, and patient comfort are also important factors to be considered in the design and implementation of patient immobilisation devices.

Fulfilment of these aspects and the additional requirements discussed in 1.2.2 below have proved technically demanding, but, as will be seen from the description of the current immobilisation system in paragraph 1.2.3 below, the mask immobilisation system has been sufficiently refined over time that the system is now in satisfactory regular clinical use.

1.2.2 Additional conditions imposed at NAC

Two criteria are discussed below and it will be seen that both criteria are fully satisfied with the current mask immobilisation method used at NAC.

(a) Immobilisation must be non-invasive

A major decision made at NAC was that any immobilisation system used should be non-invasive i.e. does not involve any cutaneous puncture. This was decided for two reasons: firstly, to eliminate any possible infection, especially during extended fractionated treatments; and secondly, for the entire radiotherapy procedure to be less traumatic to patients.

(b) The immobilisation system should allow convenient and reproducible (or permanent) attachment of fiducial reference markers

Radiopaque fiducial markers placed within the patient have traditionally been used to record the patient position relative to the treatment beam for many types of radiotherapy (Verhey *et al.*, 1982; Jones *et al.*, 1993). Recently these markers have been used for calculating adjustments necessary to correctly position the patient, these subsequently being applied in a feedback loop to the patient support couch (Gall *et al.*, 1993). The employment of the SPG system at NAC requires that the fiducial markers be clearly visible by video cameras and not located within the patient. In order to maintain the spatial relationship between the markers and the patient's anatomy, it is essential that the markers are placed on, or are rigidly registered with, the immobilisation system. As seen below the acrylic facemask allows convenient use of fiducial markers by the SPG system.

1.2.3 Description of the current immobilisation system

Following the decision to position patients at NAC with the SPG system, the usual condition in traditional radiotherapy of rigid patient immobilisation was conceptually relaxed. This was because it was envisaged that any movements by the patient during treatment could be corrected by a feedback loop from the SPG system to the treatment chair. Consequently the mask described below consists of a separate anterior and posterior section. The posterior section is used to support the patient while the anterior section provides a support structure for the fiducial markers. An important consequence is that the positioning is based on fiducial reference markers that are mounted on the patient mask rather than the anatomy directly.

A Plaster-of-Paris positive of the patient's head is made with extra care for a good fit to the patient's anterior head contour. Sandblasted 3 mm thick thermoplastic ultra-high impact acrylic (cellulose acetate) sheets are formed over the anterior half using a vacuum former, in the same way as for a conventional radiotherapy mask. The posterior half is 6 mm thick acrylic sheet, also

vacuum formed, to which are attached two 'wings' (Figure 1-1). These are subsequently attached to the head restraint mechanism on the treatment chair (Figure 1-4) during treatment. The anterior half is placed on the patient and is attached to the posterior half by means of four Velcro strips. These pull the anterior mask tightly onto the patient's anatomy.

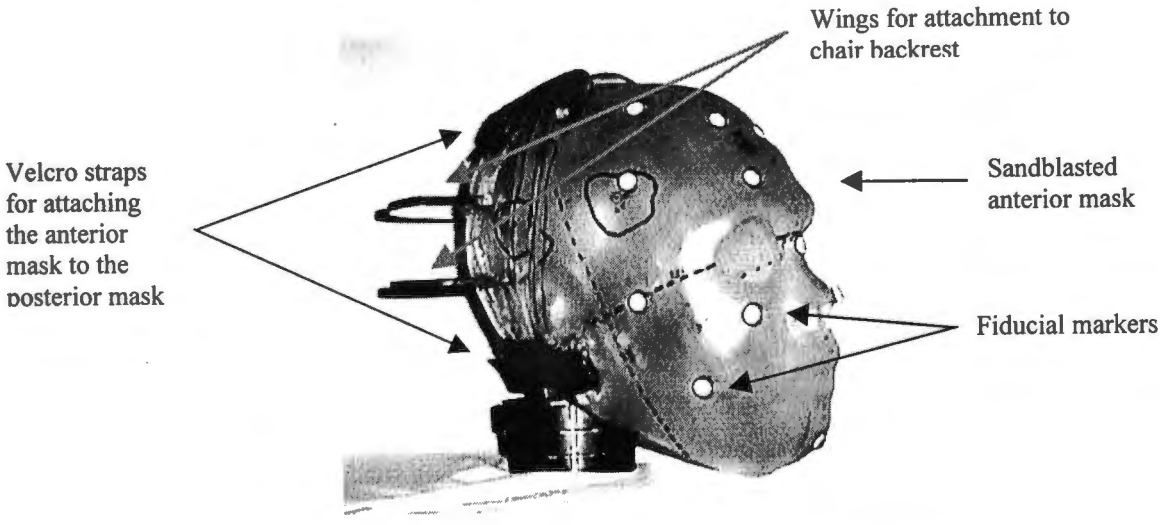

Figure 1-1 Posterior mask, wings, and restraint mechanism

The essence of a well made mask is that the anterior section is in no way prevented from being pulled as tightly as possible onto the head. Thus, the posterior half must not butt against any part of the anterior section. In addition, movement of the anterior half of the patient's head in the anterior section is minimised by requiring the patient to shave his/her head, or at least have very short hair.

Once the posterior part is attached firmly to the chair, small strains can occur between the posterior part and the patient. Because of the flexible Velcro strips, minimal distortion is transferred from the posterior to the anterior section and the patient remains firmly held inside the anterior section.

Patients report that the mask is very comfortable. This is presumably due to very even all round pressure over the head. If the mask is over-tightened patients are quick to respond, and a firm yet comfortable pressure can be easily found.

Small 1 mm diameter stainless-steel ball bearings, which are well visualised in CT, are inserted directly into 0.9 mm diameter holes drilled into the anterior mask.

Retro-reflective marker discs 8 mm in diameter are fixed accurately on the mask exactly over the centres of the steel fiducial markers. The three dimensional co-ordinates of these reflectors are known from a prior CT scan and the anterior mask, acting as the patient's "second skin", is then positioned by the SPG system.

1.2.4 Problems with the current facemask immobilisation system

The problems which have been identified in the use of the current facemask immobilisation system are listed below and were addressed in the design of the new system. The problems (a) and (b) below are concerned with time consuming preparation techniques. The problems (c) and (d) are concerned with unreliable and time wasting operation of the SPG system during patient setup and treatment.

(a) Many stages in the construction of the mask

There are many stages in the manufacturing of the mask, resulting in a process that can last for several days and involves typically about 5 hours of skilled labour. Any shortening of time in the preparation of the patient for treatment has a benefit both in terms of reduced overall cost of treatment, and more prompt treatment of the tumour.

(b) Time consuming acquisition of fiducial reference marker co-ordinates

The acquisition of the CT scan co-ordinates of up to eighteen markers is very time-consuming and therefore both costly and tiring for the radiographer and clinician involved in the image acquisitions.

(c) The plastic facemask is not rigid

Distortions of the mask due to the flexibility of the acrylic may cause inconsistent positioning of the fiducial markers between the CT scan session and subsequent treatment sessions.

(d) Dependence of successful SPG operation on the tension between the anterior and posterior mask sections

If the tension between the anterior and posterior mask sections is too great the anterior section can distort, causing erroneous SPG positioning. Alternatively, if the tension is insufficient, the patient is not immobilised properly on the chair and breathing and other patient movements may impede initial capture of the marker co-ordinates by the SPG system.

(e) Uncertain registration between the mask and the patient's anatomy

The registration of the marker carrier (facemask) on the patient is by pressure onto the face contour, and uncertainty always remains because of the possibility of movement of the head within the mask. The patient's head is hidden by the mask and cannot therefore be directly monitored for positional accuracy. Consequently a check X-radiograph is made of the patient's anatomy in the treatment position immediately prior to commencement of treatment. This is compared to a digitally reconstructed radiograph produced by the radiotherapy planning system.

(f) Expensive equipment required

The construction of the plastic mask requires expensive capital equipment. The vacuum former would cost in the region of R800 000 ($130 00).

1.3 Patient positioning

The conditions required for successful patient positioning in the radiation beam are discussed below. Then the physical components of the SPG system and the positioning procedure and monitoring of the patient position during irradiation using the SPG system are described. Thereafter the problems experienced with the SPG system are discussed.

1.3.1 Conditions required to be satisfied for successful patient positioning

A target will be successfully positioned in the radiation beam (within a given tolerance) provided both of the following two conditions are satisfied.

(a) There is minimal change in the relationship between the fiducial reference markers and the patient's internal anatomy

A patient immobilisation system consisting of an acrylic mask has been designed to ensure that this condition is reasonably assumed to be true. No measurements have yet been made to check that the skull does not move within the facemask. A direct real time confirmation would also be desirable. An additional consideration is the movement of patient anatomy within the skull. This was investigated by Urie (1995) and Serago *et al.* (1992) who found shifts of intracranial content of up to 2 mm.

(b) The fiducial reference markers are correctly positioned relative to the theoretical beam vector

The properly calibrated and operating SPG system performs this function. The initial experience at NAC showed an accuracy of less than 2 mm in positioning of the beam, as indicated by the beam line laser, on the patient (mask). In view of the limitation of the CT scanning spatial

resolution, this appears to be reasonable, but a more detailed assessment of the accuracy and possible sources of errors was required.

It is assumed as prior conditions that the proton radiation beam is correctly calibrated to align with the theoretical beam vector defined in the room co-ordinate system, and that there are no large errors in the co-ordinates of fiducial markers.

1.3.2 Positioning and monitoring of patients at NAC

The physical components of the SPG system are briefly described below and thereafter the stages from the initial fitting of the facemask to the monitoring of the patient position after the proton beam is switched on are discussed.

(a) The components of the SPG system

The major physical components of the system, shown in Figure 1-2, are the main SPG personal computer with three attached video monitors, eight charge-coupled device (CCD) video cameras, and a patient support system which is a computerised adjustable chair with 5 degrees of freedom. For more details see van der Vlugt (1991). A rotating collimator mounted on the beam gantry

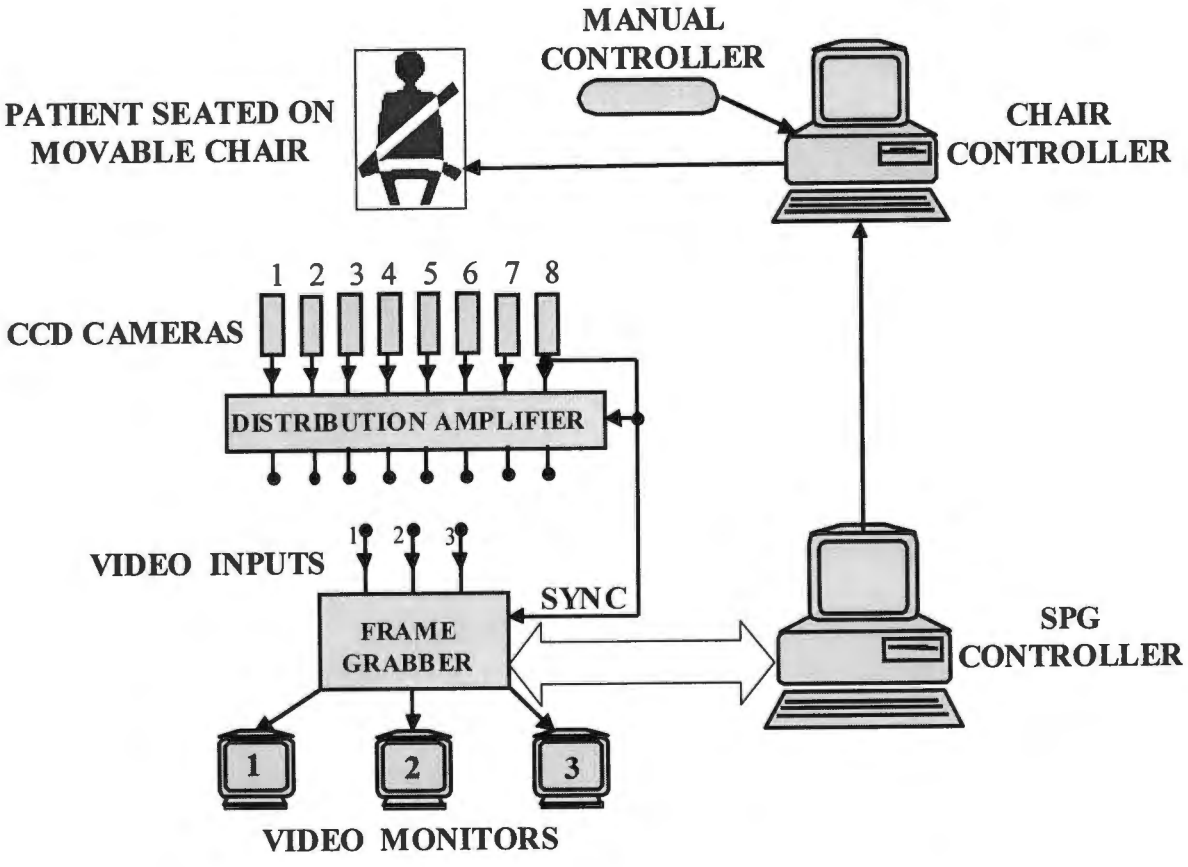

Figure 1-2 Simplified diagram of the hardware components of the positioning system

achieves the sixth degree of freedom.

The basic principle of positioning a patient for treatment is that retro-reflective fiducial markers on the patient are observed with three out of eight possible video cameras. Images of the patient from three different angles are observed on the SPG computer monitors. The SPG computer resolves the position of the patient and calculates the movements required to be made by the chair to position the patient correctly in the radiation beam.

(b) Description of the patient set-up and monitoring procedure for proton treatment

A flow diagram of the stages is presented in Figure 1-3 below. The stages involved in immobilising, co-ordinating, positioning and monitoring a patient for proton treatment are described below in the order in which they are performed, and following the numbering used in Figure 1-3 below.

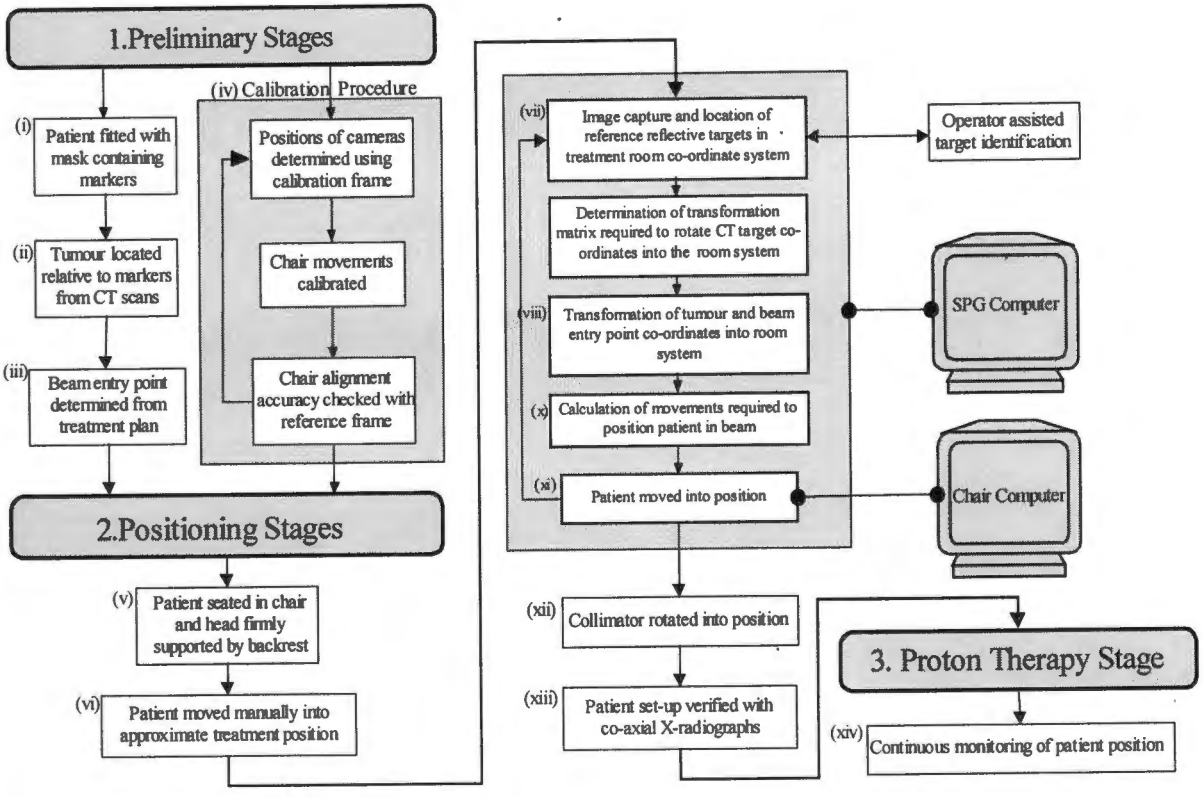

Figure 1-3 Stages in immobilising, co-ordinating, positioning and monitoring a patient for proton treatment

(i) Patient fitted with the mask

The patient is fitted with the custom-made tightly fitting moulded acrylic facemask described in 1.2.3 above.

(ii) Tumour and fiducial marker positions obtained from the patient CT scan

After immobilising the head and mask on the CT scanner[1] table, a scan is done, using a 2 mm slice-thickness, spanning the tumour and each of the markers. Each marker's slice position is found by aligning the scanner laser onto the steel sphere. The x, y, and z (table) position of each marker is read from the scanner and recorded. The x and y co-ordinates are in the axial (slice) plane in the lateral and posterio-anterior directions respectively.

(iii) Beam entry points, as determined from the treatment plan, are entered into the SPG computer and marked on the facemask

The CT scans are transferred to the radiotherapy planning system. After preparation of an acceptable treatment plan, the treatment beam parameters, viz. the co-ordinates of the beam entry points and the treatment isocentre, thus defining the planned beam central axis, are recorded. The co-ordinates of an exit point are also obtained from the planning system and are sometimes used as an additional check on the beam positioning accuracy. The point is not used directly by the SPG system. In the treatment room at NAC, the co-ordinates of the patient markers, treatment isocentre, and beam entry points, are fed into the SPG system for later use in positioning and monitoring the patient.

The distance of each beam entry and exit point from each of the fiducial markers is calculated, and by setting these distances on a divider and marking arcs on the mask it is possible to determine the beam entry and exit points on the mask.

(iv) Calibration procedure of the SPG system

The camera positions in the treatment room co-ordinate system are determined by the SPG system at regular intervals using a large calibration frame placed in a reproducible position around the treatment room isocentre. This frame contains retro-reflective markers that have been accurately co-ordinated relative to the isocentre by survey with a theodolite and whose co-ordinates are stored in the SPG control computer. The known markers are viewed by three of eight cameras, and using stereophotogrammetry techniques, the "camera model" is used to solve for the respective co-ordinates in the proton treatment-room co-ordinate system. These co-ordinates are then transformed into the co-ordinate system of the calibration frame. If the co-

ordinates match to a pre-set accuracy threshold, then the cameras are correctly calibrated. However, if the co-ordinates do not agree, then the eleven parameters defining the "camera model" are recalculated and subsequently used by the system.

The chair movements are also regularly calibrated using the chair controller computer.

The operation of the SPG system is checked once a day prior to treatment using a small check frame attached to the chair. The check frame is positioned by the SPG system using the attached retroreflective markers. The deviation of a 1 mm hole at the centre of the frame from the room isocentre is measured with a theodolite and recorded.

(v) Patient seated in chair and firmly supported by the backrest

The patient is seated on the chair and his/her facemask is attached firmly to the chair backrest by the head restraint mechanism designed at the NAC for holding the mask firmly in any comfortable position (Figure 1-4 below).

(vi) Patient moved manually into approximate treatment position

The manual chair controller is used for initial gross positioning of the mask into the field of view of each of the three cameras to be used for that particular treatment by the SPG system. The minimum condition is that at least three fiducial markers must each be seen by at least two of the three cameras.

(vii) Image capture, and location and co-ordination of fiducial reflective targets

The retroreflective markers are detected by the SPG system using three CCD cameras. Bright incandescent lights are mounted close to each camera. The camera and lights are directed towards the room isocentre, thus effectively illuminating the retroreflective markers for the cameras.

To ensure that the patient plus chair can be observed from all around the treatment room it was necessary to install eight cameras, which were roughly evenly spaced around the room. Their positions, illustrated in Figure 1-5 below were chosen so that any three adjacent cameras subtend angles of no more than 90° from each other at the isocentre. The cameras are positioned about 2.5 m from the isocentre.

[1] Picker IQ Fast (also called Premier) 1991, Picker International, Inc., 595 Miner Rd., Cleveland, Ohio 44143, U.S.A.

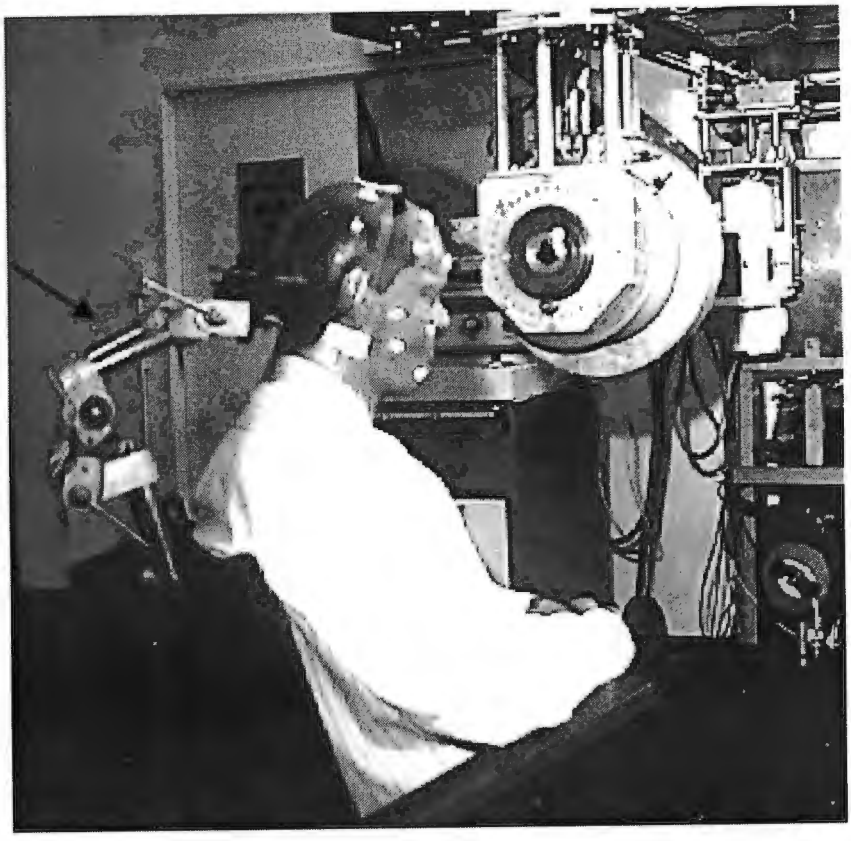

Figure 1-4 Patient seated on the treatment chair with his facemask attached firmly to the chair back-rest

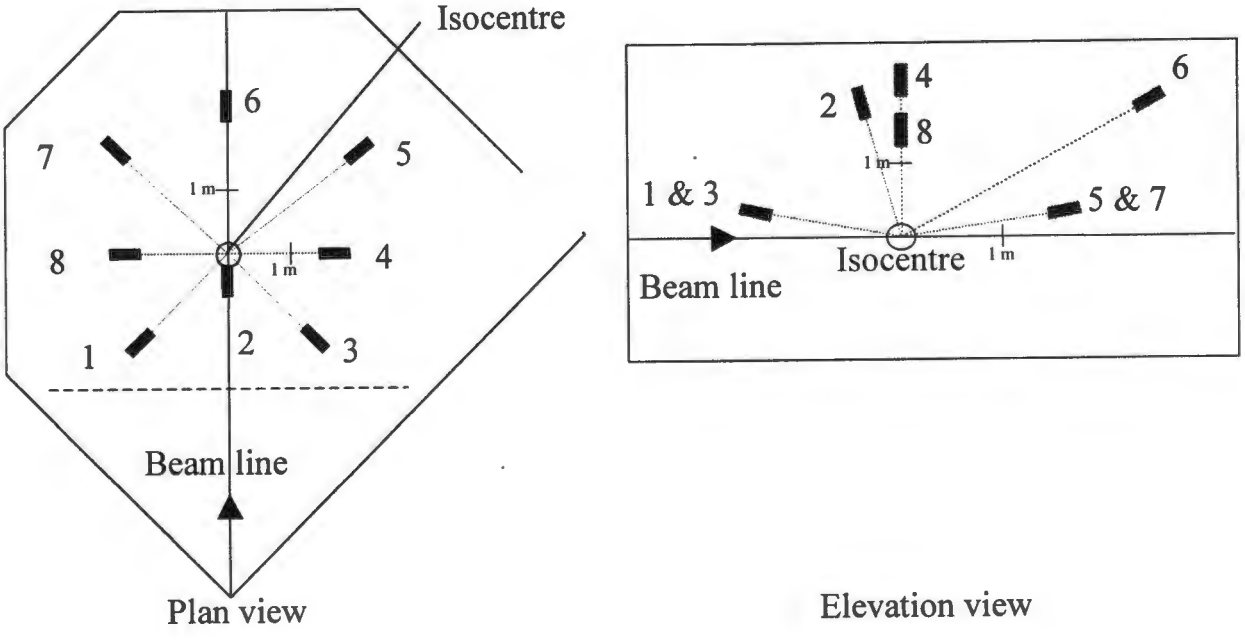

Figure 1-5 Location of CCD TV cameras in the treatment room

Sets of three cameras are pre-selected to act together. The calibration procedure using the small check frame on the chair checks each set for accuracy. The most appropriate set needs to be chosen for each treatment beam. Only two simultaneous observations of a particular marker are required for its 3D position to be reconstructed. The third observation, when available, is used to improve the overall accuracy. Each camera is connected to a separate channel of a frame grabber on the SPG personal computer.

The operator is required to adjust the image threshold for each channel such that only the retro-reflective markers are visible and spurious artefacts due to reflections are eliminated. The SPG system then searches the image and calculates the centre of gravity of each of the visible areas. The operator identifies each marker by number on each channel. On subsequent positioning iterations thresholding and marker identification are not normally required.

(viii) Transformation of tumour and beam entry point co-ordinates into room co-ordinates

The SPG system compares the observed retro-reflective marker positions with marker co-ordinates previously obtained from the CT scanner. A rotational matrix is obtained which transforms the marker CT co-ordinates into SPG/room co-ordinates. This matrix is applied to the required planned beam central axis, whose co-ordinates are also known in the CT scanner co-ordinate system from the treatment planning process, and the corresponding SPG/room co-ordinates for the beam are obtained.

(ix) Residual errors

Once the SPG system has calculated the patient position (actually the positions of the fiducial markers), it reports the residual errors of each marker point found from the transformed scanner co-ordinates. These errors are typically from 0.0 to 2.0 mm., and give an indication of whether any marker is grossly mislabelled and/or out of position.

(x) Calculation of movements required to position patient in the beam

The SPG system then calculates the spatial corrections required to align the planned beam central axis with the known proton beam central axis position in the treatment room.

If the SPG system determines that the patient is positioned within pre-set tolerances, normally 0.5 mm in each of the three orthogonal directions, the position is also checked by ensuring that front- and back-pointer lasers intersect the marked beam entry and exit points on the mask. The SPG positioning stage is then completed and step (xii) is proceeded with.

(xi) Patient moved into position

The spatial corrections are sent to the chair control computer (see Figure 1-2). The required co-ordinates of chair (containing the patient) are calculated, and the chair is moved into the treatment position with 5 degrees of freedom (3 translations, vertical rotation, and backrest rotation). Computer controlled stepper motors move the chair plus patient with an X, Y and Z translation accuracy of 0.1 mm, and a vertical axis and backrest rotation accuracy of 0.1°.

A return is made to the image capture stage, (vii) above, for the patient position to be checked.

(xii) Collimator rotated into position

The required sixth degree of freedom is achieved by the calculation of the final collimator position applicable to the treatment beam, and this angle is sent to a stepper motor which drives the collimator mechanism.

(xiii) Patient set-up verified with co-axial X-radiographs

From the detailed description above of the positioning procedure, it can be seen that it is the patient mask that is positioned and not the patient anatomy directly. The mask is constructed and fitted (as described in paragraph 1.2.3 above) in such a way that there is reasonable confidence that the patient is positioned within the mask identically to when the CT scan was done and upon which the treatment planning was based. It is however vital that a check is made of the patient anatomy position. This is currently done with a double-exposure coaxial portal X-radiograph (Figure 1-6 below).

An X-ray unit is brought into the beam line and a film cassette suspended behind the patient. One exposure is taken with the collimator out of the beam to show the anatomy while for the second the collimator is in position to show its outline and orientation. The developed film shows the collimator opening superimposed on the full head image, allowing a direct comparison with the digitally reconstructed radiograph produced by the planning system (Figure 1-7 below).

The slice spacing and spatial resolution on the CT scanner limit the spatial resolution of the digitally reconstructed radiograph, and the low contrast resolution is poor in comparison to film. This makes precise checking of patient position and collimator rotation relatively difficult. The system is nevertheless essential for alerting the users to major errors, for example wrong beam/collimator combinations.

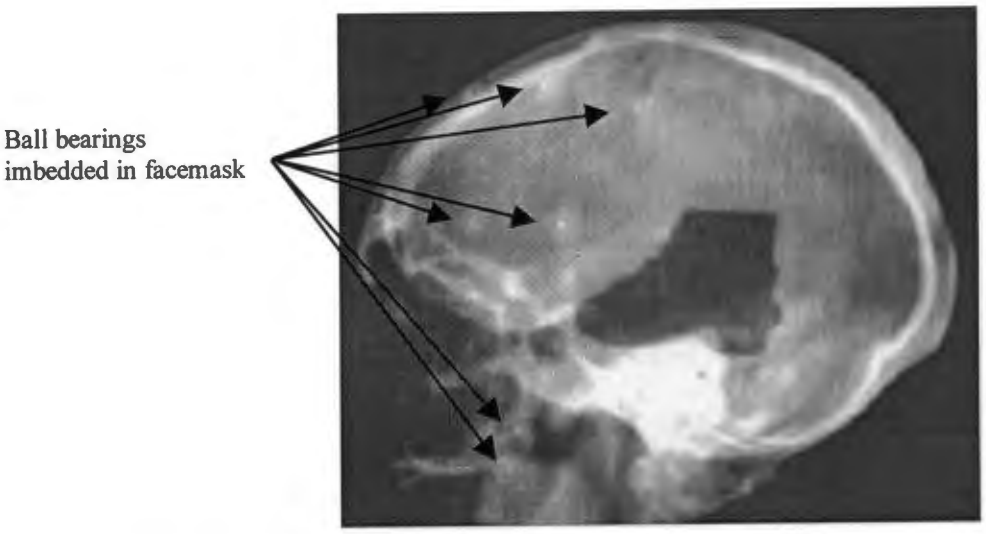

Figure 1-6 Typical verification double-exposure X-radiograph with the collimator outline superimposed on the anatomical image. The 1 mm diameter ball bearings imbedded in the patient's mask are clearly visible.

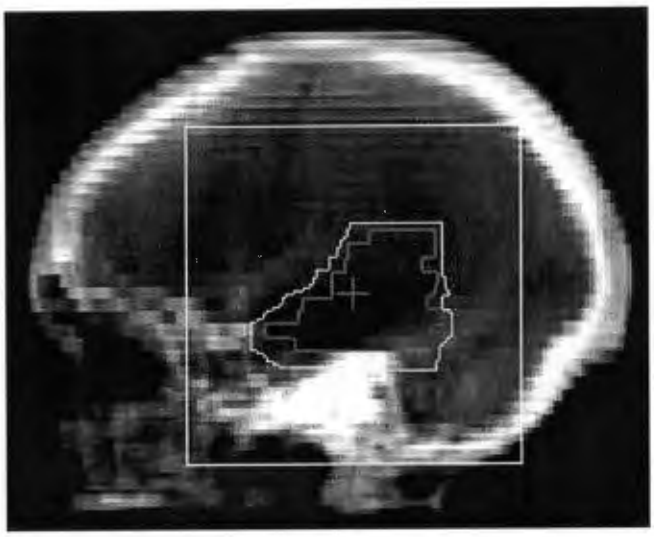

Figure 1-7 A digitally reconstructed radiograph obtained from the treatment planning system for the same beam and patient used for the X-radiograph in Figure 1-6.

(xiv) Monitoring of patient position during treatment

Once the patient position is considered satisfactory treatment can begin. The patient movement is monitored to 0.8 mm about the final set-up position. In the initial SPG software, monitoring ceased and an interlock signal to cease treatment was generated when the patient movement was

outside the tolerance limit. This proved impractical, as the movements were often relatively small transient movements. After re-doing a complete SPG re-positioning cycle it was often found that the patient was still in his original position.

It is now possible to temporarily interrupt the beam in the case of a 'small movement'. If the patient moves back into position within a certain pre-set time, the beam is restarted automatically. A 'small movement' is defined as a movement where there is a chance that the patient might move back into position during a specified time period. This is typically possible

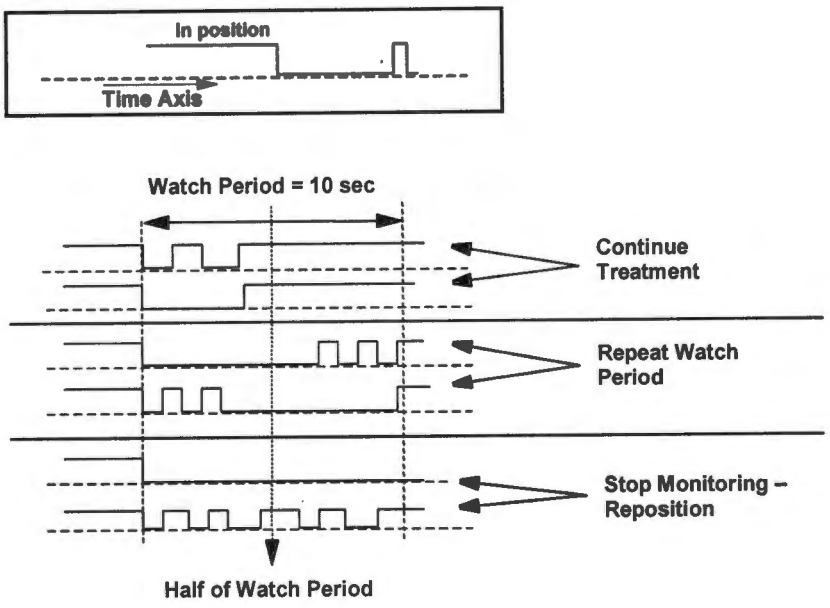

Figure 1-8 A schematic illustration of the possible scenarios during and after the watch period that is activated as soon as the patient moves out of position.

when the patient takes a deep breath or coughs. To facilitate this, a watch period (typically about 10 seconds) is implemented in the patient monitoring routine. The watch period is started as soon as the patient moves out of position. This is illustrated in Figure 1-8 below.

When the watch period expires it is possible to continue the treatment, to repeat the watch period if no explicit conclusion was possible, or to stop the monitoring process. In the latter case it is required to reposition the patient to restart the monitoring process and hence the treatment. The watch period lasts for 40 monitoring cycles where a monitoring cycle comprises of grabbing the images from three cameras and analysing them for any deviations from the final set-up images.

The length of a scanning cycle and hence the length of the watch period depends on the number of common points seen by the selected combination of cameras. A frequency of 4 scanning cycles per second is possible when six common points, which are typical for most treatments, are seen by a given set of cameras.

This amendment to allow for transient movements and to continue treatment when the patient returns to the original position is working very well.

(c) Preliminary determination of positioning precision

In addition to measuring the *accuracy* of the entire current positioning protocol, the *precision* or reproducibility of positioning can be made. Random errors are generated in the entire marker acquisition and co-ordination procedure, and by the SPG positioning system itself. By repeating the positioning procedure several times and recording each time the deviation of the position of a theoretical point from a reference position, an estimate of the overall random error, or precision, can be calculated. This is the standard deviation of the sample of position deviations. Normally the mean of the position deviations would be called the accuracy. However this is not meaningful if the "correct" position of the reference point is not known. Nevertheless, a determination of precision or variability of positioning is important as it characterises the ability of the system to position in a repeatable way. Further discussion on this topic is shown in section 2.5.2 below.

Schreuder *et al.* (1997) describe a preliminary study done to estimate the precision with which the anatomy is positioned by the SPG system. Firstly a retrospective analysis of the portal X-radiographs, for a limited number of patients treated using the SPG system, was done to examine the degree of patient movement in the mask. Only X-radiographs from coplanar AP and lateral beams were evaluated. Distances between the steel ball bearing fiducial markers, embedded in the mask, and well defined bony anatomical landmarks in the patients' heads were measured. Only ball bearings lying in a plane coplanar to the X-ray film and passing through the isocentre were considered. The measured distances were corrected for differences in magnification.

In a second study the SPG system was used to position an empty patient mask several times in the beam for coplanar AP and lateral beams respectively. Portal X-radiographs of the positioned empty mask were taken in each case. From the X-radiographs it was possible to measure distances between ball bearing markers, imbedded in the mask, and a cross hair which defined the beam axis. Only ball bearings lying in a plane coplanar to the X-ray film and passing through

the isocentre were used in this analysis and all the measurements were again corrected for differences in magnification. From this study it was possible to quantify the reproducibility of the system for a typical patient mask.

As indicated in Table 1-1 below, the registration between the reference points on the masks and anatomical landmarks varied by mean standard deviations of 0.74 cm, 0.85 cm, and 1.17 cm for the x, y, and z axes respectively during the course of a treatment. For ease of comparison with other immobilisation methods, the values for the three co-ordinates can be combined in quadrature to give a standard deviation vector (see Glossary) of 1.62 (1 SD) mm. The precision vector for repositioning of an empty mask, calculated in a similar way, was 1.61 (1SD) mm. Combining these results in quadrature, the overall positioning precision can be described by a standard deviation vector of length 2.3 mm (1SD).

Table 1-1 Results from two preliminary studies of patient movement and reproducibility of the SPG system.

STUDY	Number of measurements	AXIS	MEAN STANDARD DEVIATION (mm)	95 % CONFIDENCE INTERVAL (mm)	Vector combination of Mean Standard Deviation (mm)
Patient movement inside mask	54	x	0.74	0.62 - 0.92	1.62
	50	y	0.85	0.71 - 1.05	
	94	z	1.17	1.02 - 1.37	
Repositioning of empty mask	20	x	0.39	0.30 - 0.57	1.61
	28	y	0.96	0.76 - 1.31	
	48	z	1.23	0.98 - 1.70	
Overall positioning precision		x	0.84		2.28
		y	1.28		
		z	1.69		

1.3.3 Problems with the current SPG implementation

There are areas where the current SPG implementation could be improved. Due to the limited scope of this thesis (see paragraph 1.5 below), only those issues considered most important are dealt with. These are listed below.

(a) The positioning accuracy has not been measured in great detail.

A detailed analysis of the positioning accuracy of the SPG system is required for evaluating improvements, and for comparison with other radiotherapy positioning techniques. In addition

the positioning precision measurements in the study described in section 1.3.2(c) above need to be refined.

An analysis is required of the sources of error in the positioning of the tumour for irradiation. This knowledge is essential if the positioning accuracy and precision are to be improved.

(b) Time consuming patient set-up and monitoring procedures

Patient positioning on the treatment day is often time-consuming. Several positioning iterations are required, fiducial markers can be misidentified, stray reflections on the mask can cause the SPG system to fail, check films need to be developed and the patient can be placed in a relatively uncomfortable position on the chair resulting in mask distortions and unstable positioning. The set-up requires a high level of expertise and can be stressful for the operators. Time consuming patient set-up and monitoring is an important factor that ultimately limits patient throughput.

(c) Position of patient anatomy cannot be confirmed by the SPG system in real time

Although every effort is made to avoid it, there is a possibility that the patient's anatomy can move within the facemask. The patient anatomy position is checked by comparing X-rays to digitally reconstructed radiographs as described in section 1.3.2(b)(xiii) above. This comparison can only detect relatively major positioning errors and is time consuming. A higher level of confidence is required to confirm that the patient's anatomy, or tumour, is in the correct position, so that delays can be reduced and the entire positioning process can become more automated.

(d) Inadequate chair design for active positioning during treatment

Due to cost constraints, the patient chair was not designed to be absolutely stable. This was not thought necessary, as the SPG system would be able to adjust for any consequent positioning error. In practice, however, movements by the patients or the chair itself result firstly in a non-predictable chair position due to the patient's centre of mass being displaced when moving the patient from one beam position to another, and secondly in a wobble which takes time to stabilise.

The rigidity of the chair along its vertical axis has been improved substantially. A complete redesign of the vertical support was required. Shifts up to almost 10 mm were seen previously, while the maximum shift with the new vertical support is less than 1 mm. This allows the chair to move the patient more accurately and also allows the SPG system to automatically identify the reflective markers on the patient's mask when the patient is in a new position. Fewer positioning iterations are now required. It is important to note that in a given position the rigidity of the chair

is not important since the SPG system only uses relative chair movements and not absolute chair positions.

Due to chair wobble, active corrective positioning during treatment cannot be done.

1.4 Objectives of the thesis

The current facemask immobilisation system and the SPG positioning system are in regular use to treat patients, however a number of problems have been identified, as listed in sections 1.2.4 and 1.3.3 above, and in order to improve patient positioning, a logical sequence of studies has been undertaken. Five main objectives have been identified and are formally stated and further developed below.

1.4.1 To assess the accuracy with which the current SPG system can position tumour points placed in a sample mask

The accuracy of the total positioning procedure has not been quantified in detail as yet, and this is therefore the first objective of this thesis. The precision previously measured as described in 1.3.2(c) above was re-measured. It is impractical to use a real patient for repeated measurements, so an empty mask was used. The effect on the precision of the empty mask co-ordinates when patients wear the mask is discussed below in paragraph 1.4.2 (b).

To measure the systematic positioning error or accuracy of the tumour, requires accurate knowledge of where the "correct" position of the tumour is supposed to be located in space. This was taken to be the beam vector in the treatment room as defined by theodolite measurements. An isocentre has been defined on the beam vector. The line joining the theodolite station positioned in the proton beam line proximal to the isocentre, and the distal theodolite station containing its insert, was used to define the beam vector. The insert contains a cross-wire within a 1 mm target hole, and the beam vector was taken to be the line passing through the centre of the hole. This beam vector was initially used to position the mounting holes of the large calibration frame and is also routinely used as the 'reference' beam vector for checking the SPG positioning accuracy (described in 1.3.2(b) (iv) above).

The tumour reference point as determined using a CT scanner, is required to lie on the beam vector at the isocentre, and the SPG system attempts to achieve this. Due to difficulties in making the measurement, and the unimportance for proton therapy of small deviations along the direction of the beam vector away from the isocentre, no measurements of positioning error along the beam vector were made.

1.4.2 To investigate the sources of error of the current positioning system

In order to understand the factors affecting the accuracy, it is necessary to gain an understanding of the sources of error inherent in the current SPG implementation, and to measure or assess their relative magnitude. There are several components of the total error in the patient positioning system. Each of these was investigated separately to assess their contribution to the total error. The first three errors discussed below are concerned with the correct co-ordination of the patient tumour in the frame of reference defined by the fiducial markers. The next two sources of error concern the SPG positioning system directly.

(a) The error in co-ordinating the facemask fiducial markers on a CT scanner (with no patient in the mask)

A comparison of the fiducial marker co-ordinates obtained on the CT scanner and the co-ordinates obtained using an accurate three-dimensional mechanical measuring device was made. Techniques were investigated that could be used to improve the accuracy and precision of determining the CT scanner co-ordinates of the fiducial markers. Investigating in detail the accuracy of CT co-ordination for each axis separately by using an accurately surveyed control frame can highlight co-ordination errors due to scaling and distortional errors. The use of alternative CT scanning protocols was also investigated.

(b) The effect on the precision of the CT scanner co-ordinates of the fiducial markers

A determination was made of how the fitting of the mask to the patient affects the precision with which the marker co-ordinates can be determination on the CT scanner.

(c) Movement of the patient anatomy inside the mask in a 7-day period

An attempt was made to determine whether there is any significant movement of the patient inside the mask.

(d) The accuracy and precision of the SPG system cameras

As part of the daily SPG calibration procedure, described in 1.3.2(b) (iv) above, a small check frame whose marker positions are accurately known is positioned by the SPG system before any patients are treated. A record is kept of the error in alignment between a theoretical target point on this frame and the isocentre. The positioning data of the small check frame by the SPG system was analysed, and the inherent positioning accuracy and precision calculated. These values were compared to values obtained from positioning accuracy measurements done for this thesis.

(e) Errors in position of the proton beam

It is crucial that the theoretical geometric vector in the proton treatment room describing the path of the proton beam be precisely defined. Theodolite surveys are used to define this vector. This thesis is not concerned with the positional accuracy of the *radiation* beam which is kept on the room vector by an automatic feedback loop operating on sets of steering magnets. No attempt is therefore made to analyse the accuracy of the proton *radiation* beam alignment with the beam vector.

The treatment vault lasers are used for convenient visual location of the isocentre and are used only for approximate checking of the patient position.

1.4.3 To investigate and implement ways of decreasing the time to set-up patients in the treatment room on the current system

One factor possibly limiting the numbers of patients that are treated at NAC using the SPG system for positioning is the length of time taken to set up a treatment field, currently about 15 minutes. The relative complication of the entire co-ordinating and positioning procedure and the occasional difficulty in tracing the source of a field mispositioned by the SPG system contributes both to this time delay and to stress of the operators. Methods of improving the setup efficiency were investigated. The current SPG system implementation was investigated both with respect to software and in its physical aspects with a view to streamlining and improving the current patient set-up and SPG positioning procedures in order to decrease treatment times. Currently used techniques that can be improved upon without major efforts were identified. The use of infrared light for sensing the reflective markers was suggested in by van der Vlugt (1991). The areas of investigation are listed below.

(a) Streamlining the current SPG software system

The SPG software was analysed with a view to improving its ease of use.

(b) Improving the marker illumination

It has been found that both spurious light reflections from the patient mask and thresholding problems have been extremely disruptive to the smooth operation of the SPG system. Bright areas that are not retro-reflective markers can occur, caused by reflections of ambient light from the mask. Eliminating these by increasing the threshold (see section 1.3.2(b)(vii), page 13) can remove valid markers from the image. The use of infrared light was investigated.

(c) Reducing the number of fiducial reference markers on the mask

An investigation was made into the effect of reducing the large number of fiducial markers currently used.

(d) Investigating apparent errors in chair movements

In the course of positioning patients for treatment it has been observed that intermediate movements sent to the chair often result in an incorrect patient position (a position not linearly closer to the isocentre than the prior position). This happens mostly when the chair movements are large, and has the consequence that multiple chair movement iterations are required to reach the correct patient position (within the stated tolerances). A systematic study of the intermediate chair positions was made.

1.4.4 To devise an alternative patient immobilisation system which will simplify the immobilisation and positioning procedures

In order to reduce the complexity of the system and to increase patient throughput, the patient positioning procedures need to be simplified. Alternatives to the facemask immobilisation system, also used as the fiducial marker support, were investigated. The designs should fulfil the conditions listed in paragraphs 1.2.1, 1.2.2, and 1.3.1 above. In addition, attention was given specifically to a system that reduces the problems of the current facemask as detailed in paragraph 1.2.4. Thus the design attempted to address the following issues:

- Minimising the manufacturing time and complexity;
- Minimising fiducial marker CT co-ordinate acquisition time;
- Providing a more rigid mount for the fiducial markers
- Reducing or eliminating the need for an X-radiographic check of the patient position by allowing the patient's head to be directly monitored;
- Facilitating a reduction of time and complexity to position and monitor the patient using the SPG system.

These alternatives should have the consequence of increased convenience of use, overall reduction in patient handling time and a reduction of cost of the immobilisation procedure with at least no loss of positioning precision and accuracy.

1.4.5 To compare the positioning accuracy of the current system with the alternative system

The positioning error of the new alternative immobilisation method designed according to the principles in section 1.4.4 above was assessed with no patient and compared with the accuracy achieved with the current mask system with no patient as measured according to the principles of section 1.4.1 above.

1.5 Scope and limitations

To attempt to act on all areas of possible improvement was beyond the time and physical resources available. Those areas judged to have the greatest possible immediate impact on improving the positioning precision or the ease of use of the SPG system were investigated and implemented where possible.

1.6 Thesis structure

After a brief discussion of the characteristics of proton therapy and the consequent requirements for patient immobilisation and positioning, a full description of the positioning system in use at the NAC is given in sections 1.2 and 1.3 above. The current problems of the system are also analysed. A proper understanding of the current system operation is a necessary foundation for the work done in this thesis. This section leads on to a detailed discussion and formal statement of the thesis objectives in section 1.4.

In the literature review in Chapter 2, radiotherapy positioning techniques are reviewed with particular emphasis on the latest trends prompted by advances in conformal 3-D tumour defining techniques. Of particular relevance to proton therapy at NAC are the immobilisation techniques pioneered in radiosurgery.

It was decided to allocate a separate chapter to each of the overall objectives. Within each chapter the method, materials, results, discussion and recommendations concerning the specific overall objective are discussed. In some cases the sub-objectives within the main chapters are dealt with in a similar way.

Finally, overall recommendations made as a consequence of this work are discussed in Chapter 8.

2 Review of Patient Immobilisation and Positioning for Radiotherapy

A table of centres worldwide treating with high-energy particles is shown below. The patient immobilisation and positioning methods are also shown where known.

Table 2-1 World wide high-energy proton and heavy ion treatment facilities, and the patient immobilisation and positioning systems used

Place	Country	Beam Direction	Patient immobilisation and positioning system used
Berkeley, CA*	USA	Horizontal	No longer treating
Boston, MA	USA	Isocentric and Horizontal	Not treating yet
Cambridge, MA	USA	Horizontal	Low temperature thermoplastic mask, bite block, implanted markers, stereoscopic X-rays, feedback to positioning system; foam body mould (Rosenthal *et al.*, 1995)
Uppsala	Sweden	Horizontal	-
Moscow	Russia	Horizontal	Low temperature thermoplastic mask, bony landmarks
Faure	South Africa	Horizontal	Face-mask with steel ball fiducial markers. Stereophotogrammetric control of patient support chair (Jones *et al.*, 1995)
Bloomington, IN	USA	Horizontal	Not treating yet
Orsay	France	Horizontal	Implanted wires; position on orthogonal X-rays controls chair position
Dubna	Russia	Horizontal	-
Loma Linda, CA	USA	Isocentric and Horizontal	Low temperature thermoplastic mask, dental fixation, body mould, laser positioning, X-ray confirmation of titanium fiducials and bony landmarks, skull contours
Tsukuba	Japan	Horizontal and Vertical	-
Kashiwa	Japan	Isocentric and Horizontal	-
St. Petersburg	Russia	Horizontal	Crossfire stereotactic frame
Chiba*	Japan	Horizontal and vertical	Body cast, CT scanner used in the treatment position
Villigen, PSI	Switzerland	Isocentric	Body cast with identical mechanical docking on CT scanner and treatment unit
Darmstadt, GSI*	Germany	Horizontal	Relocatable plaster mask, stereotactic positioning frame mounted on a floor stand (Schlegel *et al.*, 1992)

* Heavy ion beams

When first implemented in 1993, the SPG positioning and immobilisation system at NAC as described in sections 1.2.3 and 1.3.2 above were unique and successful solutions to the immobilisation and positioning requirements for high precision radiotherapy. To date, January 2000, no implementation of stereophotogrammetry for routine patient positioning in radiotherapy has been found in the literature. Two commercial photogrammetric patient positioning systems have however been marketed over the last two years (RadioCameras used with the Linac Scalpel[2], and ExacTrac[3]). It is not known what the precision and accuracy of these systems are, and whether either of them is in clinical use.

The immobilisation and positioning accuracy of the relocatable Riechert/Mundinger system used at the German Cancer Research Centre, Heidelberg, Germany (Schlegel *et al.*, 1992) was investigated with a photogrammetric optical sensor system described in detail by Menke *et al.* (1993). Measurements were successfully done using two CCD cameras focussed on five 'landmarks' attached to a cross, held firmly to the head by means of a bite block. The authors state that they intend using the system to automatically control a patient positioning system, but no further developments have been published.

As described earlier (section 1.3.2(c) above) a positioning precision vector of 2.3 mm has been reported by Schreuder *et al.* (1997) in a preliminary evaluation of the NAC SPG system.

A group at the Department of Biomedical Engineering at the Milan Polytechnic have tested a high sampling rate stereophotogrammetric system which corrects for breathing motion (Baroni *et al.*, 1996). They state that the system would be suitable for precision radiotherapy positioning (Baroni *et al.*, 1997; Baroni *et al.*, 1998).

Most recently, Rogus *et al.* (1999) investigated a SPG system that is very similar to that at the NAC. In view of the fact that this paper is sponsored by Varian Associates, and that BrainLab[3] and Varian are radiotherapy development partners, it is likely that the system being tested is based on the ExacTrac system. In their conclusions they state: "Overall results show that this photogrammetry system ... may have application in positioning patients undergoing fractionated stereotactic radiotherapy. The system may be used to set up a patient, and to monitor and document the patient's position during treatment." They are presumably unaware that these uses have been in use at NAC for proton therapy for six years, as they do not reference the article by

[2] Sofamor Danek USA, Memphis, TN.
[3] BrainLAB, Heimstetten, Germany

Levin *et al.* (1993) describing the preliminary design of the NAC SPG system, or the articles by Jones *et al.*, 1995 and Schreuder *et al.*, 1997 describing the operational system and the experience gained over three years. All measurements made for the current thesis were made prior to the publication of the paper by Rogus *et al.* (1999). The aim of their paper is, however, very similar to several of the objectives of this thesis, and as a consequence their results have been extensively used as a basis for comparison.

2.1 Patient immobilisation and positioning for conventional X-ray therapy

The primary aim of radiotherapy is to deliver sufficient radiation dose to a tumour to cause cell damage within the tumour rendering it unviable and resulting in its destruction as a living entity. As a constraint to this requirement, as much of the surrounding healthy tissue as possible should be spared. The probability of controlling the local disease depends on the ability to deliver an adequate dose to the entire volume of target cells. Years of radiobiological and radiotherapy experience published in several studies have led Mijnheer *et al.* (1987) to conclude that the total error (both random and systematic) in absorbed dose should be no more than ±3.5% at the one standard deviation (1SD) level (equivalent to 68% confidence level for a 'normal' distribution). A rigid, reproducible immobilisation system is often vital to satisfying this requirement since excessive patient movement can cause parts of the tumour to lie outside the beam edges.

Apart from limiting patient motion and reducing the probability of major positioning errors, there are other benefits of a good immobilising system. Verhey (1995) pointed out that a well-constructed system can reduce the time for daily patient set-up, it can make the patient feel more secure and less apprehensive, it can reduce reliance on patient co-operation and alertness, and it can help to stabilise the relationship between external cutaneous marks and internal structures. Finally, if the immobiliser is saved at the conclusion of the treatment, it can be used to approximate the treatment position in subsequent follow-up diagnostic studies, thereby facilitating the interpretation of clinical results.

The methods for accurately positioning the patient such that the region to be treated falls in the radiation beam have followed available technology very closely. In conventional radiotherapy the most commonly used technique today is to define orthogonal horizontal, vertical and longitudinal planes by means of narrow (1 mm) laser beam lines. The lasers are placed on the walls of the treatment room and intersect at the isocentre of the treatment unit. Similar laser lines located in the treatment simulator room, image intensifier room, or on the CT scanner unit, indicate an isocentre within the patient and intersect the patient's skin or a formed plastic shell

when the tumour is imaged. These positions are marked on the patient's skin or on the body shell and are subsequently re-aligned with the treatment room laser lines on a daily basis immediately prior to treatment. In this way the position of the patient when the tumour was first identified is re-established on the treatment unit.

Once the patient has been correctly positioned at the isocentre, the treatment beam is correctly orientated according to the treatment plan by appropriate translations and/or rotations of the treatment couch, and rotations of the gantry and collimator. Port films are now frequently used to verify the position of the beam relative to the patient anatomy, often by comparison with digitally reconstructed radiographs produced by the planning system.

Apart from precise and secure fixation, the positioning accuracy and precision attainable is dependent on the correct calibration of the laser lines in orthogonal planes passing through the isocentre, line quality and positional stability of the laser lines, and the accuracy of the treatment unit and treatment couch movements. For conventional radiotherapy where tolerances of up to 5 mm are often acceptable, no further refinements are required provided regular quality control measures are instituted. Treatments requiring more precise positioning are typically intracranial irradiations, and thus advances in positioning have been developed for radiosurgery applications using conventional radiation (discussed further in 2.3 below) and in charged particle therapy where the favourable dose distribution in tissue can be exploited (discussed further in 2.4 below). The mechanical tolerances inherent in specialised localisation equipment will affect the positioning accuracy and precision attainable.

2.2 Brief history of immobilisation methods

It is useful to list here the methods commonly used for immobilisation in a historical perspective as summarised by Verhey (1995). Initial radiotherapy was for relatively superficial tumours and very rudimentary methods were used to immobilise the relevant part of the anatomy. Positioning the patient for treatment (tumour localisation) was done by aligning a light field with superficial marks on the patient. In the 1960s and 1970s treatment modalities able to treat to greater depths were developed and were gantry-mounted. Port films were used to verify the position of the beam relative to the patient anatomy. The immobilisation techniques developed to assist in the patient set-up include Plaster of Paris casts, polyurethane foam moulds, Lightcast moulds, bite-blocks attached to the treatment table, and vacuum-moulded acrylic masks. In an early paper Marks and Haus (1976) note localisation errors of greater than 1 cm in 16% of a series of

patients treated for head and neck cancer, and noted that the errors could be significantly reduced with the use of bite-block immobilisation.

CT scanners were brought into routine use for diagnostic purposes at the end of the 1970s, and within a few years were employed for planning radiotherapy treatments. This started in Boston with proton therapy (Goitein *et al.*, 1983) and later for conventional photon treatments. With the new awareness of targets defined in 3-D and the problems of positioning the target in 3-D, new immobilisation techniques emerged. These included air-evacuated bags filled with polystyrene beads, polyurethane foam casts, low temperature thermoplastics and head holders and frames with and without bite blocks (Verhey, 1995).

2.3 Positioning and immobilisation in radiosurgery

Radiosurgery refers to the treatment of small intracranial or ocular tumours using external radiation beams in a single or very few fractions. Dr Lars Leksell, the Swedish neurosurgeon, who used stereotactically directed proton beams, coined the term in 1951 (Leksell, 1983). The patient is rigidly immobilised and accurately localised for irradiation using stereotactic apparatus developed for neurosurgical procedures.

2.3.1 History

In the mid 1970s interest and development of linear accelerator based radiosurgery systems was prompted by the development of modern high-energy accelerators, mounted on an isocentric gantry. Examples of the stereotactic frames commonly used for immobilisation and positioning are listed in the next section 2.3.2.

In the early 1990s, concomitant with advances in treatment planning capabilities and beam delivery techniques (e.g. multileaf collimators), it was suggested that there might be benefits, for certain tumours, to extend the radiosurgery technique to a fractionated treatment regime typically used in conventional radiotherapy. This has been called stereotactic radiotherapy, and requires a relocatable frame system to allow reproducible daily treatments with sufficient precision. The requirements for a successful frame are well stated by Gill *et al.* (1991). "An ideal fixation device should be non-invasive, well tolerated, and accurately relocatable. When in position it should be rigidly fixed to the skull and should provide complete immobilisation. The mounting of the head should be adaptable and the frame should be compatible with all forms of imaging

and suitable for stereotactic instruments and radiotherapy." Examples of relocatable frames satisfying these requirements are listed in the next section 2.3.2.

2.3.2 Immobilisation/positioning system designs for intracranial radiation treatments

The systems widely used for single fraction radiosurgery are conventional stereotactic head frames, amongst which are the Riechert/Mundinger-frame (Riechert and Mundinger, 1955; Mundinger and Ostertag, 1978), the Leksell-frame (Leksell, 1949; Leksell, 1971) and the Brown-Roberts-Wells (BRW)-frame[4] (Brown, 1979; Heilbrun *et al.*, 1983; Lutz *et al.*, 1988).

The frames are fixed to the skull with three or four pins, under local or general anaesthetic. They can remain *in situ* for only short periods and thus are problematic for fractionated therapy. At least three groups, Betti *et al.* (1989) using a frame employing holes in the skull for relocation, the University of Miami group using the 'stereotaxic' guide (Houdek *et al.*, 1991;Houdek *et al.*, 1991 Schwade *et al.*, 1990), and McGill University group (Podgorsak *et al.*, 1993) have had satisfactory results with invasive frames. In fact Podgorsak *et al.* (1993) go on to say that they "believe that the inconvenience of the latter is outweighed by improved reliability and accuracy in the delivery of the fractionated treatment dose".

Nevertheless, several non-invasive relocatable systems have been developed for use in fractionated treatments. Here a frame providing both a measurement reference frame and fixation method is fixed to the patient in such a way that it may be easily and reproducibly removed and re-attached with adequate precision. An early system developed especially for proton treatments in Boston uses a thermoplastic mask (Verhey *et al.*, 1982). This was later improved by adding a bite block (Rosenthal *et al.*, 1995).

Other systems designed and used for fractionated treatments are:

- The Lawrence Berkeley Laboratory frame/mask (Lyman *et al.*, 1989)
- The modified Riechert/Mundinger based Heidelberg patient fixation system (Schlegel *et al.*, 1992) and a similar commercially available fixation system[5] (Hamilton *et al.*, 1996), both using a mask made from self-hardening plastic bandages[6]
- The Laitinen Stereoadapter (Laitinen *et al.*, 1985; Laitinen, 1987; Hariz *et al.*, 1990; Delannes *et al.*, 1991) using the ear canals and nasion for fixation

[4] Radionics Inc., Burlington, MA, USA
[5] Leibinger L.P., Dallas, TX, USA
[6] Scotch Cast, Scotch-Flex, 3M, St. Paul, MN, USA.

- An in-house-built stereotactic frame resembling a Leksell Stereotactic Frame, Model G[7] (Podgorsak *et al.*, 1993)
- The Gill-Thomas frame (based on the BRW frame) (Gill *et al.*, 1991; Graham *et al.*, 1991)
- The commercially available Gill-Thomas-Cosman (GTC) frame[8]
- The Boston Children's frame[9] (Kooy *et al.*, 1994; Dunbar *et al.*, 1994)
- A thermoplastic masking system by BrainLab[10] (Rogus *et al.*, 1999)

2.4 Positioning systems

As the abilities of diagnostic imaging techniques improve, the demand for both more accurate and more convenient positioning techniques increases. Innovative techniques designed specifically for integrating diagnostic and therapeutic procedures are emerging. As listed in Phillips (1993), the basic requirements that need to be fulfilled by a successful immobilisation/positioning system are:

- To provide a unique and fixed reference frame relative to the brain
- To provide the means by which this reference frame can be applied to (or correlated with) the radiologic images of the brain and surrounding structures
- To provide precise and accurate positioning for as many diagnostic and treatment procedures as necessary

For any system to be successful, it must adhere to these requirements. Consequently most of the frame systems are designed with an inherent set of accurate scales or a co-ordinate system which enables accurate positioning of the tumour reference point (or treatment plan isocentre). These are used in preference to the gantry and couch motions of the treatment unit, as is used for conventional positioning, in order to gain precision.

As the abilities of diagnostic imaging techniques improve, the demand for both more accurate and more convenient positioning techniques increases. Innovative techniques designed specifically for integrating diagnostic and therapeutic procedures are emerging. These techniques often involve an alternative method of obtaining or defining the co-ordinate system required for patient positioning.

Use has been made of implanted markers and X-ray imaging to confirm the patient position (Verhey *et al.*, 1982; Jones *et al.*, 1993). The Harvard Cyclotron Group have now instituted a

[7] Electra Instrument AB, Stockholm, Sweden
[8] Radionics Inc., Burlington, MA, USA
[9] Radionics Inc., Burlington, MA, USA
[10] BrainLab GmbH, Heimstetten, Germany

computer assisted positioning system in which three implanted markers are located by digitising stereoscopic X-ray films, and the movements required to bring the patient to the treatment position are transmitted to the treatment couch (Gall *et al.*, 1993). This system is similar to the NAC SPG positioning system, differing only in the method by which the fiducial markers are located. X-ray films are used in the Harvard system whereas video cameras are used in the NAC system. In a study investigating automated localisation of the prostate, Balter *et al.* (1995) used portal images (digital radiographs taken with the treatment unit) and automatic marker identification algorithms to calculate positioning misalignment. The complete calculation including image acquisition took 30 s and precision of better than 1 mm in translation and 1° in rotation was obtained.

A computer controlled 'stereotaxic' (*sic*) positioning and patient monitoring system using a 'space digitizer'[11] attached to a stereotactic frame is described by Houdek *et al.* (1991). This device is a magnetic field sensor that records the position and orientation in space of the stereotactic frame. Using measurements with a phantom, an "accuracy of 0.8 mm RMS in position and 0.5 degrees RMS in orientation" is claimed, and an overall radiation beam delivery precision of ± 1.5 mm.

Adler and Depp (1992) have also reported on a frameless technique that images and controls the patient position concurrently with the radiation treatment using a robot-mounted miniature linear accelerator[12]. The position of the radiation beam is dynamically controlled by on-line diagnostic X-ray images in conjunction with digitally reconstructed radiographs, thus eliminating the need for a stereotactic frame.

2.5 Positioning accuracy

2.5.1 Definitions

In September 1993, the need for standardisation of the definitions of target volumes used in radiotherapy was recognised in the publishing of an International Commission on Radiation Units and Measurements report (ICRU Report 50, 1993). In particular, the clinical target volume (CTV) is defined as the volume of tissue which includes subclinical disease, and which has to be treated adequately in order to achieve the therapeutic aim. This is an anatomical-clinical concept that has to be defined before a choice of treatment modality and technique is made. Margins have to be added around the CTV to compensate for treatment uncertainties. These are mainly beam

[11] Polhemus, Inc., Colchester, VT 05446
[12] Neurotron 1000, Accuray, Santa Clara, CA

and patient set-up errors, and patient and organ motion. This leads to the concept of planning target volume (PTV). The PTV is a geometrical concept, fixed relative to the treatment unit, defined in such a way as to take into account the net effect of all the possible geometrical variations and inaccuracies, so that the defined dose is actually absorbed in the CTV. The PTV differs from the CTV because of treatment uncertainties. The work in this thesis is concerned only with measuring and minimising the patient set-up errors. Figure 2-1 illustrates the different volumes.

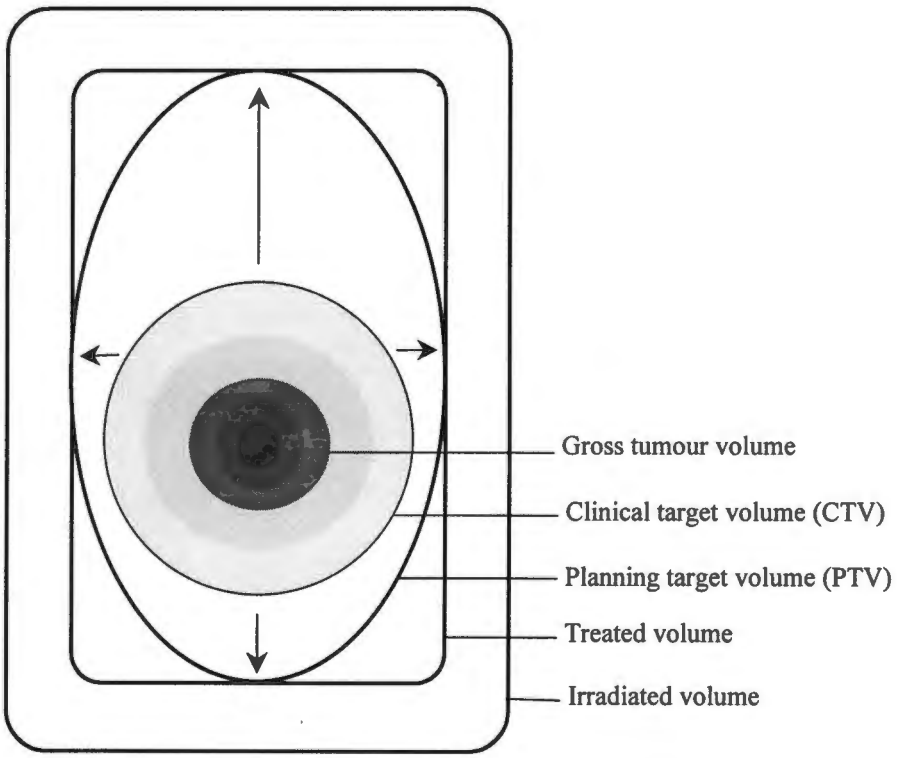

Figure 2-1 **Schematic illustration of the different volumes defined in ICRU 50.**
Gross Tumour Volume **denotes the clinically demonstrated tumour.**
Clinical Target Volume **(CTV) denotes demonstrated tumour and suspected tumour.**
Planning Target Volume **(PTV) consists of the CTV and a margin to account for variations in size, shape, and position relative to the treatment beam(s).**
Treated Volume **is the volume that receives a dose considered important for local cure or palliation.**
Irradiated Volume **is the volume that receives a dose considered important for normal tissue tolerance.**

Because the PTV is a fixed volume in space in which the CTV moves due to set-up errors, the tumour bearing regions (CTV) would receive a minimum of the prescribed dose provided those

motions were contained within the PTV, and the prescribed isodose surface on the patient did not encroach into the PTV.

2.5.2 Systematic and random errors – accuracy and precision

As with many experimental measurement errors, positioning errors can be separated into random and systematic components. This is outlined by Kutcher *et al.* (1995), and bears repeating here. Figure 2-2 represents set-up errors in which the patient can be translated away from the prescribed position in a lateral or superior/inferior direction. Each dot represents a daily set-up error measurement, that is, the difference between the patient's measured position (defined for example by a portal film) and the prescribed position (defined for example by a digitally reconstructed radiograph). No error in patient set-up would be represented by a dot at the origin. For each patient the average position (or centre-of-gravity) of the daily set-up errors is the patient's systematic set-up error, represented by the arrow from the origin. This mean error is also referred to as the accuracy of the treatment.

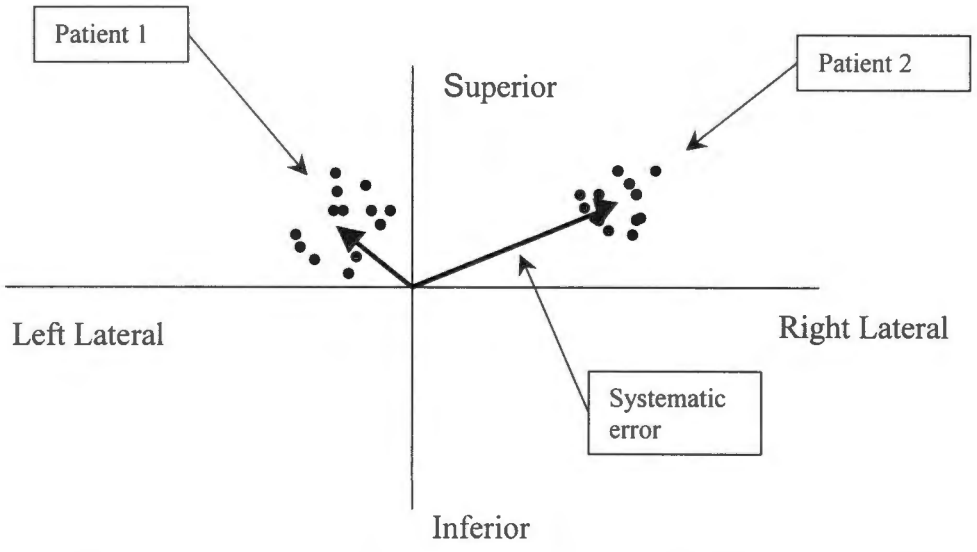

Figure 2-2 Setup error measurements. The arrow centred on the average of a group of error measurements represents the systematic error – a measure of accuracy. The differences between all the set-up errors and their mean form a distribution of random set-up errors whose standard deviation is a measure of precision of the positioning procedure for the patient

The differences between all the individual set-up errors and their mean for a patient form a distribution of random set-up errors for the patient. The standard deviation of this distribution is

referred to as the precision of the treatment. The combined data using many patients on a particular treatment, form a distribution whose parameters μ_t (mean); and σ_t (standard deviation) (see Table 2-2) are concise representations of the systematic and random set-up errors associated with that treatment or technique. The mean error is also referred to as the accuracy, and the standard deviation as the precision, of the positioning technique.

Table 2-2 Set-up error data classification

	Systematic errors	Random errors
Each patient	One systematic error per patient	Distribution of random errors per patient, ${}_p\mu_r = 0$; ${}_p\sigma_r$
Population of patients	Distribution of systematic errors, μ_s ; σ_s	Pooled random errors forming a distribution, $\mu_r = 0$; σ_r
	Combined distribution of set-up errors (for treatment technique), μ_t ; σ_t	

2.5.3 Methods of data collection and analysis

A careful analysis was done at the Massachusetts General Hospital by Rabinowitz *et al.* (1985) in which they attempted to standardise and extend the definitions of variability in patient positioning, and called on other institutions to perform similar analyses. The final simulation portal film is used as the 'correct' reference position. Several other researchers have followed a similar method (Thornton *et al.*, 1991; Gill *et al.*, 1991; Serago *et al.*, 1991; Rosenthal *et al.*, 1992; Hartmann *et al.*, 1993; Rosenthal *et al.*, 1995), but there remains poor uniformity of methods, making comparisons sometimes difficult. Rosenthal *et al.* (1992) make a strong case for reporting the total uncertainty, a root mean square of the position deviations from the initial simulation. Hamilton *et al.* (1996) follow this recommendation, with a clear and comprehensive statistical analysis.

2.5.4 Published positioning accuracy for intracranial targets

Using several newly developed techniques, Verhey *et al.* (1982) report an accuracy of 2 mm or better in immobilising the patient and CTV. Two separate alignment studies were done using a head immobilised with a low temperature thermoplastic facemask. In the first study, intra-

treatment motion was determined by comparing pre-treatment and post-treatment radiographs, separated by an average time of 5 minutes. The mean of the distribution was 0.8 ± 0.6 (1SD) mm. This distribution characterised the degree to which the mask system was able to immobilise the heads of patients. In the second study, immobilised patients were positioned initially with laser alignment to marks on the mask, and then with orthogonal radiographs. The total movement required between the initial laser alignment and the final pre-treatment position was recorded. The mean movement was 2.2 ± 1.4 (1SD) mm. This distribution characterised the degree to which the laser alignment, using cutaneous markers, and radiographic alignment coincided.

The implications for tumour margins can be examined. With laser alignment and mask immobilisation, the margins between CTV and PTV would have to be set at approximately 5 mm in order to include 2 standard deviations (2.2 + 2 × 1.4), whereas, with the anatomical radiograph alignment combined with identical immobilisation, margins of 2.0 mm (0.8 + 2 × 0.6) can be used. This smaller margin allows a higher dose to be delivered to the tumour whilst still keeping the dose to neighbouring sensitive structures within tolerable limits. Consequently, a significant increase in tumour control probability can be expected (Tatsuzaki and Urie, 1991). Verhey (1995) later summarised, "To obtain the greatest reduction of margins between CTV and PTV, both rigid immobilisation and accurate target positioning are required. It is critical that careful positioning studies be carried out to determine the size of the margins that can be safely prescribed".

Phillips (1993) reports that radiosurgery systems are capable of accuracies of 1 to 2 millimetres or better, with precisions of the same magnitude. Referring only to errors in localisation of points using a CT scanner, results analysed by Friedman and Bova (1989), Hartmann *et al.* (1993), Lutz *et al.* (1988), and Podgorsak *et al.* (1990), and summarised by Hartmann *et al.* (1993), are shown in Table 2-3 below.

Table 2-3 Vector error (random) in point localisation in CT scanners

Author	Average vector error (mm)	Maximum vector error (mm)
Friedman and Bova (1989)	0.8 ± 0.6	-
Hartmann *et al.* (1993)	1.0	½ $\sqrt{(2a^2 + d^2)}$
Lutz *et al.* (1988)	0.9	1.7
Podgorsak *et al.* (1990)	±1.0	±d/2

a = length of quadratic pixel, d = CT slice distance

Gill *et al.* (1991) report re-positioning accuracy (measured by X-radiograph) of 0.5 ± 0.5 (2SD) mm for their relocatable frame. Using mechanical measurements of the skull repositioning accuracy in the Gill-Thomas-Cosman frame, Kooy *et al.* (1994) found a total precision, adding the x, y, and z axis components in quadrature, of $\sqrt{(0.35)^2 + (0.52)^2 + (0.34)^2} = 0.71$ (1SD) mm. For the Laitinen Stereoadapter, Delannes *et al.* (1991) claim repositioning accuracy (measured by CT scanner) on 10 patients of

$$\sqrt{(1.82)^2 + (1.5)^2 + (1.9)^2} = 3.03 \pm \sqrt{(0.665)^2 + (0.535)^2 + (0.96)^2} = 1.28 \text{ (1SD) mm.}$$

It was shown by Schlegel *et al.* (1992) that the Heidelberg patient fixation system (a relocatable mask) could achieve a vector precision of $\sqrt{(0.92)^2 + (0.7)^2 + (1.3)^2} = 1.74$ mm. The follow-up paper by Menke *et al.* (1993) discusses this photogrammetry system and the precision measurements in more detail.

The paper by Rogus *et al.* (1999), using an SPG system very similar to that at NAC, reports a phantom positioning accuracy of 1 to 2 mm and a precision of ± 0.3 (1SD) mm for each of three orthogonal directions, giving a vector precision of about ± 0.5 mm.

2.5.5 Correcting for patient set-up errors

With the development of precise 3-D radiotherapy treatment planning has come an increased need to check on the patient position during a course of treatment. Portal films have been widely recognised as the most effective method of detecting patient positioning and field placement errors. Mitine *et al.* (1991) have emphasised the importance of taking port films on the first day of treatment as a means of detecting systematic errors occurring in the treatment preparation chain. The American Association of Physicists in Medicine has recommended film review of all

treatments at least once per week (Kutcher *et al.*, 1994). Because there may be gradual changes in the patient displacement over time, el-Gayed *et al.* (1993) recommend that for treatments requiring a high precision, localisation checks should be performed throughout the treatment course. Problems with the portal film approach are the increased overall treatment time, and the difficulty and expense of sufficiently accurate radiographic techniques. In recent years, however, electronic portal imaging devices (EPIDs) are being increasingly used for on-line setup error correction (van de Steene *et al.*, 1998, Boxwala *et al.*, 1999).

In an attempt to reduce the overall treatment time, protocols have been developed in which a decision, based on the set-up error measurement, is made after the treatment, and any possible correction applied at the next patient set-up (Bel *et al.*, 1993; Shalev and Gluhchev, 1994; Yan *et al.*, 1994). No attempt is made to correct for the random component of the set-up error. Thus the decision rules are based on probabilities and require knowledge of the probability distribution of each error. For example, if the set-up error measurement exceeds 3□, then there is a high likelihood that the set-up contains a systematic component.

Despite the most diligent attempts to minimise set-up errors, they persist. Kutcher *et al.* (1995) summarise two ways in which these uncorrected and uncontrolled set-up errors can be incorporated into treatment plans to 'ensure' (within a given level of probability) that the prescribed dose is delivered. One method uses margins around the CTV and calculates nominal dose distributions (without uncertainties) that are evaluated for the PTV; the other incorporates the uncertainties into the dose distributions that are evaluated for the CTV. In the former paradigm, set-up error distributions are used to derive margins around the CTV, while in the latter they are used to derive altered dose distributions.

However, as Gill *et al.* (1991) have stated, "the most significant inaccuracy in stereotactic radiotherapy remains the clinical definition of the target volume on the selected combination of imaging modalities".

3 Assessing the accuracy with which the current SPG system can position tumour points on a sample mask (with no patient in the mask)

3.1 Materials

An existing patient mask constructed as described in 1.2.3 above was modified with cut-aways such that two theoretical tumour reference points placed inside the mask could be seen from outside the mask (see Figure 3-1). The two theoretical tumour reference point positions were fixed to the mask, one near the mask surface (superficial) and one well inside the mask (deep). Both had concentric rings, of radii 1 mm to 5 mm, drawn and centred on the tumour reference point.

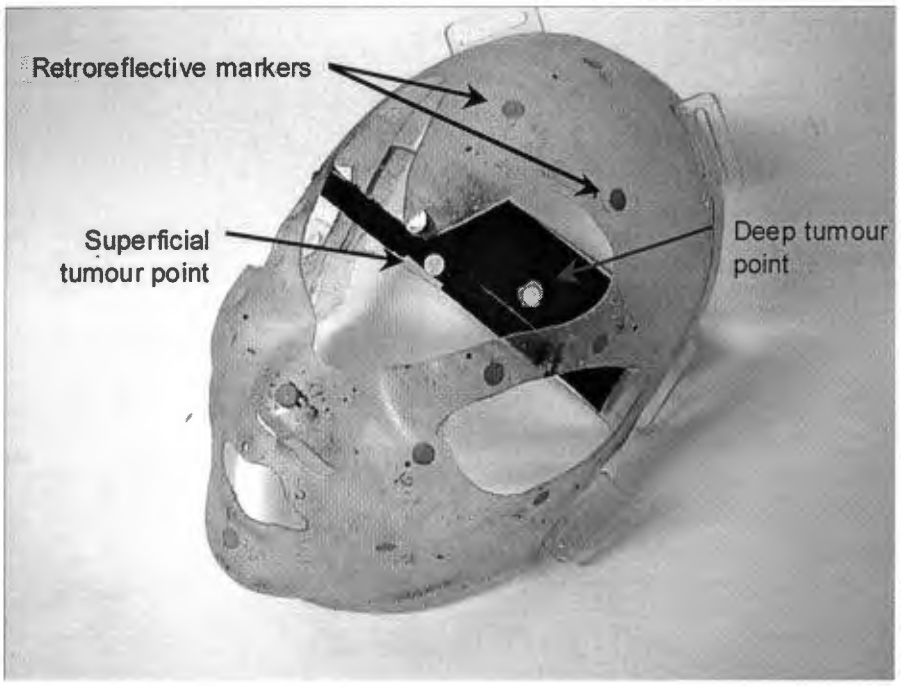

Figure 3-1 Modified patient mask

3.2 Methods

The mask was scanned on the Picker IQ Fast scanner (see footnote on page 10) to obtain the CT co-ordinates of the fiducial markers and the tumour reference points (as described in 1.3.2(b)(ii) above). The co-ordinates were input into the SPG system. A theoretical beam centred on each of

the tumour points was defined in the CT co-ordinates and input into the SPG system. The deviation of the tumour reference point from the beam vector, as observed by a theodolite and estimated using the concentric rings, was recorded after the SPG system had positioned the mask within a tolerance of 1 mm set on the SPG system. The direction of the theoretical beams were perpendicular to the plane of the rings drawn around the tumour reference points, so that the radial deviations were measured in a plane perpendicular to the beam.

In a situation when a real patient is being treated, the patient's starting position, before initiating the SPG system, is reasonably arbitrary. Eight starting positions were, however, systematically chosen here (Figure 3-2) in order to use the data for further analysis of the intermediate positions of the mask (see section 5.4). Eight readings were taken for the superficial tumour reference point and again for the deep tumour reference point, the initial mask position being at eight different positions relative to the isocentre. The readings, named Set Two, were repeated one month later.

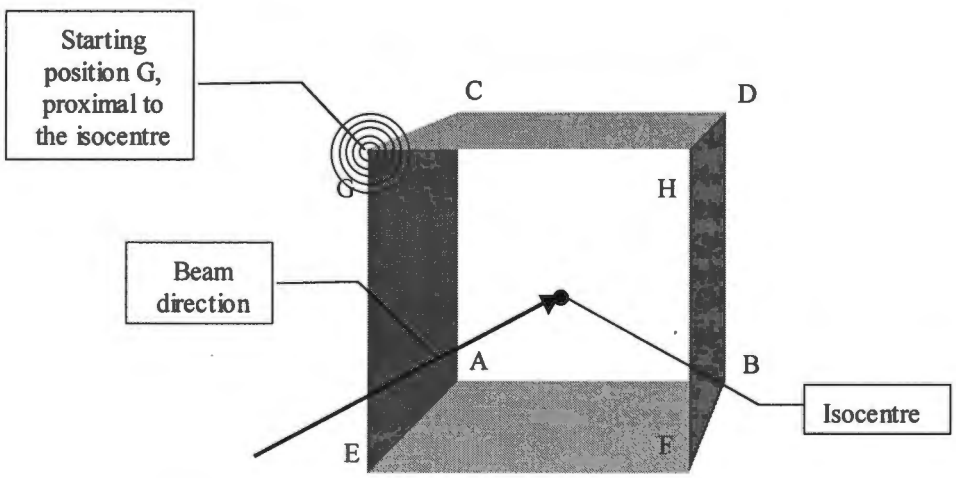

Figure 3-2 Starting positions, A, B, C etc., of the mask and frame

3.3 Results

Detailed readings are shown in Table 3-1 below. In most cases the mask was brought into its final position in two cycles of the SPG system, and in all other cases in three. The mean deviations of the tumour points from the isocentre and standard deviations are also shown.

Table 3-1 Tumour reference point to isocentre deviations (mm) on the mask after being positioned by the SPG system

Starting position	SET ONE		SET TWO (one month later)	
	Superficial	Deep	Superficial	Deep
A	1.5	1.0	1.0	1.9
B	1.5	1.3	1.0	1.9
C	1.5	1.0	1.0	1.7
D	1.5	1.2	1.0	1.7
E	1.6	0.6	1.0	1.7
F	1.7	1.4	1.0	1.5
G	2.0	1.5	1.0	1.7
H	1.6	1.2	1.0	1.7
Mean	1.61	1.15	1.00	1.73
Std. Dev.	*0.17*	*0.28*	*0.00*	*0.13*
Mean	1.38		1.36	
Std. Dev.	*0.33*		*0.38*	
Mean precision	*0.23*		*0.09*	
Mean	1.37			
Std. Dev.	0.35			
Mean precision	0.16			

For both sets there is a significant difference between the accuracy for the deep and superficial tumour points (two-tailed t test, $p = 0.0015$ for set one; $p < 10^{-4}$ for set two), and the sign is not consistent. In other words the deep tumour was more accurately located in set one, and the superficial tumour was more accurately located in set two. This inconsistency cannot be explained, although combining the readings for both locations in a set gives values (1.38 and 1.36 mm) which are not significantly different between the two sets of readings (two-tailed t test, $p=0.9$). The mean of all measured deviations is 1.37 mm with a standard deviation of 0.35 mm.

The measured precision achieved varied considerably between the deep and superficial tumours and between the two measuring occasions. However, if it is assumed that the inherent precision

possible is the same for both the superficial and the deep tumour, an average precision of 0.23 (1SD) mm and 0.09 (1SD) mm was found for the set one and set two respectively. This indicates that the measurements were more precise in set two. Assuming however that the inherent precision does not change between the two measuring occasions, the mean precision of the mask can be stated to be 0.16 (1SD) mm.

3.4 Discussion

The readings were taken on two occasions and the mean deviation of the isocentre from the tumour was found. Thus, using the mean of all readings, the positioning accuracy of the facemask can be stated to be 1.4 mm. This result corresponds very well with the results found by Rogus *et al.*, (1999). The positioning accuracy of a phantom between its position set on a simulator and measured in the treatment room is stated to be 1 to 2 mm although no detailed analysis is shown.

Concerning the precision of their system, measuring the final positioning error of a phantom repeatedly re-positioned by hand according to the corrections calculated by their system was ± 0.3 (1SD) mm in each of three orthogonal directions, giving a vector precision of ± 0.42 (1SD) mm calculated for two dimensions. This figure increased to ± 0.6 (vector = 0.85) mm for repositioning by the treatment couch. The mean precision attained with the facemask of ± 0.16 (1SD) mm is considerably better than ± 0.42 (1SD) found by Rogus. Using the overall standard deviation for all the mask measurements of ± 0.35 (1SD) (in two dimensions) still shows a slight improvement on their value.

The measured result of 1.4 mm is a baseline upper (best) limit of positioning accuracy for the SPG system since no patient was in the mask for the CT scanner and SPG position readings. It represents a sum of the constituent errors in the co-ordinating process, and is mainly affected by the precision of the CT scanner co-ordinates and the precision of the SPG positioning procedure. Distortions of the mask due to the presence of a patient, and small patient movements during the CT scan and during the positioning procedure, would contribute to increasing the error from the measured value. In the next section all the constituent errors in the positioning process are discussed.

4 Investigating the Sources of Error of the Current System

There are several components of the total random error generated in the entire marker acquisition and co-ordination procedure of the patient positioning system. Those listed below are concerned with the correct co-ordinating of the patient tumour using fiducial markers on the patient mask. As they were considered to be the largest contributors to the total random error, they were the only sources investigated. They are independent sources of error and can thus be added in quadrature to obtain an estimate of the total error.

4.1 The error in co-ordinating the facemask fiducial markers on a CT scanner (with no patient in the mask)

The error can only be determined if accurate co-ordinates of the fiducial markers are known. These were obtained using a reflex metrograph (see Glossary), and were then compared to the co-ordinates obtained on a CT scanner.

4.1.1 Materials and methods

(a) Mask survey using a metrograph

A patient mask was surveyed to obtain the 'true' positions of the fiducial markers. Measurements were taken using the reflex metrograph (see Glossary). Four sets of readings for the 20 fiducial markers on the mask were taken, and the mean co-ordinate value was taken as the 'true' marker

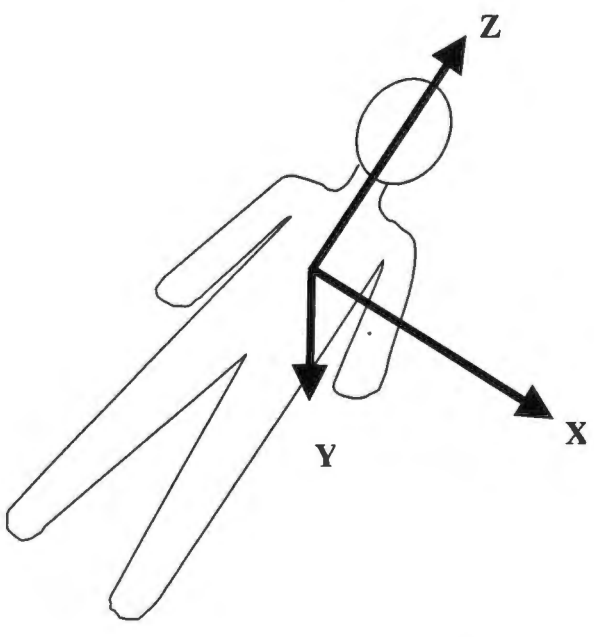

Figure 4-1 Metrograph co-ordinate system

position. By repeating the measurements several times, the precision achieved for both methods of co-ordinating could be determined. The co-ordinate system of the metrograph is shown above.

(b) Mask scanned in CT scanner

The CT co-ordinates of the fiducial markers of the same mask were obtained on the Picker IQ Fast scanner. Due to the fact that the facemask is not pre-aligned in any particular orientation on the CT scanner or metrograph, a comparison between the fiducial marker co-ordinates can only be made in an arbitrary reference frame chosen to be that of the metrograph. It is then not possible to measure a systematic error. Any possible systematic error in the CT scanner co-ordinating process is lost in the least squares transformation needed to rotate the CT scanner co-ordinate system into the metrograph co-ordinate system.

The protocol used to scan the head for diagnostic purposes uses a 5 mm slice thickness and 240 mm field of view. A 2 mm slice thickness is possible on the Picker IQ Fast and this was used for obtaining all marker co-ordinates. The table position (z co-ordinate) is reported to the nearest 0.5 mm. To obtain the z co-ordinate of a fiducial marker, the tabletop is moved until the CT scanner laser falls on the marker. At first a small series of slices at 0.5 mm intervals was taken around this position and the slice with the brightest marker used for the z position. This proved very time consuming. After the lasers (two horizontal and one vertical) were more carefully calibrated by the service technicians, the best slice was most often that found by eye using the laser. The process was thus speeded up without loss of accuracy.

The mask was placed on the CT scanner bed and the CT co-ordinates of each fiducial marker were recorded. The x and y axes are in the axial plane and the z axis is the table or slice position (see Figure 4-2 below). The mask and bed position was altered slightly, and the CT co-ordinates were recorded again. Four sets of readings were obtained. Each set of co-ordinates of 20 fiducial markers was transformed in rotation and translation (but not scaled), by minimising the least square differences, into the previous metrograph values obtained in section 4.1.1(a) above. The relation between two co-ordinate systems (x, y, z) and (X, Y, Z) is

$$\begin{bmatrix} x \\ y \\ z \end{bmatrix} = \mathbf{R}^{\mathsf{T}} \begin{bmatrix} X \\ Y \\ Z \end{bmatrix},$$

where $\mathbf{R}$ is the orthogonal matrix representing the rotation of axes and $\mathbf{R}^{\mathsf{T}}$ its transform. A computer program was written in BASIC (RODDY.TRU) in which the matrix $\mathbf{R}$ is formed by

using Caley's formula and the parameters of Rodrigues (Thompson, 1969). The program listing and sample output are shown in APPENDIX A below.

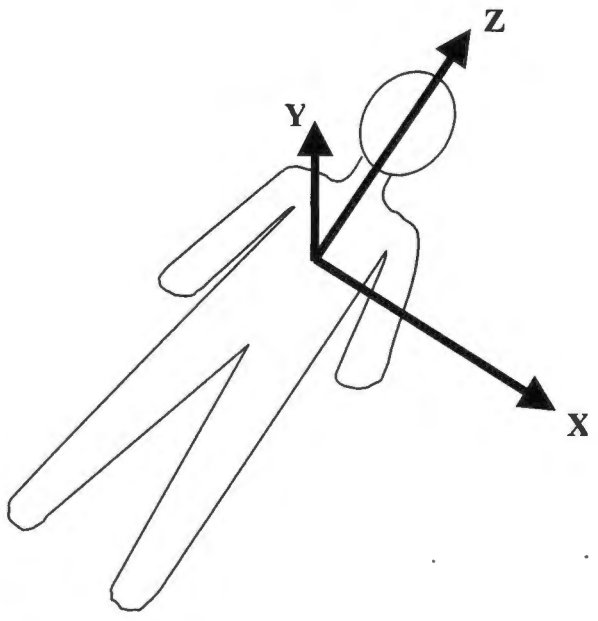

Figure 4-2 CT scanner co-ordinate system

(c) Total error in fiducial reference markers – analysis of residuals

The standard deviation of the mean of the residuals between the CT scanner co-ordinates and the metrograph co-ordinates for all the markers is a measure of the precision with which the CT co-ordinates can be obtained. This standard deviation of the mean of the residuals can be found in two ways. Theoretically the total standard deviation should be equal to the square root of the sum of the squares of the standard deviations of the metrograph readings and the CT scanner readings. This method of adding the standard deviations in quadrature is however only true for independent marker co-ordinate readings.

The CT co-ordinates need to be rotated into the metrograph co-ordinate system as a set, and therefore the marker co-ordinates are not independent of each other. In the second method, the residuals between the metrograph fiducial marker co-ordinates and the co-ordinates measured on the CT scanner are calculated for each marker in turn, after applying a least squares transformation to the set of CT scanner co-ordinates.

4.1.2 Results

(a) Mask survey using a metrograph

The detailed measurements are shown in Table 4-1. The standard deviation of the x, y, and z readings was calculated for each marker separately.

Table 4-1 Metrograph readings of facemask marker co-ordinates

METROGRAPH READINGS OF THE MARKER POSITIONS ON THE FACE MASK																						
		READINGS (mm)																				Mean
		Marker Number																				
		1	2	3	4	5	6	7	8	9	10	11	12	13	14	15	16	17	18	19	20	
Set 1	x	-14.92	47.10	-59.77	75.13	-51.27	57.18	-73.92	76.64	-75.23	74.44	-54.42	47.94	-67.18	57.93	-45.76	39.59	15.02	3.49	-3.17	-5.08	
	y	191.86	188.46	226.44	220.54	165.10	165.72	221.67	212.97	223.54	217.32	163.77	160.92	207.65	201.97	164.04	169.50	233.57	150.56	123.11	142.78	
	z	135.56	122.10	115.21	104.66	73.49	68.08	63.68	47.29	21.82	15.15	19.43	11.42	-17.19	-32.54	-27.68	-31.71	147.77	72.21	28.81	-49.83	
Set 2	x	-14.86	47.17	-59.29	75.14	-51.29	57.07	-73.88	76.89	-75.64	74.83	-54.25	47.95	-67.37	57.99	-45.65	39.57	14.69	3.73	-3.43	-5.22	
	y	191.55	188.69	226.14	220.26	165.67	165.91	221.98	213.05	222.91	216.53	163.70	160.71	207.21	201.75	163.80	169.21	233.27	149.60	122.96	142.42	
	z	135.73	122.01	115.12	104.79	73.00	67.86	63.36	47.24	21.95	15.47	19.33	11.48	-16.85	-32.42	-27.71	-31.55	147.85	72.72	28.94	-49.59	
Set 3	x	-14.89	46.94	-59.35	75.17	-51.39	57.21	-73.93	77.18	-75.49	75.00	-54.36	47.89	-67.46	58.28	-45.74	39.94	14.94	3.65	-3.19	-5.03	
	y	191.37	188.28	226.19	220.06	165.49	165.74	222.29	212.72	223.46	216.44	163.44	160.77	207.32	201.83	163.97	168.86	233.29	149.93	123.06	142.31	
	z	135.71	122.04	115.15	104.87	73.10	67.85	63.22	47.33	21.81	15.58	19.29	11.42	-16.76	-32.55	-27.77	-31.34	147.70	72.46	28.69	-49.73	
Set 4	x	-14.95	47.09	-59.43	75.06	-51.34	57.07	-73.72	76.50	-75.45	74.54	-54.49	47.99	-67.28	57.85	-45.59	39.46	15.04	3.55	-3.10	-5.04	
	y	192.13	188.30	226.56	219.91	165.57	165.86	222.67	213.30	222.91	216.86	163.63	160.45	207.28	201.67	164.06	169.25	233.15	149.44	123.03	142.43	
	z	135.27	122.08	114.70	104.77	73.03	67.79	62.98	47.14	21.83	15.26	19.35	11.55	-16.71	-32.57	-27.79	-31.77	147.68	72.78	28.78	-49.67	
Mean	x	-14.90	47.07	-59.46	75.12	-51.32	57.13	-73.86	76.80	-75.45	74.70	-54.38	47.94	-67.32	58.01	-45.68	39.64	14.92	3.60	-3.22	-5.09	
	y	191.73	188.43	226.33	220.19	165.46	165.80	222.15	213.01	223.20	216.79	163.63	160.71	207.37	201.80	163.97	169.20	233.32	149.88	123.04	142.48	
	z	135.57	122.05	115.04	104.77	73.15	67.89	63.31	47.25	21.85	15.36	19.35	11.46	-16.88	-32.52	-27.74	-31.59	147.75	72.54	28.80	-49.70	
Standard Deviation	x	0.04	0.10	0.21	0.05	0.05	0.07	0.10	0.30	0.17	0.26	0.10	0.04	0.12	0.19	0.08	0.21	0.16	0.11	0.15	0.09	0.13
	y	0.34	0.19	0.20	0.27	0.25	0.09	0.43	0.24	0.34	0.40	0.14	0.20	0.20	0.13	0.12	0.26	0.18	0.49	0.06	0.20	0.24
	z	0.21	0.04	0.23	0.09	0.23	0.13	0.29	0.08	0.07	0.19	0.06	0.06	0.22	0.07	0.05	0.19	0.08	0.26	0.11	0.10	0.14

The mean of the standard deviations for all 20 fiducial markers is shown in Table 4-2 below. This gives an idea of the precision of a co-ordinate reading obtained on the reflex metrograph. The 99% confidence interval for a single reading is also shown. This shows the range around any co-ordinate reading, within which a repeat measurement will fall 99% of the time.

Table 4-2 Statistics of the metrograph survey of the reference markers on the mask

Metrograph fiducial marker survey statistics	x	y	z	Vector
Mean Standard Deviations for 20 markers (± standard error) (mm)	0.13 ± 0.02	0.24 ± 0.03	0.14 ± 0.02	0.31 ± 0.04
99% confidence interval for a single reading (mm)	± 0.33	± 0.61	± 0.36	± 0.78
Coefficient of correlation of the mean standard deviation against marker co-ordinate.	0.2406	0.3126	0.1688	-

This table indicates for example that, in the x direction, roughly 2/3rds of the readings for each marker were within 0.13 mm of the mean value for that marker and that this value is within the interval 0.11 to 0.15 mm 2/3rds of the time. If a single marker co-ordinate reading is taken with the metrograph, the correct value will be within ± 0.33 mm of this reading 99 percent of the time. The error in the y co-ordinate is almost double that of the other two co-ordinates. The probable reason for this is that the y axis is in the direction of the depth of the mask. This co-ordinate is more difficult to measure accurately by eye on the metrograph than the height and width co-ordinates.

The data of Table 4-1 were also further analysed to check that they were 'well behaved'. For each of the x, y and z co-ordinates, a scatter diagram of the standard deviation for each marker was plotted against the magnitude of the metrograph marker co-ordinate reading for that marker. This method of comparison between two methods of measurement (in this case the marker co-ordinates) is recommended by Altman and Bland (1983) as a powerful way of investigating the data. Two characteristics of the readings can be checked in this way:

- that the points (standard deviations) are randomly scattered, and,
- that there is no correlation between the magnitude of a marker co-ordinate and the precision with which the co-ordinate can be measured.

The regression line of the standard deviations on the mean metrograph value, for the x co-ordinate, is plotted in Graph 4-1. The correlation coefficient r = 0.2406 is not significant at the 5% level (significant value = ± 0.444), indicating that there was no linear inter-dependence of the standard deviations with co-ordinate magnitude. The mean standard deviations of the marker co-ordinates, and the 99% confidence interval of a single reading, taken from Table 4-2, are also shown on this graph.

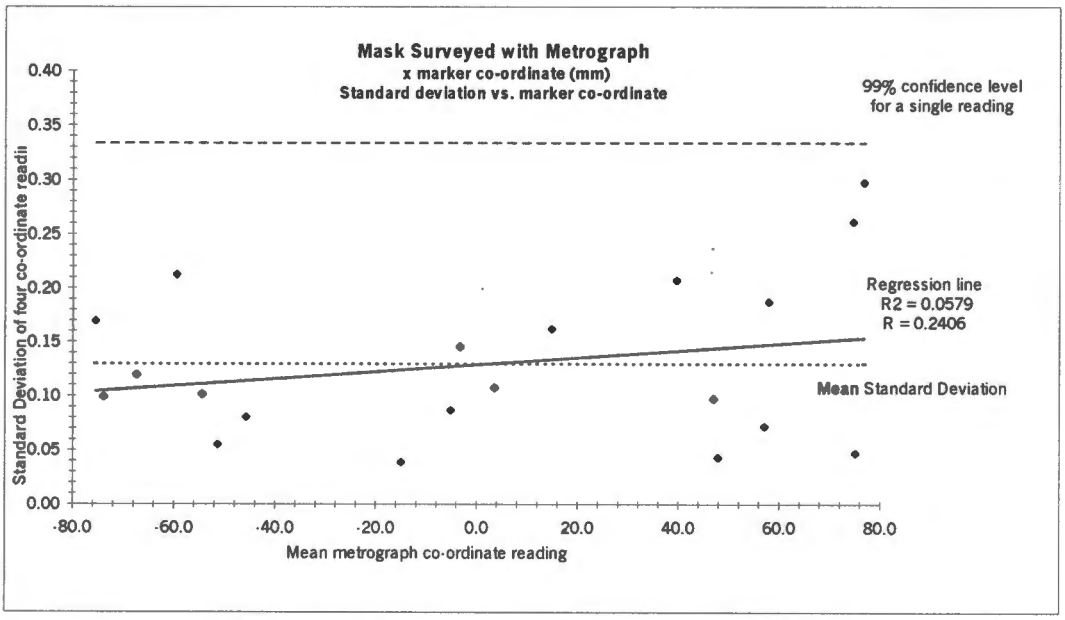

Graph 4-1 X co-ordinate of mask survey

The y and z co-ordinate measurements are shown in Graph 4-2 and Graph 4-3 respectively, and as expected there is also no linear inter-dependence of the deviations with co-ordinate magnitude.

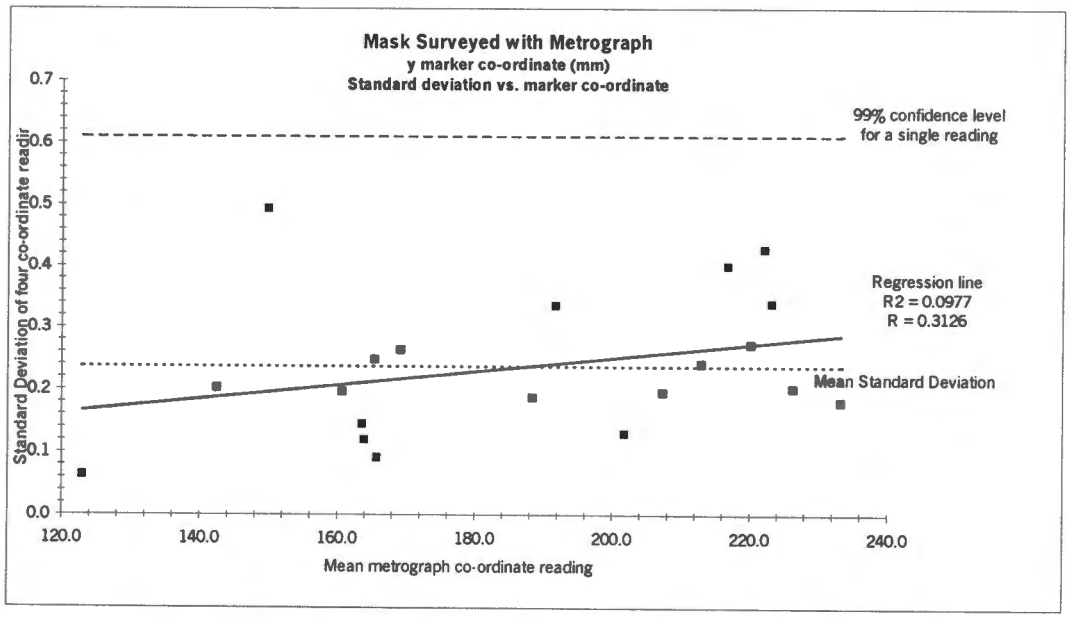

Graph 4-2 Y co-ordinate of mask survey

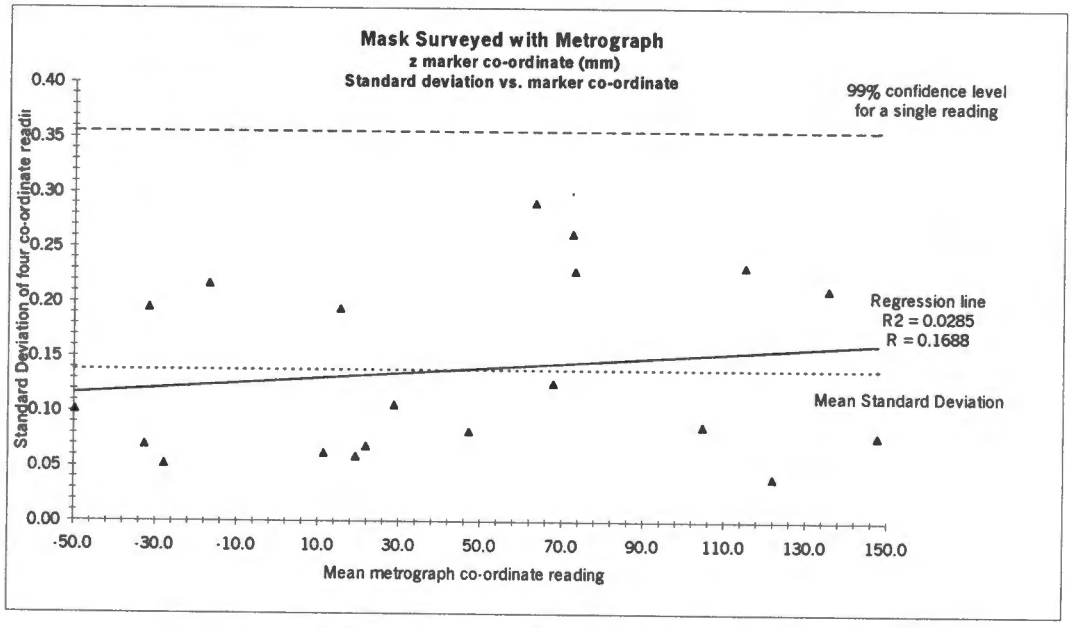

Graph 4-3 Z co-ordinate of mask survey

In summary, the metrograph co-ordinates can be determined to within 0.13, 0.24 and 0.14 mm for x, y, and z respectively (1SD), and the precision with which the co-ordinates can be obtained on the reflex metrograph is uniform over the entire measurement range.

(b) Mask scanned in CT scanner

The detailed measurements are shown in Table 4-3.

Table 4-3 CT scanner readings of facemask marker co-ordinates

CT-SCANNER READINGS OF THE MARKER POSITIONS ON THE FACEMASK (AFTER TRANSFORMATION)																						
		READINGS (mm)																				Mean
		Marker Number																				
		1	2	3	4	5	6	7	8	9	10	11	12	13	14	15	16	17	18	19	20	
Set 1	x	-14.47	48.58	-59.83	75.95	-52.22	57.66	-74.55	77.93	-76.38	75.06	-55.31	48.68	-69.14	58.68	-46.77	39.50	15.61	4.14	-3.41	-5.46	
	y	192.20	189.39	226.43	219.17	166.21	166.18	221.42	212.45	222.74	215.72	163.69	160.96	206.53	201.80	164.57	169.60	232.76	150.67	123.20	142.79	
	z	137.10	122.86	114.48	105.19	72.59	68.84	63.34	47.73	20.51	15.47	18.50	11.34	-18.04	-32.70	-27.91	-31.41	148.16	72.91	28.85	-50.09	
Set 2	x	-15.24	48.42	-59.79	76.99	-51.58	58.39	-74.63	77.68	-76.73	74.93	-55.76	48.20	-68.72	58.75	-46.99	39.44	15.89	3.91	-3.18	-5.75	
	y	192.27	189.59	226.46	219.45	166.28	166.41	221.40	211.66	222.69	215.91	163.67	161.10	206.52	200.96	164.55	169.72	232.94	150.78	123.30	142.82	
	z	135.64	122.77	114.03	105.41	72.72	68.74	62.46	47.64	20.53	15.31	19.10	12.08	-17.81	-32.65	-28.06	-31.45	148.63	72.94	29.40	-49.71	
Set 3	x	-14.79	48.62	-60.49	77.03	-52.02	58.45	-74.81	77.65	-77.28	75.43	-55.28	48.43	-69.20	58.62	-47.58	39.46	15.92	3.90	-2.44	-5.36	
	y	192.87	189.27	225.85	219.14	165.57	165.96	221.62	213.18	222.77	216.36	163.85	160.47	207.51	202.20	163.56	168.93	232.62	151.21	123.63	141.90	
	z	135.81	122.23	114.73	106.05	72.84	69.00	61.63	47.24	20.63	15.04	19.49	12.09	-17.85	-32.62	-28.51	-31.27	148.79	72.94	29.13	-49.67	
Set 4	x	-14.91	48.00	-59.99	75.86	-51.83	58.14	-74.65	77.77	-76.81	75.80	-55.89	48.11	-68.96	58.63	-47.03	39.33	15.95	4.63	-2.54	-5.37	
	y	192.27	189.54	226.39	219.35	166.15	166.30	221.26	212.53	222.49	215.77	164.47	160.91	206.25	201.70	164.29	169.46	232.95	150.70	123.15	142.55	
	z	135.70	123.24	113.69	105.06	73.09	68.98	62.36	47.34	20.97	15.47	18.98	11.20	-17.63	-32.75	-27.92	-31.94	148.84	73.43	29.30	-49.70	
Mean	x	-14.85	48.41	-60.03	76.46	-51.91	58.16	-74.66	77.76	-76.80	75.30	-55.56	48.36	-69.01	58.67	-47.09	39.43	15.84	4.15	-2.89	-5.49	
	y	192.40	189.45	226.29	219.28	166.05	166.21	221.42	212.45	222.67	215.94	163.92	160.86	206.70	201.67	164.24	169.43	232.82	150.84	123.32	142.52	
	z	136.06	122.77	114.23	105.43	72.81	68.89	62.45	47.49	20.66	15.33	19.02	11.68	-17.83	-32.68	-28.10	-31.51	148.60	73.05	29.17	-49.79	
Standard Deviation	x	0.32	0.28	0.32	0.64	0.27	0.36	0.11	0.13	0.37	0.39	0.31	0.26	0.22	0.06	0.35	0.07	0.16	0.34	0.48	0.18	0.28
	y	0.31	0.14	0.29	0.15	0.32	0.19	0.15	0.62	0.13	0.29	0.37	0.27	0.55	0.52	0.47	0.35	0.16	0.25	0.21	0.43	0.31
	z	0.70	0.42	0.46	0.44	0.21	0.12	0.86	0.23	0.21	0.20	0.41	0.47	0.17	0.06	0.28	0.29	0.31	0.25	0.25	0.20	0.32

The mean of the standard deviations of the 20 fiducial markers is reproduced in Table 4-4 below. This represents the precision of a co-ordinate reading. The 99% confidence interval for a single reading is also shown.

Table 4-4 Statistics of the CT scanner co-ordinates of the reference markers on the mask

CT scanner fiducial marker co-ordinate statistics	x	y	z	Vector
Mean Standard Deviations (± standard error) (mm)	0.28 ± 0.03	0.31 ± .03	0.32± 0.36	0.53 ± 0.06
99% confidence interval for a single reading (mm)	± 0.72	± 0.80	± 0.82	± 1.35
Coefficient of correlation of the mean standard deviation against marker co-ordinate.	0.0458	0.1077	0.5121	-

This table indicates for example that, in the x direction, roughly 2/3rds of the readings for each marker were within 0.28 mm of the mean value for that marker and that this value is within the interval 0.25 to 0.31 mm 2/3rds of the time. If a single marker co-ordinate reading is taken with the CT scanner, the correct value will be within ± 0.72 mm of this reading 99 percent of the time. The precision in all three co-ordinate axis directions is similar. The precision in the z direction (couch movement direction) is as good as for the x and y directions despite the 2 mm slice thickness. This may be ascribed to the use of a 1 mm diameter ball bearing for the markers and an accurately calibrated CT laser.

The data of Table 4-3 were also further analysed to check that it was 'well behaved'. For the x co-ordinate, the standard deviation for each marker was plotted against the metrograph marker co-ordinate reading in Graph 4-4 below. The regression line of the standard deviation of the four readings for a marker was plotted on the mean metrograph value for that marker. The correlation coefficient r = 0.0458 is not significant at the 5% level (significant value = ± 0.444), indicating that, as expected, there is no linear inter-dependence of the deviations with co-ordinate magnitude. The mean standard deviation of the differences, and the 99% confidence interval of a single reading, taken from Table 4-4, are also indicated on this graph.

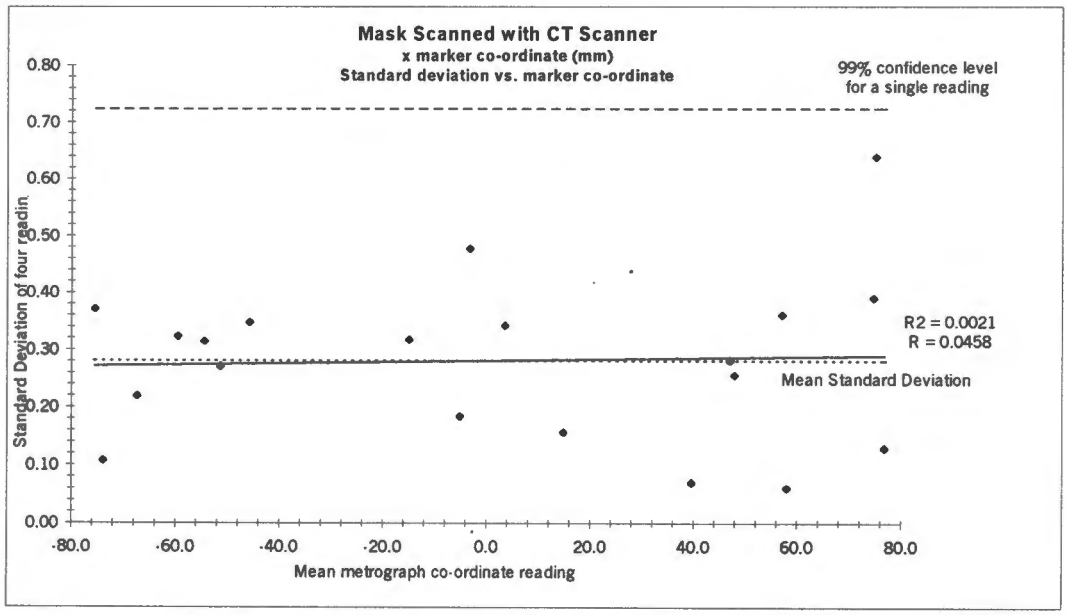

Graph 4-4 X co-ordinate of mask CT Scan

The y and z co-ordinate measurements are shown similarly in Graph 4-5 and Graph 4-6 respectively. There is no linear inter-dependence of the y co-ordinate deviations with the y co-ordinate magnitude, but the z co-ordinate deviations show a significant dependence on the magnitude of z. This seems to be due mainly to marker number one, whose z co-ordinate was more difficult to determine than most other fiducial markers due to its position on the facemask.

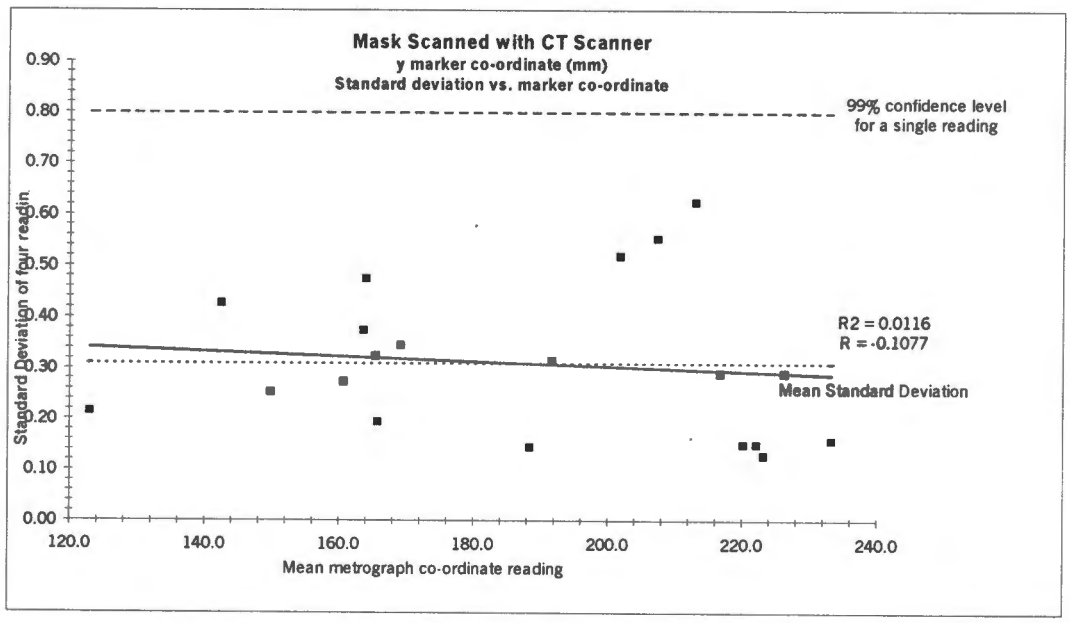

Graph 4-5 Y co-ordinate of mask CT Scan

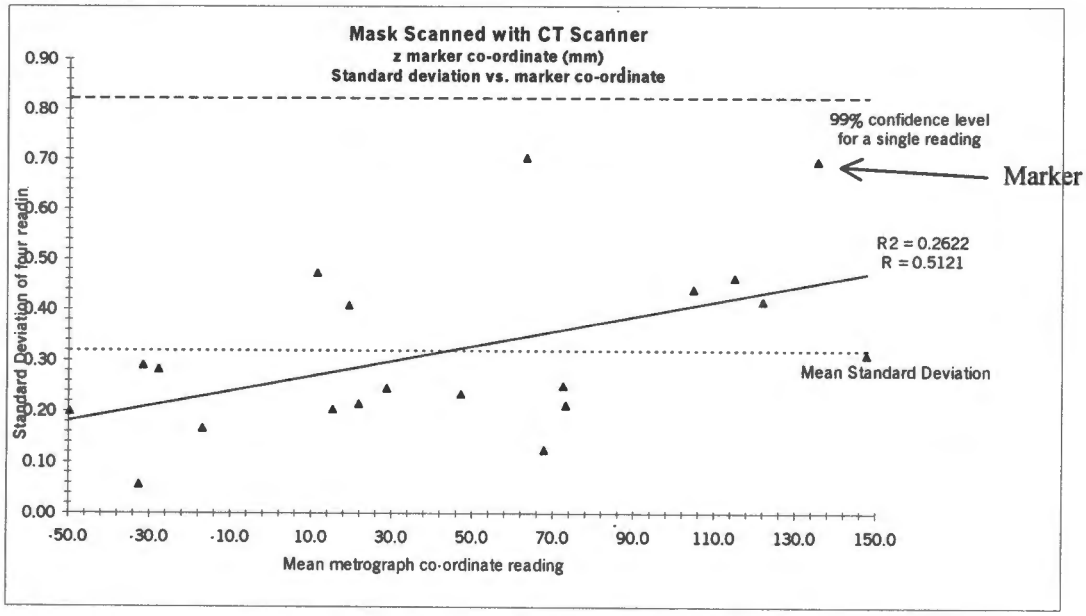

Graph 4-6 Z co-ordinate of mask CT Scan

In summary, the precision with which the fiducial marker co-ordinates can be obtained on the CT scanner is within 0.3 mm for x, y, and z (1SD). This precision is equally good over the whole range of x and y, but for the z co-ordinate, there seems to be more uncertainty in the precision for higher z values.

(c) Total error in fiducial reference markers – analysis of residuals

As the precisions achieved on the metrograph and on the CT scanner are independent variables, the total error is the square root of the sum of the squares of the standard deviations of the metrograph readings (from Table 4-2) and the CT scanner readings (from Table 4-4). For the x co-ordinate, the total standard deviation of independent residuals = $\sqrt{(0.13)^2 + (0.28)^2} = 0.31$ mm. The total standard deviation is shown for each axis in Table 4-6 below, calculated in a similar way.

In a second method of calculating the precision of the CT scanner co-ordinates, the residuals between the 'true' metrograph fiducial marker co-ordinates and the co-ordinates measured on the CT scanner are calculated for each marker in turn, after applying a least squares transformation to the set of CT scanner co-ordinates. The data used and the calculated results are shown in Table 4-5, for each of four sets of CT scanner readings.

Table 4-5 Comparison of the mean metrograph and CT scanner marker co-ordinate readings

RESIDUALS BETWEEN THE MEAN METROGRAPH AND CT-SCANNER CO_ORDINATE READINGS (AFTER TRANSFORMATION) OF MARKER POSITIONS ON THE FACEMASK																						
		READINGS (mm)																				
		Marker Number																				Standard Deviation
		1	2	3	4	5	6	7	8	9	10	11	12	13	14	15	16	17	18	19	20	
Set 1	x	-0.432	-1.504	0.376	-0.825	0.896	-0.533	0.690	-1.136	0.926	-0.361	0.928	-0.742	1.825	-0.671	1.086	0.140	-0.691	-0.537	0.192	0.374	0.87
	y	-0.477	-0.960	-0.103	1.022	-0.759	-0.375	0.729	0.554	0.465	1.069	-0.056	-0.253	0.832	0.000	-0.602	-0.393	0.554	-0.788	-0.158	-0.303	0.63
	z	-1.533	-0.803	0.562	-0.427	0.560	-0.944	-0.036	-0.481	1.343	-0.110	0.846	0.118	1.158	0.186	0.177	-0.182	-0.409	-0.373	-0.044	0.390	0.70
Set 2	x	0.335	-1.352	0.329	-1.872	0.262	-1.265	0.767	-0.879	1.282	-0.227	1.387	-0.261	1.397	-0.744	1.306	0.198	-0.974	-0.310	-0.041	0.661	0.97
	y	-0.547	-1.156	-0.136	0.734	-0.820	-0.606	0.751	1.352	0.515	0.877	-0.041	-0.393	0.847	0.846	-0.586	-0.516	0.376	-0.895	-0.261	-0.342	0.72
	z	-0.073	-0.720	1.008	-0.638	0.430	-0.846	0.852	-0.396	1.322	0.052	0.244	-0.614	0.936	0.136	0.322	-0.144	-0.882	-0.396	-0.603	0.012	0.66
Set 3	x	-0.107	-1.550	1.034	-1.904	0.697	-1.326	0.945	-0.850	1.827	-0.726	0.905	-0.492	1.884	-0.612	1.901	0.180	-0.998	-0.296	-0.779	0.266	1.15
	y	-1.148	-0.841	0.477	1.044	-0.117	-0.152	0.529	-0.171	0.432	0.428	-0.215	0.239	-0.144	-0.397	0.410	0.270	0.699	-1.333	-0.590	0.580	0.63
	z	-0.248	-0.174	0.316	-1.287	0.314	-1.112	1.680	0.005	1.219	0.322	-0.144	-0.623	0.971	0.102	0.775	-0.320	-1.041	-0.397	-0.324	-0.032	0.76
Set 4	x	0.012	-0.932	0.534	-0.743	0.507	-1.007	0.789	-0.970	1.356	-1.096	1.517	-0.171	1.643	-0.623	1.345	0.303	-1.030	-1.028	-0.685	0.279	0.96
	y	-0.540	-1.111	-0.063	0.834	-0.690	-0.492	0.893	0.477	0.717	1.012	-0.836	-0.198	1.113	0.100	-0.320	-0.258	0.371	-0.821	-0.116	-0.072	0.67
	z	-0.130	-1.183	1.354	-0.297	0.061	-1.085	0.949	-0.092	0.879	-0.109	0.361	0.267	0.752	0.230	0.181	0.345	-1.091	-0.888	-0.503	0.000	0.70
Mean	x	-0.05	-1.33	0.57	-1.34	0.59	-1.03	0.80	-0.96	1.35	-0.60	1.18	-0.42	1.69	-0.66	1.41	0.21	-0.92	-0.54	-0.33	0.40	0.99
	y	-0.68	-1.02	0.04	0.91	-0.60	-0.41	0.73	0.55	0.53	0.85	-0.29	-0.15	0.66	0.14	-0.27	-0.22	0.50	-0.96	-0.28	-0.03	0.66
	z	-0.50	-0.72	0.81	-0.66	0.34	-1.00	0.86	-0.24	1.19	0.04	0.33	-0.21	0.95	0.16	0.36	-0.08	-0.86	-0.51	-0.37	0.09	0.71

In this table the mean of the residuals of all the markers is zero because of the minimum least squares rotation algorithm used to rotate the CT co-ordinates. The standard deviations of the mean residuals were calculated from this table, and are summarised in Table 4-6 below.

Table 4-6 Characteristics of the residuals between the mean metrograph and CT scanner marker co-ordinate readings

	x	y	z	Vector
Total Std. Dev. of residuals calculated assuming independent marker positions (see paragraph (c) above) (mm)	0.31	0.39	0.35	0.61
Std. Dev. of mean residuals (from Table 4-5) (mm)	0.99	0.66	0.71	1.39
99% confidence interval (mm)	± 2.55	± 1.71	± 1.82	-
Coefficient of correlation of the mean standard deviation against marker co-ordinate.	– 0.88	0.68	0.43	-
Gradient of regression line ± standard error	– 0.015 ± 0.002	0.012 ± 0.003	– 0.0044 ± 0.0022	-
Gradient significantly different from zero (p = probability level for this happening by chance)	Extremely sig.($p<0.0001$)	Extremely sig.($p=0.00094$)	Not quite sig. ($p=0.0607$)	-

The standard deviations of the mean of the measured residuals for the 20 markers were found to be 0.99 mm, 0.66 mm and 0.71 mm for the x, y and z axes respectively. This represents the error associated with a single reading. Thus for the x axis, we expect the CT co-ordinate of a marker to be in the interval –0.99 mm to +0.99 mm from the true position 2/3rds of the time. The slightly higher value for the x axis than the other two axes is not a result of worse precision in this direction, as this was not reflected in the separate analyses of the metrograph and CT scanner co-ordinates. The scaling error discussed below is a likely cause.

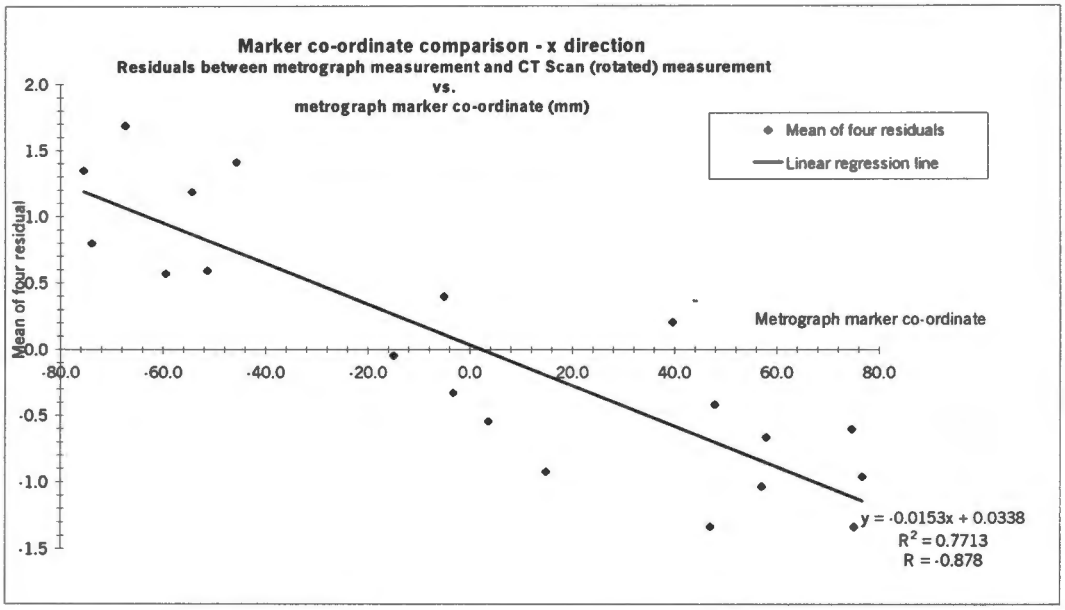

Graph 4-7 X co-ordinate residuals plotted against marker co-ordinate magnitude

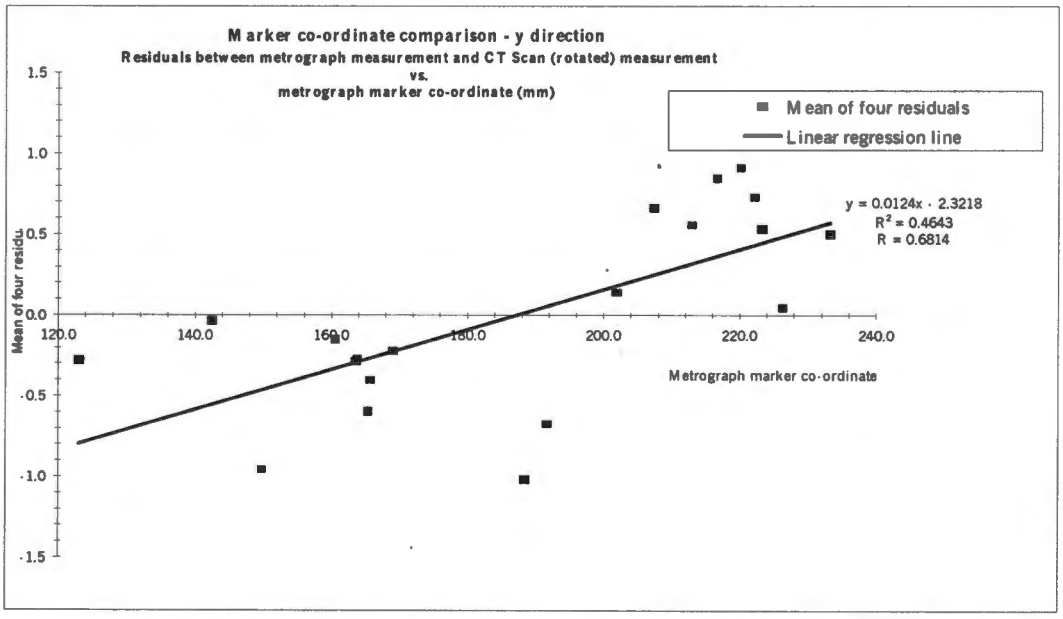

Graph 4-8 Y co-ordinate residuals plotted against marker co-ordinate magnitude

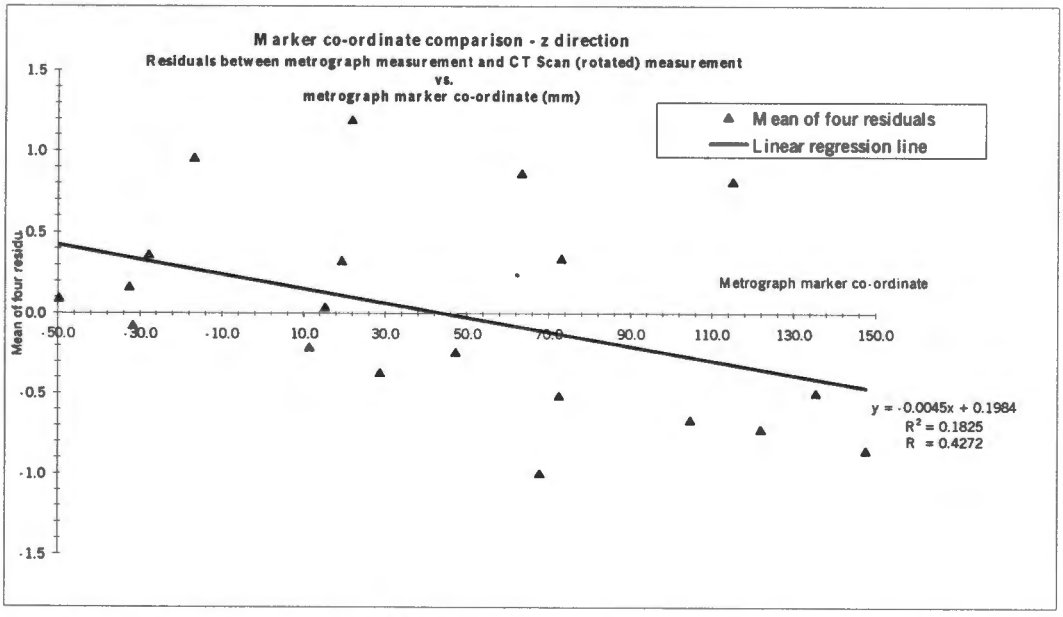

Graph 4-9 Z co-ordinate residuals plotted against marker co-ordinate magnitude

For each axis the standard deviation of the mean of the measured residuals (calculated using the second method) is greater than the calculated standard deviation of the independent residuals (the first method). The differences are 0.7, 0.3 and 0.4 mm for x, y, and z respectively. These differences represent the additional co-ordinating error introduced by the constraint that the fiducial markers on the patient mask must be considered to be a set that are fixed relative to each other. Again, the scaling error described below may be responsible for the difference between the value for the x axis and the values for the other two axes.

The 99% confidence interval of 2.55 mm, 1.71 mm, and 1.82 mm for x, y, and z respectively indicate the difference between a marker co-ordinate reading on the metrograph and the CT scanner in 99% of cases.

The mean of the residuals were plotted for each marker point against the co-ordinate magnitude for each of x, y, and z (Graph 4-7, Graph 4-8 and Graph 4-9 respectively). A linear regression analysis was performed for each co-ordinate. The results are also summarised in Table 4-6 above.

The correlation coefficients of the mean standard deviation against marker co-ordinate magnitude for x, y, and z are – 0.88, 0.68 and 0.43 mm respectively. For the x and y co-ordinate this represents a significant correlation. In addition, the gradient of the regression line for the x co-ordinate of – 0.015 ± 0.002 (1SE) mm is highly significantly different from zero ($p<0.0001$). This is probably due to a systematic scaling error between the CT scanner and the metrograph in the x-direction. For the y co-ordinate, the value of 0.012 ± 0.003 (1SE) mm is also highly significantly different from zero ($p=0.00094$). The y co-ordinate residuals are thus also significantly correlated with the co-ordinate magnitude indicating a scaling error in the y-direction. There is no significant correlation in the z co-ordinate.

4.1.3 Discussion

The fiducial co-ordinates are obtainable by metrograph to precisions of 0.13, 0.24 and 0.14 (1SD) mm and by CT scanner to 0.28, 0.31 and 0.32 (1SD) mm for the x, y and z axes respectively. Both methods show good precision, and when looked at as independent variables result in a vector precision of 0.62 (1SD) mm. When the precision of the CT scanner marker co-ordinates was calculated by analysis of the residuals of the co-ordinates from the metrograph values, the precision was found to be ± 0.99 (1SD) mm, ± 0.66 (1SD) mm and ± 0.71 (1SD) mm for the x, y and z axes respectively. These combine to give a precision vector of ± 1.4 (1SD) mm.

A significant part of the increase from 0.62 to 1.4 mm is probably due to the significant scaling error in the CT axial co-ordinate directions (x and y), i.e. the directions in which the pixel co-ordinates are calculated in the CT scanner algorithms.

For the CT scanner the z axis represents the couch position, and the precision of 0.32 mm shows that the limitation of the 2 mm slice thickness was satisfactorily overcome.

Although these results compare quite well with the target point localisation precisions of about 1 mm quoted by Hartmann (1993) (see Table 2-3), it is instructive to examine the difference more closely. The magnitude of the precision of a single point localisation on the CT scanner depends on several factors:

- the precision with which the absolute co-ordinate values are known (= $\sqrt{(0.13)^2 + (0.24)^2 + (0.14)^2} = 0.31$ mm from Table 4-2),
- the spatial resolution of the CT scanner (pixel size and slice thickness and separation),
- the number of external fiducial references used in the CT localisation technique (done in all stereotactic frames),
- the numeric resolution (number of significant figures) of the readout on the CT scanner scales, and
- the accuracy of the CT scanner linear movements and scales.

Looking in more detail at the paper of Hartmann (1993), a vector precision of single point localisation of $\sqrt{(0.5)^2 + (0.3)^2 + (0.6)^2} = 0.84$ mm was found compared to 1.4 mm found in this work. However, it should be noted that the single point positions were assumed to be perfectly known.

The accuracy and precision with which the CT scanner co-ordinates of the fiducial markers can be obtained has a vital effect on the accuracy of the SPG system. The CT scanners available at the NAC feeder hospitals are also not the most recent models and are far from state-of-the-art machines. Access to the CT scanner system software is completely closed for commercial reasons and there is thus limited scope for improvement. Care was taken to choose scanning protocols with the smallest slice thickness and the smallest field of view possible whilst still able to encompass the head.

The Picker IQ Fast pixel dimension in the scanning mode typically used for proton patients is 0.46875 mm (240 mm ÷ 512). A 2 mm slice thickness is used for obtaining all marker co-ordinates. Thus the maximum possible theoretical error in obtaining CT co-ordinates is $\frac{1}{2}\sqrt{2(0.46875)^2 + (2.0)^2} = 1.03$ mm. The maximum possible error of $\frac{1}{2}\sqrt{2(0.6)^2 + (2.0)^2} = 1.1$ mm (pixel size = 0.6 mm and slice separation = 2 mm) in the paper by Hartmann (1993) is very similar to this value.

The CT scanner table position is reported to the nearest 0.5 mm. Thus the theoretical maximum CT co-ordinate error possible, given the readout resolutions on the scanner scales and provided the table is carefully advanced 0.5 mm at a time to obtain the brightest image, is $\frac{1}{2}\sqrt{2(1.0)^2 + (0.5)^2} = 0.75$ mm.

The procedure of co-ordinate extraction from the CT scanner was investigated. There appears to be no way of obtaining a more precise reading than 0.5 mm for the CT scanner table position. Although the pixel dimension in the axial plane is 0.46875 mm, the resolution of the cursor co-ordinate readout on the CT scanner (x, and y axes) is to the nearest millimetre. A matrix is accessible as a utility on the scanner giving the pixel Hounsfield numbers at each pixel position (0 to 511) vertically and horizontally. By examination of the highest Hounsfield number in the region of a marker, representing its centre, it is possible to find the best pixel position of the marker. By interpolation, the position is obtainable to the nearest half pixel. Finding and converting pixel positions to co-ordinates in millimetres proved an extremely laborious procedure that was prone to mistakes and was not pursued. In addition, the total residual error reported on the SPG system when using a set of marker co-ordinates obtained in this way did not appear to be significantly smaller than with a conventionally obtained set of CT scanner co-ordinates. The SPG total residual error represents the total of the differences between the marker positions found by the SPG cameras, and the positions found on the CT scanner.

The CT localisation technique described by Siddon and Barth (1987) was used in the paper by Hartmann (1993). This makes use of many fiducial marks obtained from external localisation plates attached to the stereotactic head frame. In this way, using several independent fiducials to localise the point, any possible limited resolution of the CT scanner scales may be circumvented. No external fiducials are used in the SPG facemask co-ordinating technique. The CT scale resolution used by Hartmann (1993) is unknown, and no paper amongst those referenced in this

thesis refers to it. One illustration shows the CT scanner cursor co-ordinates given to several decimal places. It is reasonable to suspect that had a CT scanner readout been limited to a resolution of 1 mm, as in the Picker scanner used in this thesis, this would have been mentioned as a problem limiting resolution of the CT scanner co-ordinates. Obtaining all the marker point co-ordinates using only the CT scanner cursor position co-ordinates, as has been done in this thesis, may result in a loss of precision.

A statistically significant scaling error between the Picker CT scanner and the metrograph was detected in the x and y axes. These axes are in the transverse plane and positions on these axes are calculated as part of the CT scanner back projection calculation. Paragraph 8.3.1 below discusses what can be done about this. No error was found in the z axis (representing the CT scanner couch longitudinal movement direction).

In another example, Serago *et al.* (1991) quote a CT localisation precision of $\sqrt{(0.2)^2+(0.4)^2+(0.6)^2}$ = 0.75 mm, also surprisingly small when compared to the 1.39 mm found in this thesis, and also small when compared to the maximum error of 1 mm quoted by Serago *et al.* (1991).

The problem of obtaining accurate CT co-ordinates was addressed by Yue *et al.* (1999) who employ the pilot or scout view CT scan data in addition to the slice data. They state "Because of the finite slice thickness of transverse cuts, the longitudinal co-ordinates are more accurately obtained from the scout views". Although the improved accuracy in the longitudinal plane is clearly demonstrated on an image, no statistical analysis of the resulting accuracy is made.

4.2 The effect on the precision of the CT scanner co-ordinates of the fiducial markers of placing a patient in the mask

4.2.1 Materials and methods

This study, and the study of movement of the patient anatomy inside the face mask described in the following section (4.3), was done before the Picker CT scanner available. The first seven patients treated (palliatively) using protons were scanned in their facemasks prior to treatment on a Siemens CT scanner[13] using a 1 mm slice thickness. The initial intention of the studies was to assess whether the mask had sufficient precision, and the patient movement inside the mask was sufficiently small, to allow the mask to be used for curative (radical) proton therapy.

[13] Siemens DRH CT scanner

The specific intention in this section is to assess the magnitude of the uncertainty introduced into the mask co-ordinating process by the distortions created by the patient within the mask. Unfortunately the empty masks were not able to be co-ordinated on the Siemens scanner due to time constraints. Also repeat measurements of patients undergoing radical treatments could not be made on the Picker scanner. Thus no directly comparable data exists to be able to extract the required loss of precision, and the comparison of the Siemens data with patients in their masks and Picker data with the empty masks is shown for interest, and no conclusion is made.

The scan for each patient was repeated after a week with the patient in a different arbitrary position on the CT scanner table. Marker co-ordinate readings were obtained on both occasions. It was not possible to scan the patients repeatedly to obtain readings several times because actual patients were involved. Also, accurate marker co-ordinates obtained on a metrograph were not known. Under these circumstances, a measure of the precision with which the fiducial markers can be determined, can be obtained from the standard deviation of the residuals between the co-ordinate readings over two weeks (after rotational and translational transformation).

For each patient the set of co-ordinates obtained on the second occasion was rotated by minimum least squares into the frame of reference of the first set. The rotation matrices were retained for use in transforming the bony landmark co-ordinates as described in the next section (4.3).

4.2.2 Results

The first set of readings obtained is shown in Table 4-7.

Table 4-7 CT-scanner readings of the marker positions on patient facemasks in the first week

CT-SCANNER READINGS OF THE MARKER POSITIONS ON PATIENT FACEMASKS IN THE FIRST WEEK																			
Patient		READINGS (mm)																	
		Marker Number																	
		1	2	3	4	5	6	7	8	9	10	11	12	13	14	15	16	17	18	19
1	x	-39.00	-67.00	55.00	-70.00	-50.00	49.00	70.00	-41.00	36.00	5.00	2.00	0.00							
	y	53.00	5.00	58.00	-1.00	44.00	47.00	2.00	16.00	19.00	77.00	84.00	37.00							
	z	664.00	662.50	733.50	704.00	779.00	782.50	763.00	820.50	831.50	681.00	797.00	844.00							
2	x	-57.00	24.00	50.00	-78.00	65.00	-64.00	63.00	-52.00	56.00	-89.00	78.00	0.00	4.00	0.00					
	y	2.00	-5.00	-40.00	17.00	12.00	58.00	52.00	47.00	39.00	-33.00	-30.00	74.00	103.00	89.00					
	z	514.50	496.50	513.50	572.50	544.00	628.50	624.00	683.00	676.50	590.50	574.50	536.50	613.50	683.00					
3	x	44.00	-68.00	75.00	-47.00	74.00	-56.00	46.00	73.00	-49.00	48.00	3.00	0.00	-2.00						
	y	67.00	28.00	19.00	80.00	10.00	50.00	58.00	11.00	17.00	15.00	91.00	82.00	47.00						
	z	726.50	726.00	740.00	795.00	784.50	838.00	844.50	822.50	876.00	880.00	736.00	858.00	907.00						
4	x	55.00	51.00	-60.00	56.00	-53.00	56.00	-78.00	77.00	-62.00	65.00	-77.00	79.00	-62.00	53.00	-5.00	2.00	2.00	4.00	0.0000
	y	52.00	61.00	14.00	7.00	74.00	73.00	8.00	15.00	59.00	62.00	2.00	2.00	29.00	45.00	1.00	65.00	95.00	114.00	87.00
	z	698.00	698.00	678.00	669.00	748.00	746.00	745.00	731.00	808.00	802.00	792.00	799.50	851.50	858.50	640.50	672.00	736.00	796.00	876.00
5	x	40.00	-56.00	69.00	-48.00	49.00	-71.00	71.00	-34.00	41.00	2.00	0.00								
	y	52.00	10.00	24.00	67.00	65.00	7.00	3.00	24.00	22.00	82.00	85.00								
	z	802.50	811.00	833.00	864.00	867.50	888.50	893.00	980.00	971.00	817.50	939.00								
6	x	-46.00	33.00	-75.00	59.00	-48.00	46.00	-67.00	63.00	49.00	-7.00	1.00	3.00							
	y	70.00	65.00	18.00	22.00	67.00	61.00	22.00	19.00	26.00	87.00	78.00	13.00							
	z	790.00	790.00	804.50	799.50	838.00	829.50	845.50	843.00	884.00	804.50	895.50	939.00							
7	x	-48.00	45.00	-77.00	73.00	-44.00	44.00	-72.00	68.00	-62.00	57.00	-80.00	-63.00	-42.00	-1.00	0.00	3.00	3.00		
	y	18.00	17.00	-18.00	-25.00	77.00	79.00	24.00	26.00	62.00	65.00	2.00	22.00	73.00	38.00	80.00	113.00	93.00		
	z	634.00	633.00	664.00	666.00	692.00	694.00	694.00	682.00	749.50	751.50	737.00	797.50	803.00	620.50	662.50	742.50	825.50		

A similar set of readings was obtained after a week, and. the residuals for each marker of the first co-ordinate readings compared to the second set, after rotation into the first set reference frame, are shown in Table 4-8.

Table 4-8 Residuals of CT scanner readings of the marker positions on patients' facemasks – first set minus rotated second set

RESIDUALS OF CT-SCANNER READINGS OF THE MARKER POSITIONS ON PATIENT FACEMASKS – FIRST SET MINUS ROTATED SECOND SET																					
Patient		Marker Number																			Standard Deviation
		1	2	3	4	5	6	7	8	9	10	11	12	13	14	15	16	17	18	19	
1	x	0.55	0.17	0.59	0.11	0.48	0.49	-0.87	0.25	-0.74	-0.25	-0.20	-0.59								0.52
	y	0.42	-0.32	-0.17	0.63	-0.48	0.59	-0.06	-0.64	0.44	-0.42	-0.41	0.42								0.47
	z	0.86	0.14	-0.03	-0.05	0.62	-0.85	-0.50	-0.12	-0.09	-0.01	-0.36	0.38								0.47
2	x	-0.21	0.10	0.86	-0.05	0.25	0.39	-0.45	0.26	-0.54	0.12	-0.88	-0.32	-0.68	1.14						0.57
	y	-0.03	0.16	-0.22	0.22	0.08	-0.62	-0.23	0.52	-0.58	-0.12	0.36	-0.62	0.23	0.85						0.44
	z	-0.32	0.31	-0.59	0.05	-0.30	0.28	0.31	-0.16	0.21	-0.20	0.18	0.36	0.48	-0.61						0.36
3	x	0.43	-0.46	-0.55	0.94	0.19	-0.27	-0.34	0.93	0.55	-1.46	0.30	-0.51	0.27							0.68
	y	-0.22	0.48	-0.80	0.02	0.16	-0.06	0.39	-0.02	-1.18	1.18	-0.13	0.58	-0.41							0.61
	z	1.16	0.79	-0.10	0.76	0.09	0.35	-0.64	0.04	-0.93	-0.68	0.87	-1.97	0.24							0.87
4	x	0.19	-0.68	0.59	0.54	-0.04	-0.08	-0.44	-1.16	1.81	-0.15	0.77	-1.37	-0.45	-1.25	1.82	0.80	0.57	-0.84	-0.62	0.93
	y	-0.33	0.20	0.33	0.01	0.13	-0.31	-0.19	-0.33	-0.37	-0.22	-0.58	-1.35	-0.67	-0.52	0.25	0.12	0.22	0.41	3.18	0.88
	z	1.21	-0.62	-0.99	-0.14	0.85	-0.72	0.59	-0.62	0.75	-3.45	-0.10	0.02	0.88	-0.12	-0.14	0.35	0.20	1.27	0.79	1.07
5	x	-0.15	0.16	1.02	-0.36	0.65	-0.95	0.07	-0.22	-0.20	-0.39	0.38									0.54
	y	-0.44	-0.18	0.72	-0.20	-0.48	-0.40	-0.35	0.72	0.30	0.25	0.04									0.44
	z	-0.92	-0.15	0.08	0.46	0.61	-0.18	-0.45	-0.09	-0.47	1.06	0.06									0.55
6	x	-0.52	0.31	0.05	0.11	-0.54	0.25	1.19	0.07	-0.72	-0.02	-0.19	0.01								0.50
	y	0.61	0.36	-0.71	-0.78	0.07	0.04	0.15	-0.80	0.64	0.24	0.50	-0.31								0.53
	z	0.62	0.88	0.10	-0.55	0.18	-0.98	-0.60	0.54	-0.29	-0.24	0.11	0.23								0.55
7	x	-0.48	0.53	-0.36	-0.33	0.18	0.16	0.41	0.42	-0.85	-0.56	0.25	0.02	0.46	-0.79	0.94	-0.10	0.13			0.50
	y	-1.23	-0.83	0.48	0.57	0.44	-0.77	-0.39	0.38	-0.12	0.42	-0.76	0.54	-0.55	-0.07	0.91	0.19	0.78			0.65
	z	0.62	-0.07	-1.03	-0.74	2.20	1.70	0.89	-0.05	-1.76	-0.93	-0.32	-0.22	0.60	0.54	0.53	0.09	-2.05			1.11
Mean Standard Deviation	x																				0.61
	y																				0.57
	z																				0.71

The standard deviation of these residuals is calculated for each patient. The mean standard deviation, which represents the average precision with which the fiducial markers can be determined on patients, is reproduced in Table 4-9 below.

Table 4-9 Characteristics of the residuals over a one week interval of CT scanner co-ordinates of the fiducial markers on the facemasks of seven patients

	x (mm)	y (mm)	z (mm)	Vector
Mean Std. Dev. of residuals	0.61	0.57	0.71	1.10
99% confidence interval	*1.56*	*1.48*	*1.83*	*2.82*

The mean standard deviation for all seven patients ranges between 0.6 and 0.7 mm for the three axes, and the 99% confidence interval ranges between 1.5 and 1.8 mm. The 99% confidence interval for a single residual is largest for the z co-ordinate, presumably because of manual positioning of the CT table.

4.2.3 Discussion

Mean standard deviation of the residuals between the marker positions over two weeks was found to be a vector of $\sqrt{(0.61)^2 + (0.57)^2 + (0.71)^2} = 1.10$ mm. This represents the average precision with which the fiducial markers can be determined with patients in the mask on the Siemens CT scanner.

Due to lack of time available on the Siemens CT scanner, the empty masks for these patients were not scanned, so that no direct determination of the change in precision is possible. Measurements were obtained using empty facemasks on the Picker CT scanner as described in section 4.1.2(b) above. The two sets are compared in Table 4-10 below to see if there is any change in the precision of determining the fiducial marker positions.

The precision with patients in the mask is expected to be less (*i.e.* have a greater value) than with no patients in the mask due to possible distortion and movement of the masks by the patients during scanning. The opposite trend is shown. This may be ascribed to two factors. Firstly, the

Siemens CT scanner may have better spatial accuracy and precision, and secondly, the spatial linearity of the Picker CT scanner was found to be suspect (especially so in the x direction, but also the y direction).

Table 4-10 Comparison of marker precision with and without patients

MEAN STD. DEV. OF MARKER RESIDUALS	x (mm)	y (mm)	z (mm)	Vector (mm)
No patients (Picker CT scanner)	0.99	0.66	0.71	1.39
With patients (Siemens CT scanner)	0.61	0.57	0.71	1.10

In order to quantify separately the effect of the patients on the marker co-ordinates on the mask, this experiment should be repeated if possible on the Picker scanner. Time and availability of patients did not allow this. For the purpose of estimating the total precision of the marker co-ordinates in this thesis, this effect is taken as zero.

4.3 Movement of the patient anatomy inside the mask in a 7-day period

4.3.1 Materials and methods

Two or three bony landmarks (e.g. Crista galli) were located on each of the patients used in section 4.2 above at the first CT scan session and again located one week later. The same transformation matrices obtained in that section for the fiducial markers were applied to the anatomical points from the second week, and these transformed co-ordinates compared to the corresponding bony landmark co-ordinates obtained in the first week. Bony landmark co-ordinates were obtained for six patients in both weeks.

4.3.2 Results

All bony landmark co-ordinate measurements are shown in Table 4-11. Also shown are the co-ordinate readings of Week 2 after being transformed in rotation using the transformation matrices obtained from the marker positions (as explained above), and the residuals of these from the Week 1 readings.

Table 4-11 Co-ordinates of bony landmarks (mm)

MEASUREMENT TYPE	Patient	Anatomical points									Mean		
		Point 1			Point 2			Point 3					
		X	Y	Z	X	Y	Z	X	Y	Z	X	Y	Z
CO-ORDINATES Week1	1	12	0	728	3	52	741	-	-	-			
	2	5.6	-6.4	587.8	0	49.7	573.7	-	-	-			
	4	1.3	60	744.8	12.7	2.3	748.9	-9.3	1.9	749.2			
	5	13	17.8	871.5	-8.1	0.9	871.1	1.3	53.8	875			
	6	-2.2	57.7	828.8	-44.1	56.8	780.7	-	-	-			
	7	1.7	56.6	698.5	-37	71.9	800.6	-	-	-			
CO-ORDINATES Week2	1	12	0	700	3	52	713	-	-	-			
	2	5.6	-6.4	587.8	0	49.7	573.7	-	-	-			
	4	1.3	60	744.8	12.7	2.3	748.9	-9.3	1.9	749.2			
	5	13	17.8	871.5	-8.1	0.9	871.1	1.3	53.8	875			
	6	-2.2	57.7	828.8	-44.1	56.8	780.7	-	-	-			
	7	1.7	56.6	698.5	-37	71.9	800.6	-	-	-			
CO-ORDINATES Week2 (rotated)	1	11.9	-0.3	728	2.5	51.9	739.7	-	-	-			
	2	5.6	-6.4	587.8	0	49.7	573.7	-	-	-			
	4	1.3	60	744.8	12.7	2.3	748.9	-9.3	1.9	749.2			
	5	13	17.8	871.5	-8.1	0.9	871.1	1.3	53.8	875			
	6	-2.2	57.7	828.8	-44.1	56.8	780.7	-	-	-			
	7	1.7	56.6	698.5	-37	71.9	800.6	-	-	-			
RESIDUALS [Co-ordinates Week1 – Co-ordinates Week2 (rotated)]	1	0.12	0.34	0.04	0.54	0.09	1.31	-	-	-	With point 1 of patient 4		
	2	0.4	0.38	0.16	0.04	0.26	0.78	-	-	-			
	4	(0.67	2.99	0.17)	0.66	0.65	0.39	1.33	1.14	0.69	0.58	0.67	0.67
	5	0	0.25	0.98	0.87	0.09	0.58	0.28	0.85	0.51	(Without point 1 of patient 4)		
	6	1.83	0.66	0.67	0.11	0.17	1.25	-	-	-			
	7	0.25	1.41	0.46	1.03	0.13	1.42	-	-	-	(0.53	0.46	0.66)

By visually inspecting these residuals for each patient in turn, it can be seen that there is no significant correlation found between the movements of the first anatomy point against the second, or third. This means that if there was a relative movement between the mask and the anatomy during the week interval, it is not translational. This also means that all the residuals can be pooled together, and the mean taken, to assess the average error in locating anatomical points week to week for each co-ordinate axis.

The y residual of 2.99 mm for point 1 of patient number 4 can be regarded as an outlier. The results with and without this point eliminated are shown in Table 4-12 below.

Table 4-12 Residuals of bony landmarks

	RESIDUALS OF BONY LANDMARKS	x (mm)	y (mm)	z (mm)	Vector (mm)
With point 1 of patient 4	Mean error of bony landmarks	0.58	0.67	0.67	1.11
	Standard deviation	*0.53*	*0.78*	*0.44*	*1.04*
	99% confidence interval	*1.38*	*2.01*	*1.13*	*2.69*
Without point 1 of patient 4	Mean error of bony landmarks	0.53	0.46	0.66	0.96
	Standard deviation	*0.56*	*0.43*	*0.45*	*0.84*
	99% confidence interval	*1.43*	*1.10*	*1.17*	*2.15*

This shows that the error vector of movement of the bony landmarks over a week was 1.0 ± 0.8 (1SD) mm.

4.3.3 Discussion

The vector error of bony landmark movements over three occasions using six patients was 1.0 ± 0.8 (1SD) mm. This shows excellent accuracy and reproducibility even when compared to the results quoted below from the literature using stereotactic frames, although very special care is required for a well fitting mask.

In a study similar to that done in this thesis, Graham *et al.* (1991) show a worse result using their cellulose mask, but a similar result for the relocatable Gill-Thomas frame, although with a possibly

larger range. These results are summarised in Table 4-13 and were obtained from orthogonal X-radiograph measurements which are typically more precise than CT based measurements.

Table 4-13 Results of study by Graham *et al.*, 1991 Graham *et al.* (1991) of relocation accuracy using bony landmark and 1 mm ball bearing markers on the mask and frame using X-ray films for four patients and 20 repositionings.

	MASK (mm)	RELOCATABLE GILL-THOMAS FRAME (mm)
AP displacement	1.2 (range 1.0 – 1.3)	1.0 (range 0.7 - 1.2)
Lateral displacement	1.8 (range 1.4 – 2.5)	1.0 (range 0.4 - 1.6)
3D Vector assuming zero caudal displacement	2.2	1.4

Using mechanical measurements of the skull repositioning accuracy in the Gill-Thomas-Cosman frame, Kooy *et al.* (1994) found a total vector precision of $\sqrt{(0.35)^2 + (0.52)^2 + (0.34)^2} = 0.71$ (1SD) mm. In the discussion the authors state "The GTC frame has shown excellent relocation accuracy on the order of ± 0.4 mm". This is in each of three directions and 0.71 mm should be used instead for comparison purposes. The results are summarised in Table 4-14 below.

Table 4-14 Results of study by Kooy *et al.*, 1994 Kooy *et al.* (1994), of relocation precision derived for 20 patients from mechanical measurements

	RELOCATABLE GILL-THOMAS-COSMAN FRAME (mm)
Lateral movement	0.35 (range 0.07 – 0.79)
Superior movement	0.52 (range 0.00 - 1.77)
Occipital movement	0.34 (range 0.00 – 1.30)

4.4 The accuracy and precision of the SPG system cameras

4.4.1 Materials and methods

As part of the daily SPG calibration procedure, described in 1.3.2(b) (iv) above, a small check frame whose marker positions were accurately determined by surveying with a theodolite is positioned by the SPG system before any patients are treated. The records kept of the error in alignment between a theoretical target point on this frame and the isocentre were analysed.

103 records for the period May 1996 to December 1996 and 149 for the period January 1997 to November 1997 were analysed. The displacement of the isocentre, as indicated by a theodolite, from the centre of the 1 mm diameter hole at the centre of the check frame was recorded for both the horizontal and vertical axis, for four camera combinations.

The deviations were measured in only the two orthogonal directions perpendicular to the beam vector, as explained in 3.2 above, and the third error, in the direction of the beam, was ignored as small deviations are not important for proton therapy.

4.4.2 Results

The data were superpositioned in Figure 4-3 below to show the distribution of the isocentre positions within the 1 mm diameter hole at the centre of the check frame. There appears to be some systematic error in the data. The summarised data are shown in Table 4-15 below. The accuracy of positioning the check frame varied between the camera combinations and there was a consistent systematic bias in the negative vertical direction averaging 0.21 mm. The accuracy of the SPG system was found to be 0.36 mm, and the precision was found to be 0.17 mm.

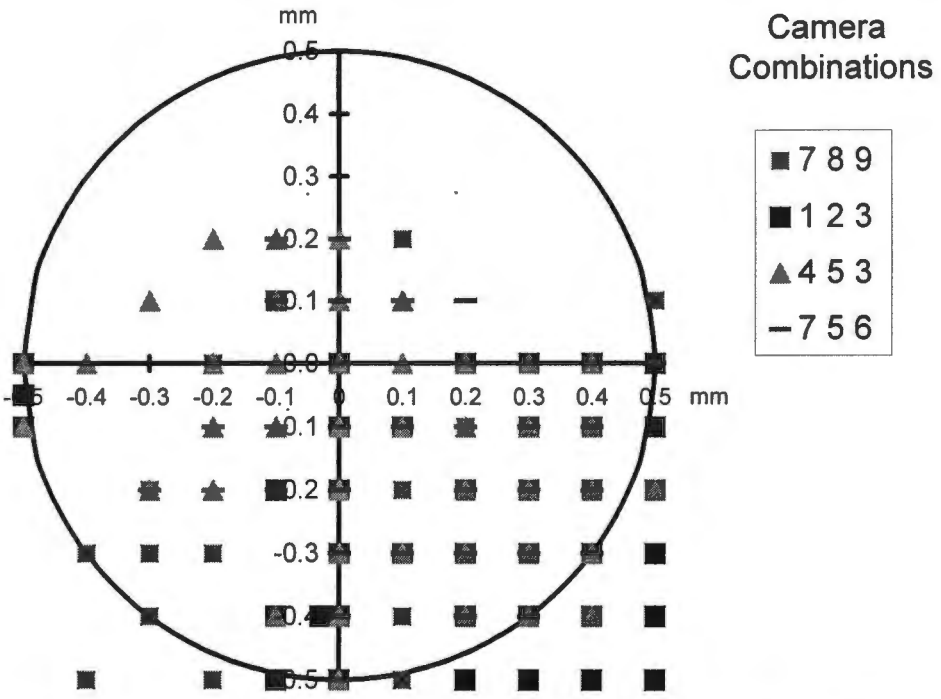

Figure 4-3 Positions of the isocentre as seen through a theodolite within the 1 mm diameter check frame positioning hole. Each position shown represents at least one observation.

Table 4-15 Displacements of the centre of the SPG system check frame from the treatment room isocentre recorded daily before treatment (mm)

Camera combinations	7 8 9		1 2 3		4 5 3		7 5 6		All combined
	Hor	Vert	Hor	Vert	Hor	Vert	Hor	Vert	Vector
Mean	0.07	-0.36	0.10	-0.32	-0.10	-0.09	0.10	-0.05	0.36
Std. Dev.	*0.21*	*0.13*	*0.29*	*0.14*	*0.32*	*0.18*	*0.17*	*0.16*	*0.17*

4.4.3 Discussion

No attempt was made to correct for the systematic error because it was considered small in relation to the other errors of the system. A possible reason for this error is a calibration error occurring in the use of the large camera calibration frame for determining the camera positions (see section

1.3.2(b)(iv) above); possibly an incorrect alignment of the calibration frame centre with the room isocentre.

The precision of 0.17 mm indicates good repeatability of positioning by the SPG system. In order to confirm these measurements, it was also possible to analyse further the positioning accuracy measurements of the mask and the specially designed patient frame, as recorded in Table 3-1 and Table 6-8. The standard deviations found are repeated in Table 4-16 below.

Table 4-16 Standard deviations (precisions) of the distances of the tumour reference point from the isocentre after positioning with the SPG system (mm)

	MASK				FRAME			
	SET ONE		SET TWO		SET ONE		SET TWO	
	Superficial	Deep	Superficial	Deep	Superficial	Deep	Superficial	Deep
	0.17	*0.28*	*0.00*	*0.13*	*0.05*	*0.00*	*0.05*	*0.18*
Mean	*0.23*		*0.09*		*0.025*		*0.115*	
Mean	0.16				0.07			
Mean	0.12							

The standard deviations for each set of readings are very small. This may reflect the limited measurement resolution of the method using the theodolite and concentric rings. The standard deviations are also rather inconsistent in that the precision of the mask in Set One was much worse than that of the frame, but was slightly better than the frame precision in Set Two. However, on average it appears that the precision has been influenced by the fiducial marker support structure, and, for the frame, is about half the value for the mask. This possibly reflects

- the better imaging capabilities of a retroreflective spheres as used on the frame compared to the discs used on the mask since the spheres always present a circular face to the cameras, and
- the better mechanical rigidity of the frame over the mask.

After consideration of the overall mean SPG precision, as shown in Table 4-16 to be 0.12 mm, and the value of 0.17 mm found from the check frame analysis, a rounded average value of 0.2 mm will be used as an estimate of the precision of the SPG system, irrespective of the fiducial support

structure used. This indicates that the SPG system is able to position a given point with a precision of better than 0.2 mm which is more than adequate for proton patient positioning.

Menke *et al.* (1993) report the accuracy and precision that is achievable by their SPG system. They found an average repositioning error for two patients of $\sqrt{(0.9)^2 + (0.8)^2 + (0.9)^2}$ = 1.50 mm and a immobilisation accuracy (sic) (calculated as the standard deviation of the distribution of positioning errors, this is actually the precision according to the definition in section 2.5.2 above) for one patient of $\sqrt{(0.122)^2 + (0.061)^2 + (0.054)^2}$ = 0.147 mm. The authors state that this measurement should not be extrapolated to imply that a similar precision for localising a beam isocentre using a set of fiducial markers attached to a bite block can be achieved.

Rogus *et al.* (1999) quote a system precision of less than 0.1 mm and an accuracy of 0.5 mm across the 40 cm wide camera field of view for each orthogonal direction. These values can be compared to the values of 0.17 mm and 0.36 mm, for precision and accuracy respectively, found above for the check frame. The difference may be due to the fact that for precision, they quote a camera calibration precision that does not test the positioning ability of the system, and that for accuracy, they have investigated the entire camera fields of view, which was not done in this thesis.

4.5 Estimate of total SPG positioning error

An estimation of the precision, or total standard deviation of the error vector between the correct tumour position and the treatment isocentre as found by the SPG system, for patients treated with the facemask can be calculated by adding the precisions found in sections 4.1 (CT scanner co-ordinates of the mask markers), 4.2 (effect of the patient on the mask marker co-ordinates), 4.3 (movement of the patient anatomy) and 4.4 (SPG system cameras) in quadrature, *viz.* $\sqrt{(1.39)^2 + (0)^2 + (0.8)^2 + (0.2)^2}$ = 1.6 (1SD) mm. Thus, assuming no systematic error, about two thirds of patients treated using the facemask, will be irradiated within 1.6 mm of their prescribed tumour reference points, while 95% of patients will be irradiated to within 3.2 (2SD) mm of the prescription point. Stated in another way, a planning target volume (PTV) drawn with a margin of 4.1 (2.56SD) mm around the CTV will ensure that in 99 % of patients the complete CTV will be irradiated.

5 Decreasing the Time to Set-up Patients in the Treatment Room

Four studies were done with a view to reducing the patient set-up time in the treatment room. Two areas of improvement in the current SPG system are investigated below, *viz.* the software, and the target illumination. The effect on the positioning accuracy of reducing the number of markers was also investigated, and lastly the behaviour of the chair movements as the final patient position -was approached was analysed.

5.1 Streamlining the current SPG software system

5.1.1 Materials and methods

Several logical flow problems in the SPG system were identified. In addition a facility to remove problematic individual markers from being used in the positioning process via software was identified as being important to aid in eliminating positioning delays. Some reasons for problems with markers were that they could be very oblique to the cameras and be barely visible at the thresholding level; or there could be a relatively large CT co-ordinate error for the marker which causes the SPG matrix transformations to fail.

The program is written in 'C' code. Source code printouts were obtained for most of the program modules. A schematic diagram of the SPG computer system subroutine calling structure is shown in Figure 5-1 below for the modules directly concerned with positioning and monitoring.

The relevant modules to be altered were identified. The necessary coding and flow changes were made and the program was re-compiled and extensively tested. The existing version was kept as a backup.

In addition to flow corrections, and facility to remove individual markers, some new features were added, two program errors were corrected, and all compiler warnings (mostly data type definitions) were eliminated. The changes made are briefly described in Table 5-1 below.

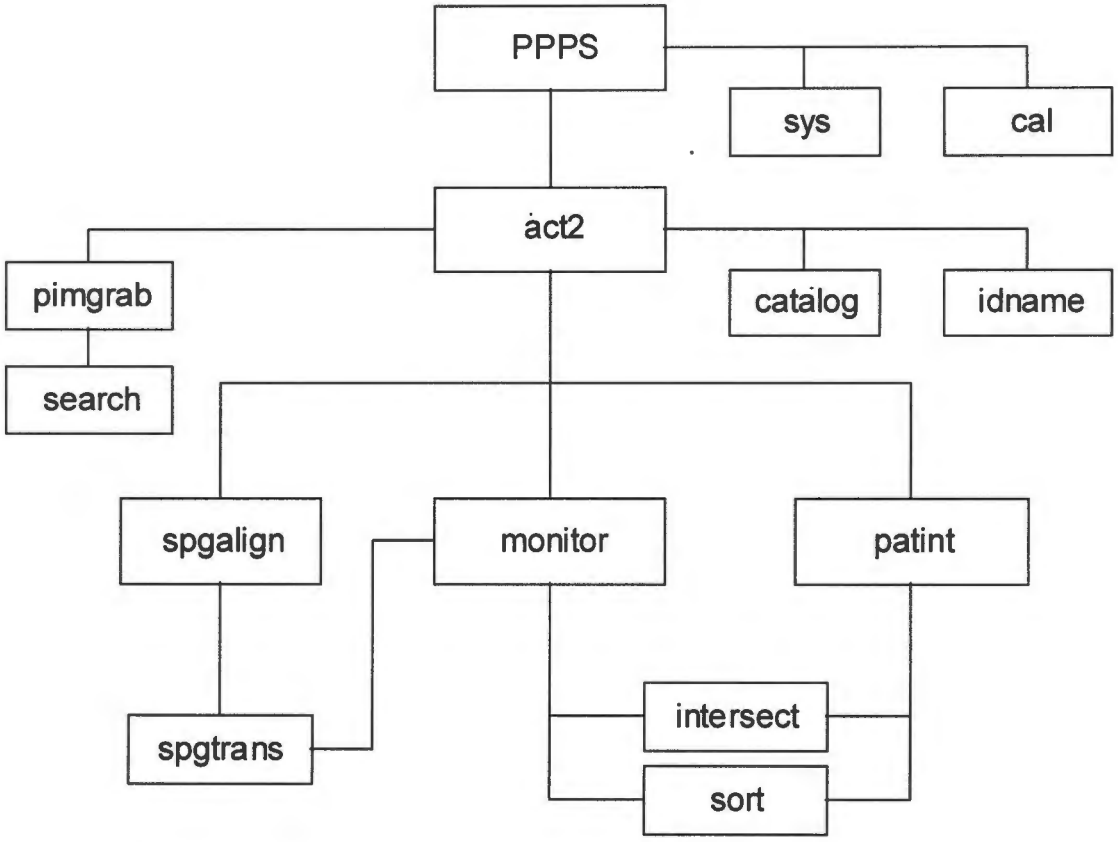

Figure 5-1 SPG computer system subroutine calling structure

Table 5-1 Alterations made to the SPG computer system

PROGRAM MODULE	CHANGE
act2	Flow improvements: Allow exit if beam data not found for specified patient Allow continuation with next beam for curent patient Allow new patient
Spgalign	Add option to check and adjust tolerances Move decision if patient in position to this module from act2
Spgtrans (does Rodrigues transformation of camera co-ordinates)	Add provision to delete a marker from observation To aid in positioning difficulties: Add display of number of cameras (2 or 3) a marker was observed with in the previous cycle Display a "change indicator" for quick assessment of additional or missing markers, or different number of camera observations Add a facility to optionally inspect the transformation parameters (including the sample standard deviation of all residuals)
Intersect	Distinguish between a singular matrix and "no convergence" error for reporting in module patint
Patint	Out of bounds loop found and corrected
Monitor	Out of bounds loop found and corrected
All modules	Add variables containing old positioning information to relevant modules Eliminate all compiler warnings

5.1.2 Results

Six modules were substantially altered, and the program was fully implemented and is in satisfactory daily use.

5.1.3 Discussion and recommendations

The software development environment was very restrictive, as the computer was able to run only a very basic C compiler/debugger. In addition, it is not possible to develop the software on another computer as the graphics card and other hardware components are required for the program to run.

5.2 Improving target illumination

5.2.1 Materials and methods

Infrared diodes were mounted on a ring surrounding each camera lens. These were already in place, but had not been put into use. Standard photographic high quality infrared filters were obtained, and the sheets were cut out into discs to fit each lens. Most are held in place by the polarised, clear, protective lens covers.

5.2.2 Results

The filters reduce the amount of available light, but by opening the apertures fully, the retroreflective fiducial markers are sufficiently visible. The depth of field of the cameras was thus reduced, resulting in possible lack of focus of the fiducial markers. No immediate effect on the residual errors and overall accuracy was noticed.

In order to assist the SPG computer system to identify the fiducial markers on the video image, the image is thresholded by the operator such that only the marker reflections appear. A small disadvantage of the reduced intensity images is that the background is darkened. The fiducial markers' identification numbers are consequently more difficult to identify on the patient's facemask. However, this problem can be overcome as the 'F3' button on the SPG system computer allows the image to be viewed without thresholding, and is convenient to use.

5.2.3 Discussion

It was thought that infrared lamps with higher luminosity may be preferable to diodes, but these have not been necessary so far. By introducing the infrared diode target illumination, there has been a marked reduction in erroneous marker identification due to stray reflections. In addition, the patient position monitoring during irradiation can also now be done with gas discharge lamps fully illuminating the room. The patients are much more comfortable in a well-lit room.

5.3 Reducing the number of reference markers on the mask

5.3.1 Materials and methods

The following experiments were performed to test the dependence of the positioning algorithm on the number of fiducial markers used for positioning by the SPG system.

A mask was made of an anthropomorphic head phantom[14] in the way currently done for patients, with 15 steel sphere markers. The mask was positioned on the patient chair using the SPG system. The number of fiducial markers on the mask was gradually reduced by covering each successive marker, chosen at random, with matt black tape. The angular horizontal and vertical deviations of the tumour reference points on the mask from the isocentre, as measured with a theodolite, were recorded. A calibration factor for converting readings in degrees into millimetres was found by measurement, and all readings were converted. Two readings were taken by moving the chair away from the alignment position between readings. The mean values are shown in the results below.

The above experiment was repeated using both the modified mask (Figure 3-1) and the check frame in order to test whether there was any difference in positioning accuracy between these two devices. For each of these devices two different arbitrary points were chosen as the intended tumour point, and a different set of cameras was used for the SPG system This was done to test consistency in the behaviour of the deviation vector.

The conversion of the theodolite angles into distances was found by taking the angle subtended at the theodolite by the ends of a 5 mm long line that was placed at the isocentre perpendicular to the direction of view along the beam line.

5.3.2 Results

The angular spread of the 5 mm line was found to be = 0° 6′ 24″.

Thus 1 mm = 0° 6′ 24″÷5 = 0° 1′ 18.8″ = 0.021333° = 1.28′.

Theodolite reading at the isocentre (zero):	Vertical:	90° 0′ 0″
	Horizontal:	0° 0′ 0″

The deviation readings using the Rando Phantom head with mask, with all eight fiducial markers used, are shown in Table 5-2 below. The mean residual vector is obtained from the SPG system and

reflects the mean vector value of the residuals of all the visible fiducial markers positions found by the SPG system, and their positions found on the CT scanner. The conversion to millimetres of the angular deviation of the tumour reference point from the isocentre is also shown.

Table 5-2 Typical theodolite readings for one of eight markers used

	Vertical	Horizontal	Mean Residual Transformation Vector on SPG system (mm)
Measured Theodolite Angle	90° 0′ 00″ 90° 0′ 06″	0° 2′ 40″ 0° 2′ 48″	0.91 0.87
Mean	90° 0′ 03″	0° 2′ 44″	0.89
Less zero reading	90° 0′ 00″	0° 0′ 00″	
Deviation from isocentre	3″	2′ 44″	
	0.06 mm	2.1 mm	

A summary of all the measured deviations using the Rando Phantom head with mask is shown in Table 5-3 below.

Table 5-3 Deviations of tumour reference point from the isocentre using the Rando Phantom head with mask

No. of markers used	Mean Residual Transformation Vector on SPG system (mm)	Deviation (mm)		
		Vertical	Horizontal	Vector
8	0.89	0.06	2.1	2.1
7	0.85	-0.5	2.0	2.1
6	0.84	-0.4	1.5	1.6
5	0.76	-0.1	1.4	1.4
4	0.60	-0.5	0.1	0.5
3	0.48	-0.6	0.2	0.6

[14] RANDO, The Phantom Laboratory, Salem, NY, USA.

Unexpectedly the deviation vector decreases from 2.1 mm with all eight fiducial markers to 0.6 mm with 3 fiducial markers. This implies that the fewer the number of fiducial markers used the better the accuracy of positioning the tumour reference point! This could only logically be true if the marker points which were eliminated were also co-incidentally those whose positions were most inaccurately known. The mean residual transformation vector obtained from the SPG system computer also diminishes as the number of fiducial markers used decreases. This would also seem to confirm that the fiducial markers with the most inaccurate CT scanner co-ordinates were eliminated first. However, when the order in which the markers were eliminating was changed, there was no change in the general pattern of decreasing deviations as the number of markers decreases.

Unfortunately the standard deviation of the mean residual vector is not known. This statistic would presumably increase as the number of fiducial markers decreases, thereby indicating the expected loss of positional precision.

The summary of all the measured deviations of the tumour reference point 1 from the isocentre, using the sample mask is shown in Table 5-4 below.

Table 5-4 Deviations of tumour reference point 1 from the isocentre using the modified patient mask

No. of markers used	Mean Residual Transformation Vector on SPG system (mm)	Deviation (mm)		
		Vertical	Horizontal	Vector
8	0.93	0.6	2.0	2.1
7	0.84	0.5	1.6	1.7
6	0.64	0.5	0.9	1.0
5	0.42	0.7	1.4	1.6
4	0.23	0.9	0.9	1.3
3	0.23	0.9	0.8	1.2

Although once again there was an unexpected general decrease in the deviation as the number of markers decreased, the removal of the sixth marker (5 markers used) increased the positioning error.

The summary of all deviations using the same sample mask as above, but with a different tumour reference point and different positioning cameras, is shown in Table 5-5 below.

Table 5-5 Deviations of tumour reference point 2 from the isocentre using the modified patient mask

No. of markers	Mean Residual Transformation Vector on SPG system (mm)	Deviation (mm)		
		Vertical	Horizontal	Vector
11	0.97	1.7	0.3	1.7
10	0.81	1.5	-0.2	1.5
9	0.66	0.7	-0.9	1.1
8	0.52	0.1	-1.3	1.3
7	0.42	1.6	-0.4	1.6
6	0.37	1.6	-0.4	1.6
5	0.29	1.3	-0.4	1.4
4	0.18	1.3	-0.7	1.5

In this case the deviation vector increased and decreased randomly as the markers were eliminated indicating that the positioning accuracy depended on exactly which markers were used by the SPG system rather than the total number of markers used.

The summary of the deviations of the tumour reference point 1 using the check frame is shown in Table 5-6 below.

Table 5-6 Deviations of tumour reference point 1 from the isocentre using the check frame

No. of markers	Mean Residual Transformation Vector (mm)	Deviation (mm)		
		Vertical	Horizontal	Vector
6	1.59	-0.7	0.0	0.7
5	0.60	-0.5	-0.2	0.5
4	0.16	-0.9	-0.5	1.0
3	0.08	-0.9	-0.6	1.1

The positioning markers were accurately co-ordinated on the check frame. The deviation vector decreased when the sixth marker was removed, implying that this one may have been less well positioned by the SPG system. The positioning became progressively less accurate as the fifth and fourth markers were removed.

The summary of all deviations using the check frame but a different tumour reference point and with different positioning cameras is shown in Table 5-7 below.

Table 5-7 Deviations of tumour reference point 2 from the isocentre using the check frame

No. of markers	Mean Residual Transformation Vector (mm)	Deviation (mm)		
		Vertical	Horizontal	Vector
6	1.59	-0.7	0.0	0.7
5	Not recorded	-0.7	0.2	0.7
4	1.57	-0.9	0.2	0.9
3	1.30	-0.6	0.5	0.8

This experiment shows little change in deviation as the number of markers used was reduced from 6 to 3.

5.3.3 Discussion and recommendations

To summarise the results, with the Rando phantom and starting with eight visible markers, the measured deviation vector decreased from 2.1 mm to 0.6 mm when using three markers. The mean residual vector decreased from 0.89 to 0.48 mm. A similar pattern of a reducing deviation vector as the number of visible markers is reduced was also seen for the mask. For the check frame the deviation increased using point 1, and stayed much the same in using point 2. The mean residual vectors decreased from 1.6 mm to 0.08 mm in the first case and changed little in the other.

These results show no consistent pattern. Only when using the check frame did reducing the number of observed markers result in an increased positioning error. All markers on the check frame have been very well co-ordinated, and the deviation vector was small to start with (of the order of 0.7 mm).

With the sample mask there were occasions when the deviation increased, as expected, after an individual marker was removed. Generally, though, the deviation vector decreased when fewer markers were used as was the case with the Rando phantom, and changing the order of removing the markers had no effect on this general pattern. A possible reason is that the algorithm used in the SPG program is either relatively weak at handling many points whose mean residual vector is large, or is incorrectly coded. Another result pointing to a possible faulty algorithm is that the mean residual vector obtained from the system always decreases dramatically as the number of markers is decreased, even in the isolated cases on the mask when the removal of a marker caused the deviation vector to increase.

In summary, this experiment shows little change in deviation as the number of markers used decreased from 6 to 3 suggesting that it may not be necessary to use more than say 4 markers for any given field.

5.4 Investigating apparent errors in chair movements

5.4.1 Materials and methods

The reproducibility of overall positioning by the SPG system was tested by varying only the initial position of the specially constructed mask (see Figure 3-1) prior to allowing the SPG system to position the tumour reference point.

The starting point was placed successively at each corner, A, B, C, etc. of a cube centred at the isocentre (see Figure 3-2 above), so that the direction of approach to the isocentre was different each time. In this manner any possible positioning error consistent with the direction of approach could be observed. The measurements were repeated using the frame (see Figure 6-4 below). The SPG system was set to a tolerance of a maximum deviation of 1 mm of the entry point position from the isocentre.

The radial deviation of the tumour reference point from the tumour reference point, as seen through a theodolite and estimated from the marker rings, was recorded after one SPG cycle. This intermediate distance is thus only measured in a plane perpendicular to the beam. The readings were taken on two occasions separated by about one month, at the same time as the measurements used in Chapter 7.

5.4.2 Results

The tabulated measurements are shown in Table 5-8 below. In most cases the mask was brought into position in two cycles of the SPG system, and in all other cases in three.

Table 5-8 Distances (mm) of superficial and deep tumour reference points of the mask from the isocentre after one SPG positioning movement.

The starting positions of the mask, represented by ◎ , relative to the isocentre, □ , are shown, and the positions of the isocentre relative to the tumour reference point are shown at this position. The arrows, – ⇒, show the direction of the isocentre from the tumour when its position is too far to be shown on the diagram.

				Distal to isocentre				Proximal to isocentre					
Direction of starting position from isocentre (see Figure 3-2 above)				A	B	C	D	E	F	G	H	Mean	Standard Deviation
				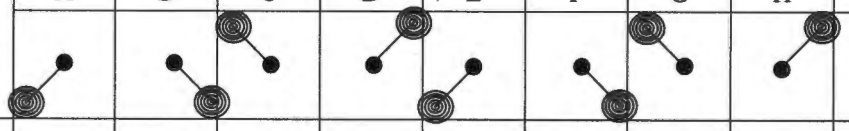									
MASK	SET ONE	Superficial	Distance	-	-	-	-	6.00	6.00	4.00	4.50	5.13	1.03
			Position	Not recorded	Not recorded	Not recorded	Not recorded	Not recorded				Final Position	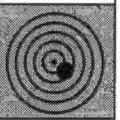
		Deep	Distance	-	-	-	-	-	-	-	-	-	-
			Position	Not recorded	Not recorded	Not recorded	Not recorded	Not recorded	Not recorded	Not recorded	Not recorded	Final Position	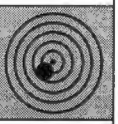
	SET TWO	Superficial	Distance	5.50	6.00	2.50	8.00	6.00	5.50	3.50	4.50	5.19	1.69
			Position						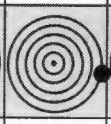		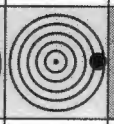	Final Position	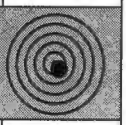
		Deep	Distance	3.00	7.00	8.00	8.00	3.50	4.00	8.00	5.00	5.81	2.17
			Position				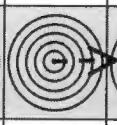					Final Position	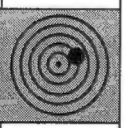
FRAME	SET ONE	Superficial	Distance	2.20	3.00	1.50	3.50	5.00	5.00	3.50	4.00	3.46	1.24
			Position	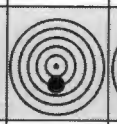								Final Position	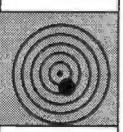
		Deep	Distance	2.70	4.50	2.20	3.20	5.00	6.00	3.00	4.00	3.83	1.29
			Position									Final Position	
	SET TWO	Superficial	Distance	5.00	5.00	1.50	4.00	8.00	7.00	2.50	4.50	4.69	2.14
			Position									Final Position	
		Deep	Distance	5.00	6.00	3.00	5.00	10.00	5.00	4.50	3.00	5.19	2.20
			Position									Final Position	

As summarised in Table 5-9 below, the intermediate distance between the isocentre and the tumour reference point was essentially the same for both measuring occasions for the mask (mean = 5.38 mm), irrespective of whether the tumour point was superficial or inside the mask. The mean intermediate distances for the frame were significantly different on the two measuring occasions. The mean intermediate distance for the frame is 4.47 mm. On the occasion when complete measurements were made (Set Two), the intermediate distance of the frame was 0.6 mm closer to the isocentre than mask for the deep tumour point, and 0.5 mm closer for the superficial tumour point.

Table 5-9 Intermediate positioning distances between the isocentre and the tumour point (mm)

		MASK		FRAME	
		Superficial	Deep	Superficial	Deep
SET ONE	Mean	5.13	-	3.46	3.83
	Std Dev	*1.03*	-	*1.24*	*1.29*
SET TWO	Mean	5.19	5.81	4.69	5.19
	Std Dev	*1.69*	*2.17*	*2.14*	*2.20*

5.4.3 Discussion and recommendations

The intermediate position from the isocentre of the mask and frame tumour point before moving to within the given tolerance of the isocentre was between 3.5 and 5.8 mm. It is not known why the first movement of the chair is not closer to the isocentre. It results in lengthening the SPG positioning process unnecessarily, and should be eliminated if possible. Possible areas of investigation could be the accuracy of the chair movements or the design and accuracy of the SPG computer system algorithm.

It was also noted that the intermediate positions of the mask (a few were not recorded) were all on a straight line joining the starting position and the final position. This implies a well-behaved or

consistent SPG positioning algorithm, although the possibility of the existence of an initial systematic error as implied in the previous paragraph still remains.

In summary, there appears to be a small decrease in intermediate distance for the frame, which may result in a small increase in accuracy of, and efficiency in, obtaining the final position. Of more concern however is the fact that the intermediate position is so far away from the isocentre.

6 Simplifying the Patient Immobilisation and Positioning Procedures

In traditional radiotherapy it is common that the method used to immobilise the patient is also used to position (or localise) the patient. The reason for this is convenience, especially if a mask is used, in that the fiducial markers used to position the patient are placed on the mask, the latter also being used to hold the patient in place. This is the case with the current proton facemask, except that a certain separation of function is achieved by having a separate posterior section, used for fixation purposes, and anterior section, used for marker placement. In designing an improved system, it was found useful to conceptually separate the patient immobilisation function from the fiducial marker support function.

Structures upon which the fiducial markers could be supported were developed and evaluated, and ways in which the structure could be held in a fixed relationship to the patient's anatomy were also developed. Although clearly interrelated, there are two separate aspects to this:

- the spatial configuration of the fiducial reference markers, and,
- the means of fixing the fiducial marker matrix to the patient.

These are dealt with separately below.

Once a means of fixing the marker support structure to the patient anatomy is found, it is tempting to use this also to support or immobilise the patient. Such a method, an oral fixation device, is proposed.

6.1 Design and assessment of alternative fiducial marker spatial configurations

The fiducial markers used to accurately determine the patient position need to be fixed to a rigid structure. The 'true' co-ordinates of the markers, tumour reference points and treatment beam need to be obtained in the co-ordinate same reference frame. This is normally done on a CT scanner. For some of the alternative structures investigated below the more accurate metrograph was used to obtain the 'true' co-ordinates. The structures investigated all involve fiducial markers located further away from the tumour than with the current mask. This may ultimately lead to less accurate positioning by the SPG system. To investigate this theory an idealised two-dimensional computer model of a set of fiducial markers was constructed, and is discussed below.

Concerning the effect on the precision of the SPG system of placing the markers further away from the tumour, as they are positioned closer to the cameras the precision of locating the fiducial markers

increases, however the projection of any errors onto the tumour position is also increased. These effects on the precision of locating the tumour were not investigated.

6.1.1 Theoretical analysis of the relationship between parameters governing the fiducial marker precision and the precision of locating the tumour

(a) Materials and method

A computer model was developed to investigate whether there is any change in the tumour position precision introduced by increasing the distance of the fiducial markers from the tumour. The marker positions are determined from a CT scanner, and their position co-ordinates are thus subject to random (and possibly systematic) variations. It can be postulated that the further a marker is from the tumour, the smaller the effect any errors in the positions of the marker will have on the calculation of the tumour position. This should be reflected in a smaller standard deviation of the calculated tumour position, for greater distances of the markers from the tumour.

The principle used in the program is called resampling (Simon and Bruce, 1993). This is simply a technique of modelling an experiment using a random process (e.g. drawing balls out of a drum, or using a random number generator) and repeating the simulation over many trials. This technique is also used in Monte Carlo simulations, but is advocated by Simon and Bruce (1993) for use in simple problems and in teaching statistics.

The model is calculated in two dimensions only and is diagrammatically represented in Figure 6-1. A variable number of markers (> 3) can be selected. These are distributed evenly over a circle of radius ir centred on the original tumour position. This is equivalent to an accurately surveyed frame with an accurately known tumour.

A minimum CT scanner resolution, res, can be fed in. Each marker is then positioned at a random position around a circle of radius res centred on its original position. This is equivalent to a CT scanned frame with each marker position determined to within a distance res of the true position. On average the marker's position is at the 'true' position. A program listing in True Basic code is shown in APPENDIX B below.

The randomly positioned markers forming the set of 'CT scanner' co-ordinates are transformed into the accurate original marker positions equivalent to a surveyed frame. The transformation residuals are calculated and from these a vector is calculated. This is a measure of the goodness of fit of the transformation.

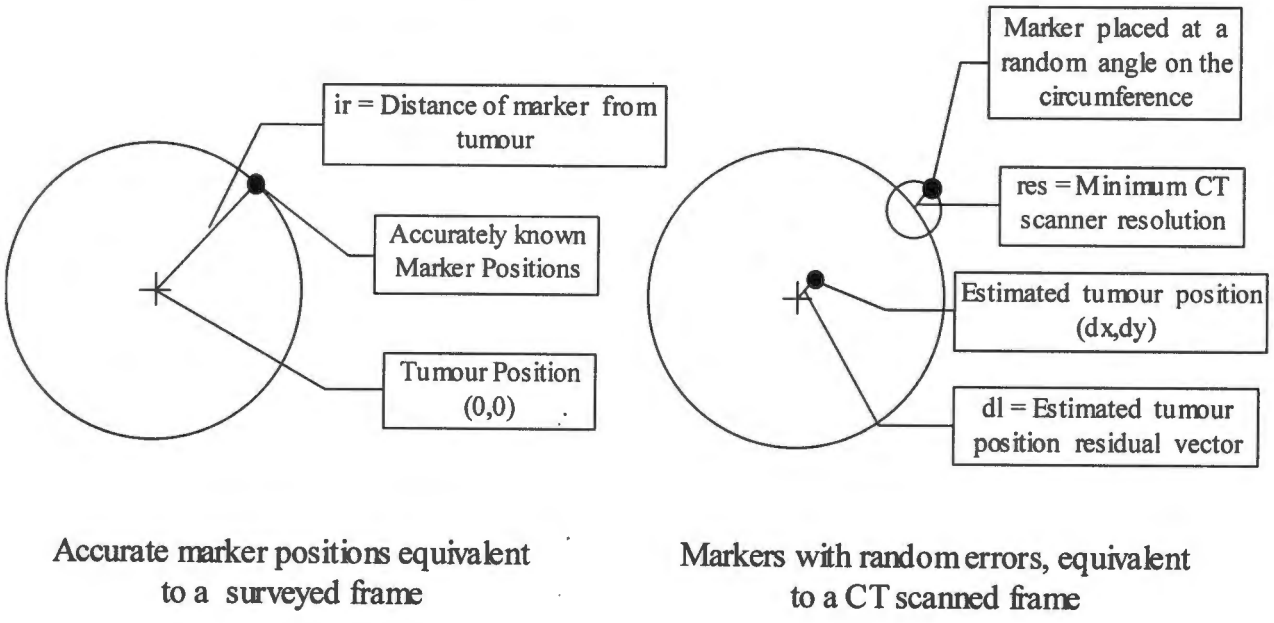

Figure 6-1 Diagram of model used to investigate the effect of parameters governing the marker precision on the precision of locating the tumour

The transformation matrix is then applied to the tumour point and the residuals of the new transformed tumour position from the original position are calculated. A residual vector is also calculated.

The number of trials can be input, and the randomised calculation is repeated for this number of trials. The mean of the tumour residuals for all axes added together, the mean of the tumour residual vectors, the standard deviation of the tumour residual vectors and the mean of the transformation vector are output to file. Finally the calculation cycle is repeated for radii from 4 to 30 mm in steps of two millimetres to assess the effect of changing distance of the markers from the tumour position.

(b) Results

A sample of the output file is shown below for 1000 trials, 8 markers, with each marker set being from 4 to 30 mm from the tumour, and a minimum CT scanner error of 0.5 mm in Table 6-1. The means of the calculated variables for all the radii used have been calculated. As explained below, this is because no dependence of the variables on the marker distance was found.

Table 6-1 Output from program RAN.TRU for 8 marker points with a CT scanner error (res) of 0.5 mm and for 1000 trials, showing the dependence of four variables, MuResidual, MudRVect, SigdRVect and MuTr.res.vec on the distance of the markers from the tumour, ir.

No of trials	No of markers	ir (mm)	res (mm)	Mean of tumour residuals (mm)	Mean of residual vector (mm)	Std Dev of residual vector (mm)	Mean transformation residual vector (mm)
1000	8	4	0.5	-0.0092	0.1878	0.1131	0.3355
1000	8	6	0.5	-0.0060	0.1943	0.1119	0.3395
1000	8	8	0.5	-0.0080	0.1934	0.1164	0.3328
1000	8	10	0.5	0.0083	0.1871	0.1101	0.3364
1000	8	12	0.5	-0.0012	0.1882	0.1107	0.3373
1000	8	14	0.5	-0.0001	0.1936	0.1133	0.3367
1000	8	16	0.5	-0.0046	0.1971	0.1147	0.3340
1000	8	18	0.5	-0.0007	0.1868	0.1083	0.3362
1000	8	20	0.5	-0.0045	0.1961	0.1128	0.3381
1000	8	22	0.5	0.0002	0.1895	0.1123	0.3368
1000	8	24	0.5	0.0051	0.1898	0.1129	0.3392
1000	8	26	0.5	0.0020	0.1935	0.1123	0.3370
1000	8	28	0.5	-0.0007	0.1974	0.1149	0.3352
1000	8	30	0.5	0.0057	0.1938	0.1088	0.3381
			Means	-0.0010	0.1920	0.1123	0.3366

The mean tumour residual for all marker distances shown in Table 6-1 is -0.0010 mm and was calculated as a check. It should be zero over many trials since on average the tumour will be at the origin. The mean residual vector for all marker distances is 0.1920 ± 0.1123 (1SD) mm reflecting the mean distance that the tumour moves away from the origin due to the marker errors. The mean transformation residual vector of 0.3366 mm is the sum of the squares of the residuals of the markers after transformation and reflects the magnitude of the transformation.

The linear regression line of the four variables: Mean of tumour residuals, Mean of residual vector, Std Dev of residual vector and Mean transformation residual vector, were plotted against the marker distances, ir, and no dependence was found (see Graph 6-1).

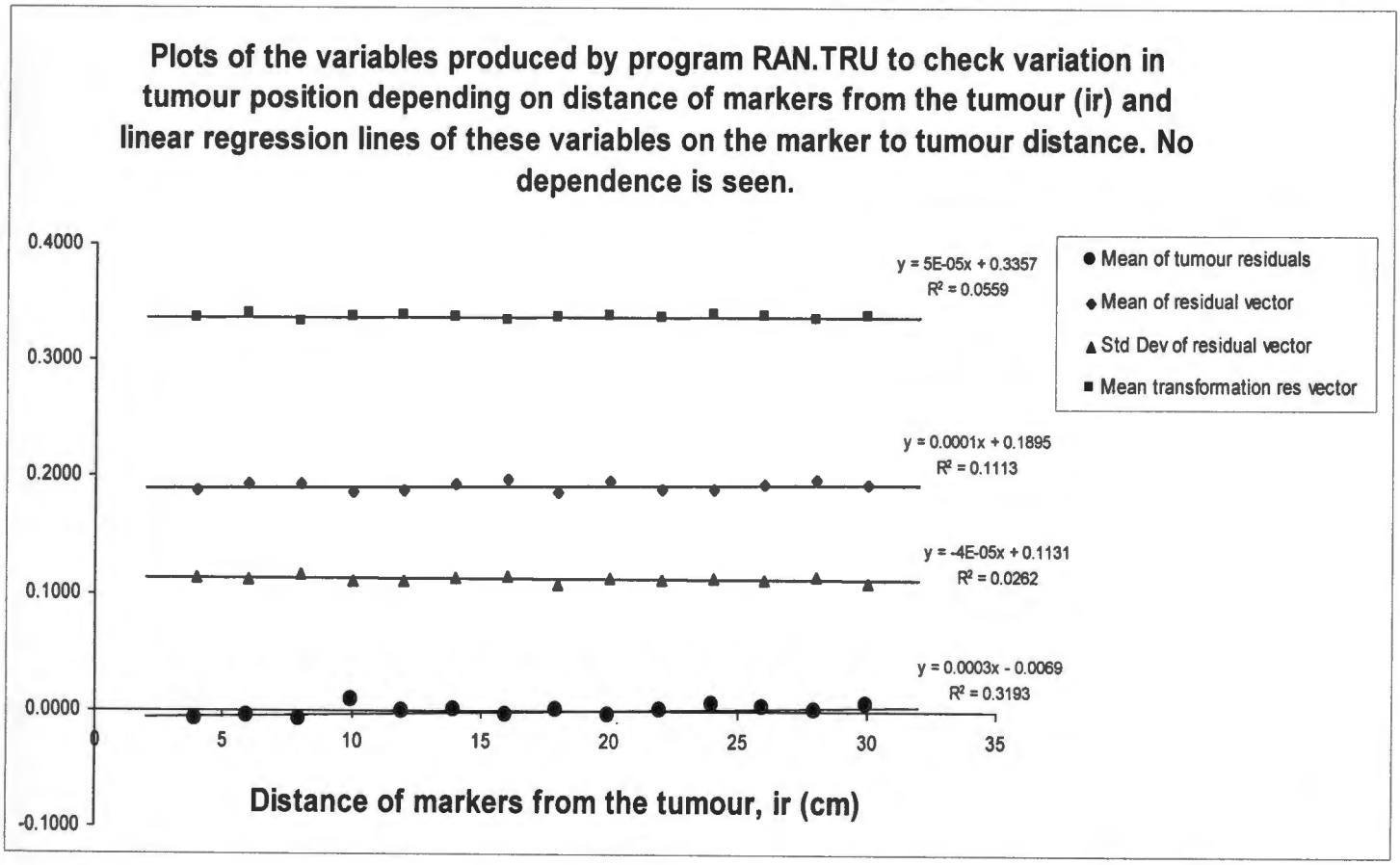

Graph 6-1 Plots of the variables produced by program RAN.TRU in Table 6-1 to check dependence on marker distance. No dependence is seen

(c) Discussion

The tumour position can thus be predicted equally accurately irrespective of how far the markers are placed from the tumour. This conclusion assumes that the markers themselves can be located perfectly by the cameras, i.e. no errors occur in the SPG system calculation of the marker positions. This is clearly no the case, as the closer the markers are to the cameras, the more accurately their positions can be determined by the SPG system. On the other hand, the projection of these positions onto the tumour is further away and any positioning error is magnified. It is not known what the net result of these opposing effects is, although the cameras are placed at distances between 191 and 320 cm from the isocentre (tumour). Thus the effect on the SPG system precision of moving the markers from about 4 cm (on average with the mask) to about 10 cm (as proposed in the structures developed below) from the isocentre is negligible.

6.1.2 Materials and methods

Three structures upon which the fiducial markers could be supported were developed:

(a) a rectangular 'plate' with four markers

(b) a 'crown' plus plate assembly

(c) a 'frame'

The 'true' positions of the fiducial markers and simulated 'tumour'; reference points were found using the metrograph. The structures were then tested for re-positioning accuracy using the metrograph, a laboratory stereophotogrammetric system employing two cameras, and the SPG system. As is discussed below, both the rectangular plate and crown were found to have unacceptably high positioning errors. Thus only the frame was used in the proton treatment room using the SPG system for further measurements in an identical way as the mask, as described in Chapter 3, so that a direct comparison of positioning accuracy could be made between the mask and the frame.

(a) Rectangular plate

A rectangular plate was constructed with four markers, one at each corner, and two simulated 'tumour' points were attached on a jig as shown in Figure 6-2 below.

Positioning accuracy was assessed by evaluating how well the co-ordinates of the four markers on the rectangular plate in one frame of reference could be used to predict the position of two simulated tumour points if the plate was moved to another position and only the marker co-ordinates were re-measured. Firstly the marker and tumour point co-ordinates were measured several times as accurately as possible using a metrograph to get their 'true' positions. A baseline ability to predict tumour positions using only these readings was determined. This procedure was then repeated with a laboratory camera system (Adams *et al.*, 1990) and again on the SPG system. Finally, the accuracy of predicting the tumour points from the laboratory camera system and from the SPG system was determined, using the best set of metrograph readings as a comparison

The plate fiducial markers were co-ordinated in three dimensions on the improved reflex microscope as described by Scott (1981), and repeated again on 7 occasions on the reflex metrograph . The plate fiducial marker co-ordinates were then compared to each other using the program listed in APPENDIX A. One set of marker co-ordinates was rotated into the reference frame of several other sets in order to estimate the precision attainable in the co-ordinate sets. The rotation matrix obtained

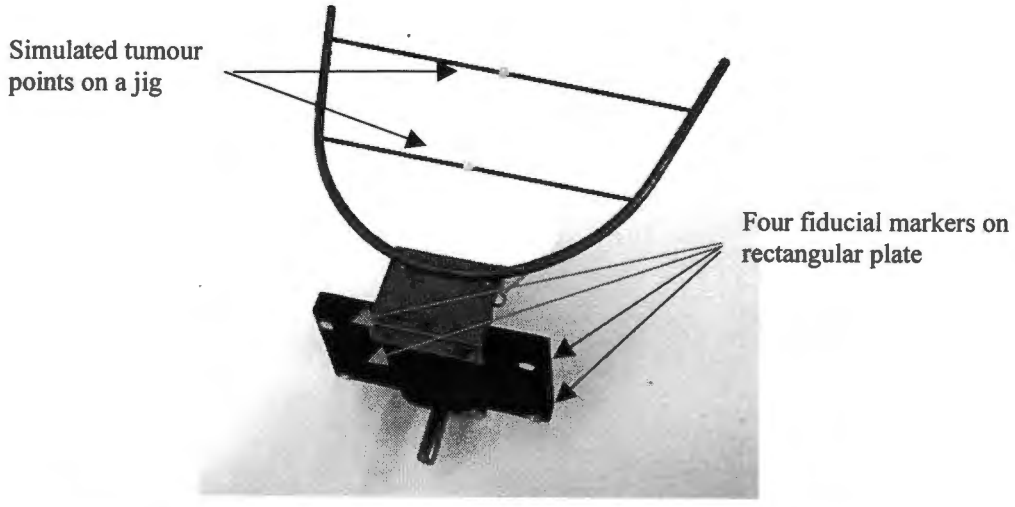

Figure 6-2 Rectangular plate with two 'tumour' points attached on a jig

was stored for subsequent use. The simulated tumour points were co-ordinated on the reflex metrograph only. The tumour co-ordinates in the frame of reference of a rotated rectangular plate were transformed using the stored transformation matrix into the stationary reference frame and the two sets of tumour co-ordinates were compared to each other.

In a similar way, the plate marker and tumour co-ordinates were measured three times using the laboratory camera system, and once using the SPG system, and the sets compared to each other.

(b) Crown plus rectangular plate

The crown was developed in an attempt to add more markers in such a way that firstly, they surrounded the tumour point better, and, secondly, that they could easily and reproducibly be added to or removed from the rectangular plate (Figure 6-3 below). Any upright marker support could be removed if it was in the beam path by unscrewing the upright support rod.

It was later reasoned that this feature could be eliminated as the support could be constructed entirely of thin carbon fibre tubing which is sufficiently rigid, and also thin enough to remain in the beam.

The crown and plate assembly could not be co-ordinated on the metrograph due to its size. The laboratory camera system and the SPG system were used to obtain both the 'true' and rotated sets of

Figure 6-3 Crown attached to the plate and bite block

marker and tumour co-ordinates for the assembly. The tumour residual vector was calculated in a similar way as for the plate only.

(c) Frame

A frame looking similar to a lampshade was designed and built from steel wire (see Figure 6-4 below). Two supporting cross members were added for rigidity. No supporting cross members would be required if the construction were from Delrin as proposed in section 8.4 (page 110). A simulated superficial and a deep tumour point were added.

Unfortunately the frame could not be co-ordinated on the metrograph due to its size. Thus, in order to be able to make a direct comparison of the accuracy and precision between the facemask and the frame, both of these were co-ordinated and assessed in an identical manner using the CT scanner to obtain the 'true' co-ordinates. The CT scanner co-ordinates of the markers attached to the frame were measured as described in section 3.2, and in order to assess the positioning accuracy of the frame, it

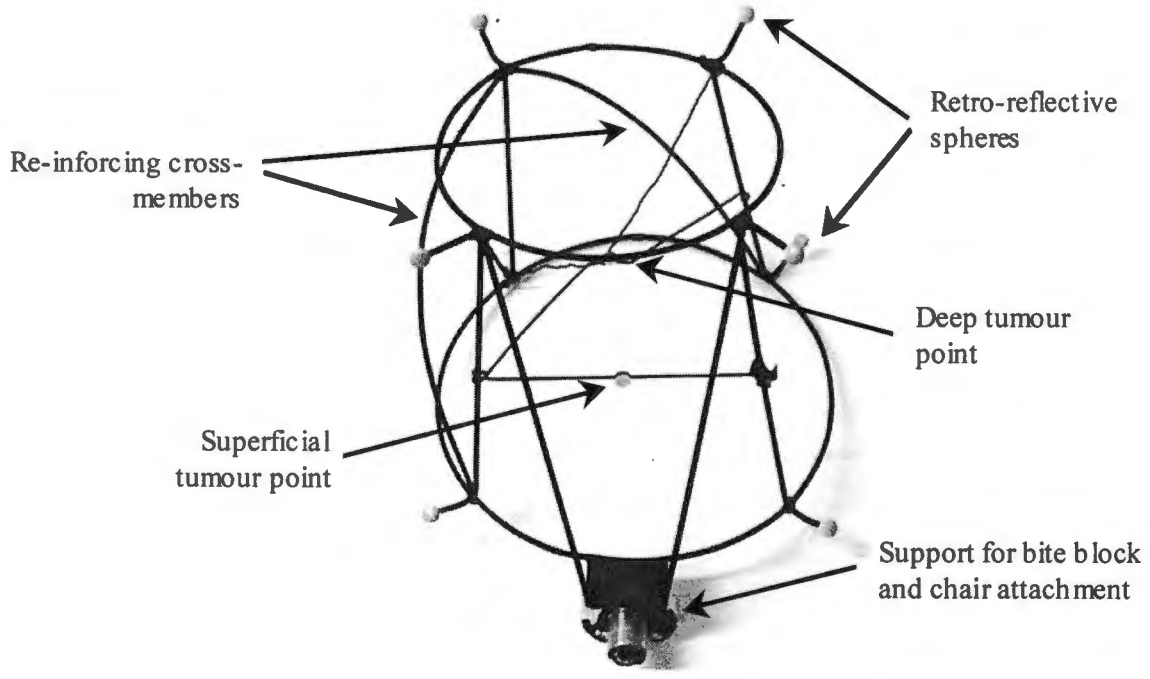

Figure 6-4 Frame showing simulated tumour points

was positioned using the SPG system, and the positioning errors were observed and recorded, also as described in section 3.2. Generally the final position (within the 1 mm tolerance) was achieved within two cycles. The readings for the frame were taken on two occasions.

6.1.3 Results

(a) Rectangular plate

Individual readings are not shown, however a summary of the results is shown in Table 6-2. In the sample printout of the Rodrigues transformation program (APPENDIX A) shown in Figure 6-5 below, the co-ordinates of markers obtained in one measurement by metrograph (named `tt1pl.txt`) are rotated into the frame of reference of the marker co-ordinates found in another measurement by metrograph considered to be the stationary set (named `met2.txt`). The estimated standard deviation vector (or residual vector) of the transformation is 0.6 mm. This result is shown in Table 6-2 below as co-ordinate comparison number 1. Eleven comparisons were made altogether, having a mean residual vector of 0.6 mm. Thus, even in ideal measuring conditions, using co-ordinates from the metrograph only, the residual vector of the transformation is unlikely to be better than 0.6 ± 0.1 (1SE) mm.

Table 6-2 Residual vectors of plate marker and tumour position differences as measured on the metrograph

Co-ordinate comparison	Transformation Residual Vector of plate markers (mm)	Transformation Residual Vector of tumours (mm)
1	0.6	3.6
2	0.4	-
3	1.0	-
4	0.7	-
5	0.3	-
6	0.8	2.8
7	0.7	-
8	0.2	0.4
9	0.6	1.6
10	0.6	-
11	0.4	-
Mean	0.6	2.1
Standard Deviation	0.2	1.4
Standard Error of Mean	0.1	0.7

The rotation matrix was applied to the simulated tumour co-ordinates measured at the same time as the co-ordinates named `tt1pl.txt`. The printout shows a comparison of the stationary simulated tumour co-ordinates (in `met2.txt`) with these transformed tumour co-ordinates (in the file named `tt1.txt`). A vector of the standard deviations of the residuals for x, y and z was calculated for the two simulated tumour points. This was found to be 3.6 mm and is shown in Table 6-2 above, co-ordinate comparison number 1. This means that using only the metrograph, the tumour points could be predicted with a precision vector of 3.6 mm. Three other similar comparisons were made, resulting in a mean precision vector for the two tumour points of 2.1 ± 1.4 (1SD) mm.

```
Date (yyyymmdd): 19990301    Time (hh:mm:ss): 00:16:01

Name of stationary input file   met2.txt

Name of rotated input file      tt1pl.txt

Scale is          1.0013605

TEST OF PRECISION
 POINT      Dx         Dy         Dz
   1     -  .436       .263    -  .086
   2        .265    -  .349    -  .265
   3        .447       .180       .333
   4     -  .276    -  .094       .018

Sum of squares of deviations

SdX2=    .537 SdY2=    .232 SdZ2=    .189

Estimated Population Standard Deviations

SDx=    .4 SDy=    .3 SDz=    .3     Vector=    .6

Residuals stored          resid            .txt

Co-ordinate values BEFORE transformation. From file:       tt1.txt
   1     162.67    - 75.42    - 37.90
   2     107.88    - 76.56    - 38.60
   3     107.46    -108.14      61.50
   4     164.31    -106.07      62.40
  11   -   3.62    - 33.61      43.60
  12      47.81      85.64      57.30

Co-ordinate values AFTER transformation. Stored          trans.txt
                                    TEST OF PRECISION using file:  met2tum.txt
                                          Dx         Dy         Dz
   1   - 64.56     108.14    - 86.01                                    1
   2   - 64.76     117.62    - 32.04                                    2
   3     40.18     115.82    - 31.53                                    3
   4     40.31     106.86    - 87.72                                    4
  11      2.16     202.72      64.47        3.073       .406       .405   11
  12   - 18.70     308.58    -  9.11        1.698    -  .651       .176   12

                                        Est Pop Standard Deviations

                                      SDx=  3.5 SDy=    .8 SDz=    .4 Vec.= 3.6
```

Figure 6-5 Printout of program RODDY.TRU showing the precision of a co-ordinate transformation from the marker point readings in file tt1pl.txt into a stationary set called met2.txt, and applying the rotation matrix to file tt1.txt which includes the tumour points 11 and 12 with the marker points of tt1pl.txt

The residual vectors when measured on the laboratory camera system are shown in Table 6-3 indicating a slightly worse average vector of 0.7 mm for the plate markers compared to the value of

Table 6-3 Residual vectors of plate marker and tumour position differences as measured on a laboratory camera system

Co-ordinate comparison	Transformation Residual Vector of plate markers (mm)	Transformation Residual Vector of tumours (mm)
1	0.7	1.6
2	0.8	-
3	0.7	2.6
Mean	0.7	2.1
Standard Deviation	0.1	0.7
Standard Error of Mean	0.1	0.7

0.6 mm as shown above for the metrograph. The average tumour precision vector for two comparisons was 2.1 ± 0.7 mm. This is the same as for the metrograph readings.

The plate fiducial marker and tumour point co-ordinates were measured using the SPG system, and the co-ordinates were compared to each other. The residual vectors are shown in Table 6-4 indicating a vector of 1.0 mm for the plate markers compared to the value of 0.6 mm for the metrograph, and a tumour residual vector of 2.8 mm compared to 2.1 mm for the metrograph readings.

Table 6-4 Residual vectors of plate marker and tumour position differences as measured on the SPG system

Co-ordinate comparison	Transformation Residual Vector of plate markers (mm)	Transformation Residual Vector of tumours (mm)
1	1.0	2.8

In order to determine how well the tumour point co-ordinates could be predicted from the laboratory camera system and from the SPG system when compared to the accurate metrograph readings, a set of co-ordinates measured on the metrograph was chosen as the stationary system, and the co-ordinates from the laboratory camera system and the SPG system were transformed into this system. The resulting residual vectors of the predicted tumour positions were calculated and are shown in

Table 6-5. The tumour precision vectors shown (mean = 4.5 mm) are too large to be acceptable for clinical proton positioning.

Table 6-5 Residual vectors of plate marker and tumour position differences using the metrograph readings (met2.txt) and the measured co-ordinates on the camera system and the SPG system

Co-ordinate comparison with met2.txt	Transformation Residual Vector of plate markers (mm)	Transformation Residual Vector of tumours (mm)
Laboratory camera set 1	0.6	2.9
Laboratory camera set 2	0.5	3.7
Laboratory camera set 3	0.7	4.6
SPG set 1	0.7	3.3
SPG set 2	1.5	7.9
Mean	0.8	4.5
Standard Deviation	0.4	2.0

It was thought that a possible reason for the poor accuracy of predicting the tumour positions was that the plate markers were all on one side only of the tumour points and their positions were thus found by extrapolation. The crown described below was an attempt to address this issue. The results of positioning accuracy measurements using the crown are shown next.

(b) Crown plus rectangular plate

The tumour residual vector using the laboratory camera system was calculated in a similar way as for the plate only, and the results are shown in Table 6-6, together with those calculated for the plate only for comparison purposes. There is no improvement in the tumour positioning precision by using the crown and rectangular plate.

Table 6-6 Residual vectors of tumour position differences for the plate only and the plate and crown measured on a laboratory camera system

Co-ordinate comparison	Tumour Transformation Residual Vector of plate (mm)	Tumour Transformation Residual Vector of plate and crown (mm)
1	1.6	2.3
2	-	-
3	2.6	1.8
Mean	2.1	2.1
Standard Deviation	0.7	0.4

The tumour residual vector using the SPG system was calculated in a similar way as for the plate only, and the result is shown in Table 6-7 below, together with those calculated for the plate only for comparison.

Table 6-7 Residual vectors of tumour position differences for the plate only and the plate and crown measured on the SPG system

Co-ordinate comparison	Tumour Transformation Residual Vector of plate only (mm)	Tumour Transformation Residual Vector of plate and crown (mm)
1	2.8	5.6

No further work was done using this crown arrangement, as the results appear to be worse than using the plate only.

(c) Frame

Detailed readings using the SPG system are shown in Table 6-8 below, and the mean final deviations of the tumour reference point from the isocentre are shown. In most cases the frame was brought into position in two cycles of the SPG system, and in all other cases in three.

There is a significant difference between the mean deviations in Set One and Set Two, for both the superficial and deep tumour points (two-tailed t test, $p < 10^{-4}$). This points either to a real but unexplained difference in the system accuracy between the two measuring occasions for the frame, or to an observer error. No significant difference was found for the mask between the two sets. The measurement should be repeated in order to decide this issue.

If the measurements for the two sets are combined, there is a significant difference between the accuracy for the deep tumour point (1.42 ± 0.32 (1SD) mm) and the superficial tumour point (1.68 ± 0.36 (1SD) mm), indicating that deep tumours, which are better surrounded by the frame fiducial markers, are positioned more accurately than superficial tumours. The mean of all readings combined is 1.55 ± 0.36 (1SD) mm.

Table 6-8 Tumour reference point to isocentre deviations (mm) on the frame after being positioned by the SPG system

Starting position	SET ONE		SET TWO (one month later)	
	Superficial	Deep	Superficial	Deep
A	2.1	1.7	1.3	1.2
B	2.1	1.7	1.3	1.1
C	2.0	1.7	1.4	1.0
D	2.0	1.7	1.3	1.0
E	2.0	1.7	1.3	1.5
F	2.0	1.7	1.4	1.3
G	2.0	1.7	1.3	1.0
H	2.0	1.7	1.3	1.0
Mean	2.03	1.70	1.33	1.14
Std. Dev.	*0.05*	*0.00*	*0.05*	*0.18*
Mean	1.86		1.23	
Std. Dev.	*0.17*		*0.16*	
Mean precision	*0.025*		*0.115*	
Mean	1.55			
Std. Dev.	0.36			
Mean precision	0.07			

DATA GROUPED DIFFERENTLY

	SUPERFICIAL		DEEP	
	Set One	Set Two	Set One	Set Two
Mean	2.03	1.33	1.70	1.14
Std. Dev.	*0.05*	*0.05*	*0.00*	*0.18*
Mean	1.68		1.42	
Std. Dev.	*0.36*		*0.32*	
Mean	1.55			
Std. Dev.	0.36			
Mean precision	0.07			

6.1.4 Discussion and recommendations

Three alternative structures for supporting the fiducial markers were investigated. Using the rectangular frame, the tumour points were able to be positioned by the SPG system to an accuracy of 3.3 mm and 7.9 mm on two occasions. The addition of the crown was not found to improve the accuracy, and the lampshade shaped design (Figure 6-4) was found to have the best result, with a mean accuracy of 1.55 ± 0.36 (1SD) mm. Other advantages of this design are:

- The same frame is used for all patients. Thus the fiducial markers can be accurately co-ordinated and the CT-scan co-ordinates can be pre-checked for consistency before use on the SPG system.
- Only eight fiducial markers are used
- At least six fiducial markers are observable by any one camera
- The markers fully surround the patient's head
- The open construction allows fiducial markers on the patient's forehead to be observed. Fiducial markers on the patient's nasion and forehead could be co-ordinated on the CT scanner and could be used as a crosscheck that the mask had not moved relative to the patient's head. Such a crosscheck is not possible with the current immobilisation system. A very time consuming method of taking X-rays along the beam line is used to check the patient position. While this method is crucial as a final positioning confirmation, errors would be automatically reported at a much earlier stage in the positioning process, as part of the SPG positioning process, if the patient can be directly observed. Changes to the computer program incorporating these two patient fiducial markers would be fairly straightforward.
- Less expensive running costs in the longer term in that repeated and time consuming mask construction for each patient would be replaced by individualised bite block construction only.

6.2 Means of fixing the fiducial marker supporting structure to the patient

6.2.1 Materials and methods

The fiducial marker support structures must be rigidly attached to the patient anatomy in some way. It is possible to attach it to any system used to immobilise the patient and a review of these was done. There are many such systems of immobilising patients used for radiosurgery, in which accurate positioning is required, and which are in current use worldwide (see paragraph 2.3.2). Following the requirement of a non-invasive system discussed in paragraph 1.2.2 (a) above, only these were more closely investigated. In the author's opinion the most successful ***non-invasive*** patient restraint system in use is based on using a biteblock. This is because the biteblock firmly holds the upper jaw. The lower jaw is used merely for support. A biteblock that is easy and inexpensive to construct, and is conveniently attached to the chair, was developed. The apparatus is shown in Figure 6-6 below.

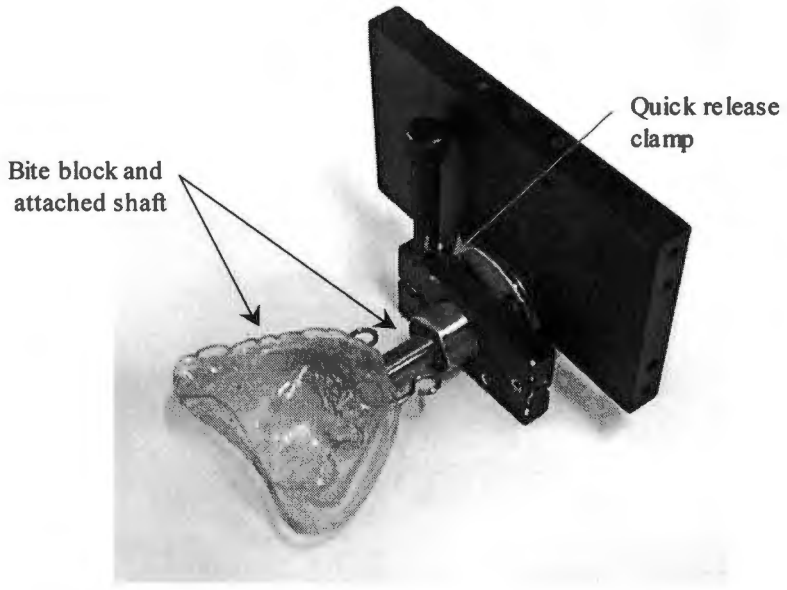

Figure 6-6 Bite block and quick release clamp

A separate dental plate as shown below is made for each patient. It has two attached mounting lugs that fit into the shaft assembly, and are held in place by two stainless steel pins. These can be inserted or withdrawn by the patient. Radiographs are currently the most common method of confirming the treatment setup. Three radiopaque markers or a steel wire (Rosenthal *et al.*, 1995) should be inserted in the dental plate to aid in ensuring that the position of the bite block stays fixed relative to the cranium.

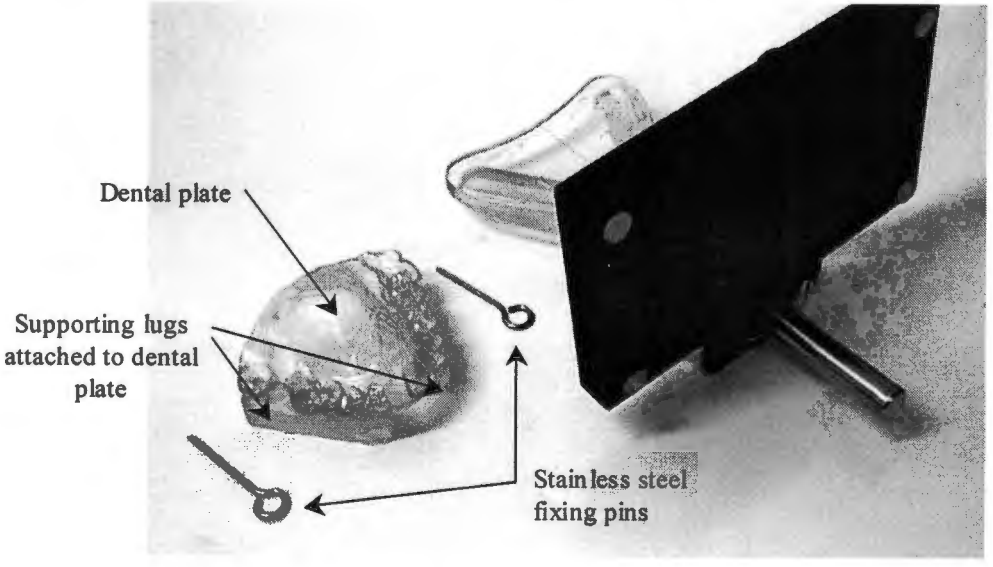

Figure 6-7 Bite block components

A dental fixation device was obtained from Dr R Shulte[15], for evaluation (see Figure 6-8 below). It is constructed from several materials making it a difficult and expensive process, but it is very comfortable for the patient. A unique feature is that a small vacuum system can be attached to the carbon fibre supporting tube. Air is extracted into the tube, via a non-return valve, from any small spaces between the bite block and upper palate, resulting in a very firm fit.

Since the patients are CT scanned on one occasion, and typically have more than one fraction of radiotherapy on other occasions, it is essential that the marker support system is attached to the patient, or to the bite block in our case, in a convenient and reproducible way. It should be easily removable in case of an emergency. A quick release clamp similar to that illustrated in Figure 6-6 is proposed, but self-locating and magnetic systems could be investigated.

Figure 6-8 Loma Linda dental fixation device (bite block)

6.2.2 Discussion and recommendations

There are several non-invasive cranial immobilising systems in use worldwide (see 2.3.2 above). The biteblock is used successfully at Harvard (Rosenthal *et al.*, 1995) and Loma Linda, and is ideal in terms of cost in the author's opinion. Consequently, a simple and effective biteblock, and a clamp for attaching the marker frame to it, were designed. For edentulous patients and children a bite block may not be suitable, and the Laitinen Stereoadapter (Laitinen *et al.*, 1985; Laitinen, 1987; Hariz *et al.*, 1990; Delannes *et al.*, 1991) using ear canals and nasion for fixation may be more suitable.

[15] Loma Linda University Cancer Institute, California, U.S.A. (http://www.llu.edu/llu/ci/)

6.3 Means of immobilising the patient for CT scanning and treatment

A proposed system of supporting the patient on the CT scanner is to use a neck rest which fits between the frame uprights. The patient's head can be held in place using Velcro strips attached to the CT table and there must be no pressure on the frame itself. This system is illustrated in Figure 6-9 above. For treatment, the patient's head needs to be firmly supported by the chair and a similar system could be used.

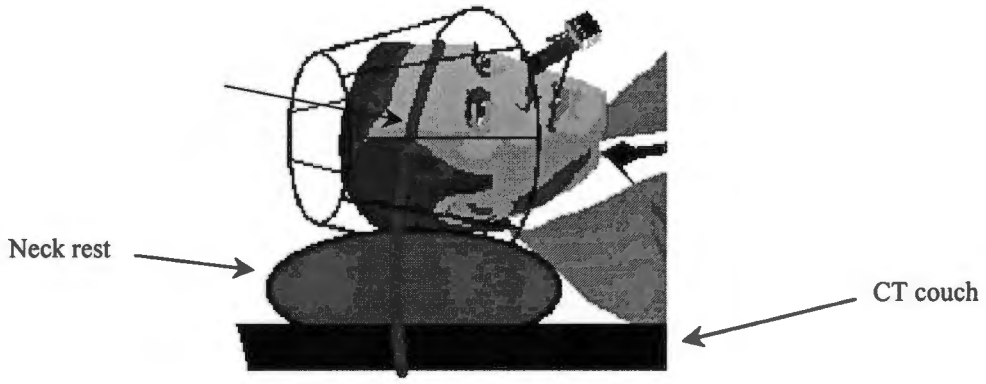

Figure 6-9 Method of immobilising patient on CT scanner

Alternatively, the following is a suggested design of a 'brace' to hold the bite block and frame directly. The brace is firmly attached to the chair backrest allowing fine adjustment for patient comfort. A clamp attached to the brace holds the biteblock shaft. This system illustrated in Figure 6-10 was not tested on a patient.

Figure 6-10 Frame and bite block support brace

6.3.1 Discussion and recommendations

Methods of fixing the patient firmly to the CT scanner and the treatment chair have been proposed. These should work adequately but need to be further tested and refined using patients.

7 Comparing the Positioning Accuracy of the Current System with the Alternative System

7.1 Materials and methods

A frame was constructed with two theoretical tumour points with concentric rings, of radii 1 mm to 5 mm, centred on the tumour reference point (see Figure 6-4 and section 6.1.2(c)). The frame was co-ordinated on a Picker IQ Fast CT scanner, positioned in the SPG system, and deviations measured exactly as was done for the facemask as described in section 3.2.

7.2 Results and discussion

This frame was found to be the most acceptable alternative to the facemask. The detailed results are presented and discussed in section 6.1.3(c) above. A comparison of the positioning accuracy achieved with the frame and with the mask is shown in Table 7-1 below.

As stated previously, with the frame the deep tumour is more accurately positioned (1.42 mm) than the superficial tumour (1.68 mm), and with the mask the superficial tumour is more accurately positioned (1.31 mm) than the deep tumour (1.44 mm). This may be a function of the fact that the fiducial markers surround the deep tumour on the frame, whereas the fiducial markers are nearer the superficial tumour on the mask. The deep tumour is slightly more accurately positioned with frame (1.42 mm) than with the mask (1.44 mm), but the superficial tumour is positioned much less accurately (1.68 mm) than with the mask (1.31 mm). The mean tumour reference point to isocentre deviation for the frame of 1.86 mm in Set One of Table 7-1 is disappointingly high. It would be interesting to repeat this measurement, and if it proved to be an observer error, then the frame system promises improved accuracy over the mask. The accuracy of the mask is more consistent over the two measuring occasions and overall (1.37 mm) is better than that of the frame (1.55 mm).

Overall the precision of the mask and frame are almost identical (± 0.35 (1SD) mm). Thus switching to a frame based system would have a small effect on the accuracy and precision, but would bring benefits in terms of easier observation of the markers by the SPG cameras, the possibility of direct patient anatomy position checking, convenience of use, less expensive running costs in the longer term, etc, as mentioned in detail in 6.1.4 above.

Table 7-1 Comparison of tumour reference point to isocentre deviations (mm) for the mask and frame

	MASK				FRAME			
	SET ONE		SET TWO		SET ONE		SET TWO	
	Superficial	Deep	Superficial	Deep	Superficial	Deep	Superficial	Deep
Mean	1.61	1.15	1.00	1.73	2.03	1.70	1.33	1.14
Std. Dev.	*0.17*	*0.28*	*0.00*	*0.13*	*0.05*	*0.00*	*0.05*	*0.18*
Mean	1.38		1.36		1.86		1.23	
Std. Dev.	*0.33*		*0.38*		*0.17*		*0.16*	
Mean	1.37				1.55			
Std. Dev.	0.35				0.36			

DATA GROUPED DIFFERENTLY

	MASK				FRAME			
	SUPERFICIAL		DEEP		SUPERFICIAL		DEEP	
	Set One	Set Two	Set One	Set Two	Set One	Set Two	Set One	Set Two
Mean	1.61	1.00	1.15	1.73	2.03	1.33	1.70	1.14
Std. Dev.	*0.17*	*0.00*	*0.28*	*0.13*	*0.05*	*0.05*	*0.00*	*0.18*
Mean	1.31		1.44		1.68		1.42	
Std. Dev.	*0.34*		*0.36*		*0.36*		*0.32*	
Mean	1.37				1.55			
Std. Dev.	0.35				0.36			

8 Summary of Results and Recommendations

The results found are summarised in Table 8-1.

Table 8-1 Summary of results

	Accuracy (mm)	Precision (1SD) (mm)	
CT co-ordinates of facemask markers	-	1.4	1.6
Movement of anatomy in face mask	1.0	0.8	
SPG system cameras	0.4	0.2	
SPG positioning of facemask	1.4	1.6	
SPG positioning of frame	1.6	< 1.6	

As constant striving for improved accuracy and precision should be a primary aim of any proton therapy facility, the recommendations made below are to improve the performance of the SPG system. For ease of reference, the recommendations are discussed under the main headings used in this thesis. No specific recommendations are made under some headings.

8.1 Assessing the accuracy with which the current SPG system can position tumour points on a sample mask (with no patient in the mask)

The current accuracy of positioning a facemask using the SPG system was found to be 1.4 ± 0.2 (1SD) mm. This compares well with the literature for high precision relocatable immobilisation techniques.

8.2 Investigating the sources of error of the current system

8.2.1 The error in co-ordinating the facemask fiducial markers on a CT scanner (with no patient in the mask)

This precision with which CT co-ordinates can be found on the facemask has been quantified as 1.4 (1SD) mm in this thesis. The operation of the SPG system depends on knowledge of the co-ordinates of the fiducial markers. Improving the accuracy and precision of the fiducial marker co-ordinates would have a marked effect on the overall accuracy and precision as the largest error found is due to the CT scanner co-ordinates. Using the currently available CT scanner hardware and software no improvement in precision could be found.

As consistently found by a number of authors in the literature, the precision obtainable from CT scanners is considerably worse than with X-ray films, therefore using orthogonal films to obtain the co-ordinates would result in improved accuracy and should be investigated. Alternative strategies for improving the marker position accuracy as determined with a CT scanner should be pursued. The procedure of locating individual fiducial markers in the CT scan with 2 mm slice-thickness is tedious and would be considerably speeded up by using a Spiral scanner to scan the whole head. Also the use of a scanner with a 1 mm slice thickness would lead to greater accuracy in the z direction.

Another approach to increasing the z-axis accuracy of the markers is to use the scout (or pilot) views of the CT scanner rather than the axial scan couch position to obtain the z co-ordinate. The paper proposing this method (Yue *et al.*, 1999) is aimed at resolving 50 to 100 small radioactive seeds easily using 5 or 3 mm slice thicknesses. The marker size will need to be increased so that it is large enough to resolve in the skull in the scout views, and small enough to avoid imaging artefacts. 3 mm diameter steel spheres may be adequate. A disadvantage of this method is that the markers may need to be removed from both the treatment planning images and the mask, prior to proton treatment, to avoid interaction with the beam.

The newly developed LODOX linear X-ray scanner (Vaughan, 1999) holds promise as a fast and accurate co-ordinating modality. However the lack of axial slice information for diagnostic and radiotherapy planning purposes prevents its use at present.

The difference in scale between the metrograph and Picker CT scanner discussed in paragraph 4.1.3 needs to be investigated in detail. Using an accurately surveyed control frame, the accuracy of CT co-ordination for each axis separately can be tested. Corrective action for the slice positions may be possible, but would be difficult for the image pixels.

8.2.2 The effect on the precision of the CT scanner co-ordinates of the fiducial markers of placing a patient in the mask

The result was inconclusive and should be repeated using the Picker IQ Fast scanner if an accurate value is required.

8.2.3 Movement of the patient anatomy inside the mask in a 7-day period

The mask design shows a error vector of 1.0 ± 0.8 (1SD) mm, an excellent accuracy and precision in comparison to stereotactic frames, although the inability to check whether there has been any movement of the patient inside the mask remains a problem. The new frame design addresses this.

8.2.4 The accuracy and precision of the SPG system cameras

The accuracy of the SPG system using a check frame was found to be 0.4 mm, and the precision was found to be extremely good at around 0.2 mm, implying that no major effort is required to improve the SPG system precision. Although the contribution of the SPG camera system of 0.4 mm to the total systematic error is small in relation to the other errors, it may be relatively easy to eliminate. A possible reason for this error is a calibration error occurring in the use of the large camera calibration frame; possibly an incorrect alignment of the calibration frame centre with the room isocentre. The congruence of the room isocentre defined on the theoretical beam vector and the SPG isocentre determined in the calibration procedure should be checked and corrected if necessary.

8.2.5 Estimate of total SPG positioning error

A total patient positioning precision using the SPG system was found to be $\sqrt{(1.39)^2+(0)^2+(0.8)^2+(0.2)^2}$ =1.6 (1SD) mm. This incorporates the errors in co-ordinating the mask on a CT scanner without a patient (1.39 mm), the error introduced by having a patient in the mask (0 mm), the error due to patient motion inside the mask (0.8 mm) and the error in the SPG system cameras (0.2 mm), and compares very well to international standards. The largest component of the positioning error observed during the course of patient treatments can be explained by the error in the CT co-ordinates, and consequently most effort should be given to reducing this.

8.3 Decreasing the time to set-up patients in the treatment room

Several aspects of the positioning system were investigated for the purpose of improving its performance. Two of these features, the software and the target illumination, have been successfully implemented.

8.3.1 Streamlining the current SPG software system

It is recommended that the standard deviation of the mean residual transformation vector is calculated and shown on the SPG computer monitor as a summarising statistic to be able to easily evaluate the precision of the CT scanner marker co-ordinates when compared to those obtained by the SPG system.

8.3.2 Improving target illumination

This has been successfully done.

8.3.3 Reducing number of fiducial markers

The inconsistent results of reducing the number of fiducial markers point to a possible faulty algorithm. This should be investigated as soon as possible.

Although it was found that using only four fiducial markers for positioning a particular beam could retain sufficient accuracy, this information does not mean that fewer markers need to be used on the facemask. This is because it is not known exactly which of the 20 markers currently used on all patient masks before the radiation plan is designed, will be required for a particular beam. The knowledge that fewer points are sufficient for positioning could be useful in practice if individual points were giving trouble in some way during the positioning procedure on the SPG system. Due to one of the changes made to the SPG program, the troublesome point can be simply removed from those used by the program for positioning.

8.3.4 Investigating apparent errors in chair movements

There is a consistent error of about 5 mm of the prescribed tumour reference point from the isocentre, when the SPG chair is moved for the first time. This should be eliminated if possible by investigating the accuracy of the SPG computer system algorithm and the accuracy of the patient chair movements. This would lead to quicker and more accurate positioning.

8.4 Simplifying the patient immobilisation and positioning procedures

The lampshade shaped frame shown in Figure 6-4 above was found to have a positioning accuracy of 1.6 ± 0.1 (1SD) mm. It should be constructed and implemented so that the ability to monitor the patient's anatomy position relative to the frame using the SPG system can be exploited. This will give added confirmation of correct patient positioning. Appropriate modification of the SPG system will be required.

Ideally the frame should be constructed of 2-mm diameter Delrin AF[16] plastic carbon fibre tubing. Delrin is produced from iso-oriented teflon fibres and acetyl resin and "was judged superior to other CT and MRI compatible materials, including nylon and carbon-fibre based materials, because of its dimensional rigidity, abrasion resistance, and relatively high transmission of both diagnostic and therapeutic beams" (Houdek *et al.*, 1991). This would be sufficiently rigid to support the fiducial markers and withstand normal wear and tear, and is thin enough to remain in the path of a beam.

8.5 Additional areas of investigation

Other possible areas of investigation are:

- implementing an automatic fiducial marker identification system. This would be a major improvement as the setup time and complexity could be greatly reduced.

[16]Commercial Plastic & Supply Corp., Cornwells Heights, PA 19020, USA

- implementing the NAC proton chair geometry in the virtual simulation module of Proxelplan[17]. The current positioning geometry for simulating and planning proton radiotherapy is based on the conventional LINAC 'gantry', and changing to the NAC treatment geometry should result in more efficient patient planning and a closer correspondence of the treatment plan parameters and the parameters use to set-up and treat the patient in the treatment room.
- investigating the SPG transformation algorithms. Stereophotogrammetry techniques rely on knowledge of the position, orientation and image linearity of each of the CCD cameras. The camera system is calibrated in order to determine the first two of these parameters.

Errors can occur in the calibration of the cameras for various reasons. One is the neglect of camera imperfections, such as lens distortion. A test for geometric distortions across the individual camera's fields of view should be performed as was done by Rogus *et al.* (1999). They found a scale factor distortion of 0.6 mm at a distance of 15 cm from the isocentre. The computer calibration routines could be re-assessed and scrutinised. Techniques do exist for the incorporation of such camera imperfections. These techniques are not implemented in the SPG system design at the time of calibration (see van der Vlugt, 1991).

Two major determinants of inherent *accuracy* of the SPG system are the camera calibration accuracy and the computational accuracy used in the SPG computer transformation algorithms. The inherent *precision* will depend mainly on the CCD camera resolution and the camera and video adapter electronic noise. With the algorithms used in the SPG system, systematic or random errors can occur in calculating either the co-linearity or conformal transformations because of the numeric approximations and coding complexity. As the transformations are non-linear in nature and the system is over-determined, the following well-established technique is used. The transformation functions are first linearised, by retaining only the first two terms of the Taylor series expansion of the function. Next an iterative linear least squares technique is employed to minimise the residual error in the computation. A non-linear least-squares technique could be employed. The problems resulting from algorithm approximation techniques are recognised by Li *et al.* (1999) who state " ... a significant error could (also) be produced by an approximation in the co-ordinate system", and consequently give a revised transformation algorithm. (This particular example is not directly applicable to the SPG system, as no co-ordination shortcut assumptions are made.) It is however unlikely that any major inaccuracies which significantly influence the position of patients exist in the SPG system software as

[17] VOXELPLAN developed at DKFZ, Heidelberg, Germany, updated by, and currently in use at, NAC for Proton planning.

unacceptable errors would be intercepted by both the daily check frame measurements and the X-ray checks done for every field, and it is questionable if the gain in precision will warrant the effort.

APPENDIX A - Rodrigues transformation program

```
REM This is program "RODDY.TRU"
LIBRARY "f:\truebasic\shell.tru"
OPTION BASE 1

DIM x(1),y(1),z(1),na(1)
DIM x1(1),y1(1),z1(1),nb(1)
DIM xl(1),yl(1),zl(1)
DIM xll(1),yll(1),zll(1),nnp(1)
DIM xp(1),yp(1),zp(1),np(1)
DIM r(3,3)
DIM x6(1),y6(1),z6(1),x7(1),y7(1),z7(1)
DIM x4(1),y4(1),z4(1),x5(1),y5(1),z5(1),d(1,1),f(1,1),g(1,1)
DIM a(1,1),l(1,1),b(1,1),c(3,3)

CLEAR

PRINT "            ********************************************************"
PRINT "            *                RODDY.TRU                            *"
PRINT "            *        Calculating Rodrigues Parameters              *"
PRINT "            *         and Test of Precision for an                 *"
PRINT "            *         (un)scaled 3D transformation.                *"
PRINT "            *                                                      *"
PRINT "            *    The second file entered will be rotated into the  *"
PRINT "            *        first entered file's co-ordinate system.      *"
PRINT "            *  (The number of points in the second file can be     *"
PRINT "            *       smaller than in the first file).               *"
PRINT "            ********************************************************"
PRINT


FOR ii = 1 to 20
DO
 LET Err1 = 0
 WHEN ERROR IN

PRINT " Current first (static) file is :",NA$
INPUT PROMPT " Is this OK? (y/n) ":qqq$
IF qqq$ <> "y" and qqq$ <> "Y" then
 INPUT PROMPT " Enter the file name of the first (static) 3D system : ":NA$
END IF
PRINT
OPEN #1: NAME NA$ &".txt", ACCESS OUTIN, CREATE NEWOLD,organization text

SET #1: POINTER BEGIN
INPUT #1:a$
LET s=val(a$)
MAT REDIM x(s),y(s),z(s),na(s)
FOR I = 1 to s
    INPUT #1:a$
    LET na(i)=val(a$[1:3])
    LET x(i)=val(a$[5:11])
    LET y(i)=val(a$[13:19])
    LET z(i)=val(a$[21:27])
    PRINT  na(I),x(I), y(I), z(I)
NEXT I
PRINT
PRINT
CLOSE #1
INPUT PROMPT " Do you want to print the results? (y,n): ":qp$
PRINT
CLEAR
IF qp$ = "y" or qp$ = "Y" then
DO
 LET Err = 0
 WHEN ERROR IN
   OPEN #7: NAME NA$ &".wri", ACCESS OUTIN, CREATE NEWOLD,organization text
  USE
   PRINT "Error: "; ExText$
   LET Err = 1
   INPUT PROMPT " Press any key when error corrected":junk$
 END WHEN
LOOP UNTIL Err = 0
```

```
   PRINT #7, using "################ ########    ################ ########":"Date
(yyyymmdd):",DATE$,"Time (hh:mm:ss):",TIME$
   PRINT #7
   PRINT #7:"Name of stationary input file ",NA$;
   PRINT #7:".txt"
   PRINT #7
END IF

PRINT " Current second (rotating) file is :",NAM$
INPUT PROMPT " Is this OK? (y/n) ":qqq$
IF qqq$ <> "y" and qqq$ <> "Y" then
 INPUT PROMPT " Enter the file name of the second (rotating) 3D system : ":NAM$
END IF
PRINT
OPEN #1: NAME NAM$ &".txt", ACCESS OUTIN, CREATE NEWOLD,organization text
SET #1: POINTER BEGIN
INPUT #1:a$
LET n=val(a$)
MAT REDIM x1(n),y1(n),z1(n),nb(n)
FOR I = 1 to n
    INPUT #1:a$
    LET nb(i)=val(a$[1:3])
    LET x1(i)=val(a$[5:11])
    LET y1(i)=val(a$[13:19])
    LET z1(i)=val(a$[21:27])
    PRINT  nb(I),x1(I), y1(I), z1(I)
NEXT I
PRINT
PRINT
CLOSE #1

LET j = 1
FOR i = 1 to s
 IF j <= n then
  IF na(i) = nb(j) then
   LET x(j)=x(i)
   LET y(j)=y(i)
   LET z(j)=z(i)
   LET j=j+1
  END IF
 END IF
NEXT i

IF qp$ = "y" or qp$ = "Y" then
   PRINT #7:"Name of rotated input file ",NAM$;
   PRINT #7:".txt"
   PRINT #7
END IF
!PRINT "Press any key to continue"
!GET KEY trash
!CLEAR

MAT REDIM x6(n),y6(n),z6(n),x7(n),y7(n),z7(n)
MAT REDIM x4(n),y4(n),z4(n),x5(n),y5(n),z5(n)
MAT reDIM a(3*n,3),l(3*n,1),b(3,3*n),c(3,3),d(3,3),f(3,3*n),g(3,1)

!Deriving centroid coordinates
LET x2=0
LET y2=0
LET z2=0
LET x3=0
LET y3=0
LET z3=0
FOR i = 1 to n
    LET x2=x(i)+x2
    LET y2=y(i)+y2
    LET z2=z(i)+z2
    LET x3=x1(i)+x3
    LET y3=y1(i)+y3
    LET z3=z1(i)+z3
NEXT i
LET x2=x2/n
LET y2=y2/n
LET z2=z2/n
LET x3=x3/n
LET y3=y3/n
LET z3=z3/n

FOR i= 1 to n
```

```
    LET x(i)=x(i)-x2
    LET y(i)=y(i)-y2
    LET z(i)=z(i)-z2
    LET x1(i)=x1(i)-x3
    LET y1(i)=y1(i)-y3
    LET z1(i)=z1(i)-z3
NEXT i

LET total = 0
!FOR I = 1 to s-1
FOR I = 1 to n-1
!    FOR J = I+1 to s
    FOR J = I+1 to n
       LET ddd=sqr( (x(J)-x(I))^2 + (y(J)-y(I))^2 + (z(J)-z(I))^2 )
       LET total=total+ddd
    NEXT J
NEXT I

LET total1 = 0
FOR I = 1 to n-1
    FOR J = I+1 to n
       LET ddd=sqr( (x1(J)-x1(I))^2 + (y1(J)-y1(I))^2 + (z1(J)-z1(I))^2 )
       LET total1=total1+ddd
    NEXT J
NEXT I

LET scale = total /total1

PRINT "Scale is ",scale
PRINT
IF qp$ = "y" or qp$ = "Y" then
   PRINT #7: "Scale is ",scale
   PRINT #7:
END IF
INPUT PROMPT  " Do you want to apply the scale factor (y,n)? ": qs$
IF qs$ = "y" or qs$ = "Y" then
   PRINT "Scaled input values:"
   FOR I = 1 to n
      LET x1(i)=x1(i)*scale
      LET y1(i)=y1(i)*scale
      LET z1(i)=z1(i)*scale
      PRINT  x1(I), y1(I), z1(I)
   NEXT I
   PRINT "Press any key to continue"
   GET KEY trash
END IF

FOR i = 1 to n
    LET x4(i)=x1(i)+x(i)
    LET y4(i)=y1(i)+y(i)
    LET z4(i)=z1(i)+z(i)
    LET x5(i)=2*(x1(i)-x(i))
    LET y5(i)=2*(y1(i)-y(i))
    LET z5(i)=2*(z1(i)-z(i))
NEXT i

! solving Lambda , Mu and Nu

FOR i = 1 to n
    LET a(3*i-2,1)=0
    LET a(3*i-2,2)=-z4(i)
    LET a(3*i-2,3)=y4(i)
    LET a(3*i-1,1)=z4(i)
    LET a(3*i-1,2)=0
    LET a(3*i-1,3)=-x4(i)
    LET a(3*i,1)=-y4(i)
    LET a(3*i,2)=x4(i)
    LET a(3*i,3)=0
    LET l(3*i-2,1)=x5(i)
    LET l(3*i-1,1)=y5(i)
    LET l(3*i,1)=z5(i)
NEXT i
MAT b=trn(a)
MAT c=b*a
MAT d= inv(c)
MAT f=d*b
MAT g= f*l
LET l1=g(1,1)
LET m1=g(2,1)
```

```
LET n1=g(3,1)
! forming rotation matrix
LET d1=1+(l1^2+m1^2+n1^2)/4
LET d2= 2-d1
LET r(1,1)=(l1^2/2+d2)/d1
LET r(1,2)=(l1*m1/2-n1)/d1
LET r(1,3)=(l1*n1/2+m1)/d1
LET r(2,1)=(l1*m1/2+n1)/d1
LET r(2,2)=(m1^2/2+d2)/d1
LET r(2,3)=(m1*n1/2-l1)/d1
LET r(3,1)=(l1*n1/2-m1)/d1
LET r(3,2)=(m1*n1/2+l1)/d1
LET r(3,3)=(n1^2/2+d2)/d1
! to test precision of the transformation
FOR i = 1 to n
    LET x6(i)=x1(i)*r(1,1)+y1(i)*r(1,2)+z1(i)*r(1,3)
    LET y6(i)=x1(i)*r(2,1)+y1(i)*r(2,2)+z1(i)*r(2,3)
    LET z6(i)=x1(i)*r(3,1)+y1(i)*r(3,2)+z1(i)*r(3,3)
    LET x7(i)=x(i)-x6(i)
    LET y7(i)=y(i)-y6(i)
    LET z7(i)=z(i)-z6(i)
NEXT i
CLEAR
IF qs$ = "y" or qs$ = "Y" then
   PRINT "TEST OF PRECISION - SCALE FACTOR APPLIED"
ELSE
   PRINT "TEST OF PRECISION - SCALE FACTOR NOT APPLIED"
END IF
PRINT "    POINT     Dx     Dy     Dz"
FOR i = 1 to n
    PRINT using "  ##    ###.###   ###.###   ###.###":nb(i),x7(i),y7(i),z7(i)
NEXT i
PRINT

LET sx=0
LET sy=0
LET sz=0
FOR i = 1 to n
    LET sx=sx+x7(i)^2
    LET sy=sy+y7(i)^2
    LET sz=sz+z7(i)^2
NEXT i
PRINT  "Sum of squares of deviations"
PRINT
PRINT  using "##### ##.### ##### ##.### ##### ##.###":"SdX2=",sx,"SdY2=",sy,"SdZ2=",sz
PRINT
PRINT  "Estimated Population Standard Deviations"
PRINT
PRINT  using "#### ##.# #### ##.# #### ##.#  ####### ##.#":"SDx=",(sx/(n-1))^0.5,"SDy=",(sy/(n-
1))^0.5,"SDz=",(sz/(n-1))^0.5,"Vector=",((sx+sy+sz)/(n-1))^0.5
PRINT

IF qp$ = "y" or qp$ = "Y" then
   IF qs$ = "y" or qs$ = "Y" then
     PRINT #7: "TEST OF PRECISION - SCALE FACTOR APPLIED"
   ELSE
     PRINT #7: "TEST OF PRECISION"
   END IF
   PRINT #7:" POINT     Dx       Dy       Dz"
   FOR i = 1 to n
      PRINT #7, using "  ##    ###.###   ###.###   ###.###":nb(i),x7(i),y7(i),z7(i)
   NEXT i
   PRINT #7:
   PRINT #7: "Sum of squares of deviations"
   PRINT #7:
   PRINT #7, using "##### ##.### ##### ##.### ##### ##.###":"SdX2=",sx,"SdY2=",sy,"SdZ2=",sz
   PRINT #7:
   PRINT #7: "Estimated Population Standard Deviations"
   PRINT #7:
   PRINT #7, using "#### ##.# #### ##.# #### ##.#    ####### ##.#":"SDx=",(sx/(n-
1))^0.5,"SDy=",(sy/(n-1))^0.5,"SDz=",(sz/(n-1))^0.5,"Vector=",((sx+sy+sz)/(n-1))^0.5
   PRINT #7:
END IF

INPUT PROMPT "Write residual values to disc? (y,n) : ":ans$
IF ans$ = "Y" or ans$ = "y" then
   INPUT PROMPT "Enter file name for residuals : ":NA9$
   OPEN #5: NAME NA9$ &".txt", ACCESS OUTIN, CREATE NEWOLD,organization text
   !        SET #5: POINTER BEGIN
```

```
   ERASE #5
   PRINT #5, using "####":n
   FOR i = 1 to n
      PRINT #5, using "###.###   ###.###   ###.###":x7(i),y7(i),z7(i)
   NEXT i
   CLOSE #5
   IF qp$ = "y" or qp$ = "Y" then
    PRINT #7 :"Residuals stored In File "  ,NA9$,".txt"
    PRINT #7 :
   END IF
END IF
CLEAR
INPUT PROMPT "Any points to be transformed using RODDY parameters? (y,n): ":qq$
PRINT
IF qq$ = "y" or qq$ = "Y" then
   PRINT "Co-ordinates transformed from system two to (static) system one"
   PRINT
   INPUT PROMPT "Enter the file name of the 3D co-ords to be transformed : ":NA7$
   PRINT
   OPEN #1: NAME NA7$ &".txt", ACCESS OUTIN, CREATE NEWOLD,organization text
   SET #1: POINTER BEGIN
   INPUT #1:a$
   LET n=val(a$[1:3])
   MAT REDIM xl(n),yl(n),zl(n),nnp(n)
   MAT REDIM xll(n),yll(n),zll(n)

   IF qp$ = "y" or qp$ = "Y" then
     PRINT #7, using "################################################### >#######":"Co-ordinate
values BEFORE transformation. From file:",NA7$;
     PRINT #7:".txt"
   END IF
   PRINT "Co-ordinate values BEFORE transformation"

   FOR I = 1 to n
      INPUT #1:a$
      LET nnp(i)=val(a$[1:3])
      LET xl(i)=val(a$[5:11])
      LET yl(i)=val(a$[13:19])
      LET zl(i)=val(a$[21:27])
      PRINT  nnp(I), xl(I), yl(I), zl(I)
      IF qp$ = "y" or qp$ = "Y" then
        PRINT #7, using "  ##   ####.##   ####.##   ####.##":nnp(I),xl(I),yl(I),zl(I)
      END IF
      LET xl(i)=xl(i)-x3
      LET yl(i)=yl(i)-y3
      LET zl(i)=zl(i)-z3
   NEXT I
   IF qp$ = "y" or qp$ = "Y" then
     PRINT #7
   END IF
   CLOSE #1
   FOR I = 1 to n
      LET xll(i)=xl(i)*r(1,1)+yl(i)*r(1,2)+zl(i)*r(1,3)
      LET yll(i)=xl(i)*r(2,1)+yl(i)*r(2,2)+zl(i)*r(2,3)
      LET zll(i)=xl(i)*r(3,1)+yl(i)*r(3,2)+zl(i)*r(3,3)
   NEXT I
   PRINT
   INPUT PROMPT "Write transformed values to disc? y/n : ":ans$
   IF ans$ = "Y" or ans$ = "y" then
     INPUT PROMPT "Enter file name for 3D transformed co-ords : ":NA6$
     OPEN #4: NAME NA6$ &".txt", ACCESS OUTIN, CREATE NEWOLD,organization text
     SET #4: POINTER BEGIN
     PRINT #4, using "####":n
   END IF
   INPUT PROMPT "Compare transformed values to file on disc? y/n : ":anss$
   IF anss$ = "Y" or anss$ = "y" then
     INPUT PROMPT "Enter comparison file name : ":NA9$
     OPEN #5: NAME NA9$ &".txt", ACCESS OUTIN, CREATE NEWOLD,organization text
     SET #5: POINTER BEGIN
     INPUT #5:a$
     LET s=val(a$)
     MAT REDIM xp(s),yp(s),zp(s)
     MAT REDIM np(s)
     FOR I = 1 to s
        INPUT #5:a$
        LET np(i)=val(a$[1:3])
        LET xp(i)=val(a$[5:11])
        LET yp(i)=val(a$[13:19])
        LET zp(i)=val(a$[21:27])
```

```
    NEXT I
    CLOSE #5
  END IF
  IF qp$ = "y" or qp$ = "Y" then
    IF ans$ = "Y" or ans$ = "y" then
       PRINT #7:"Co-ordinate values AFTER transformation. Stored In File ",NA6$;
       PRINT #7:".txt"
    ELSE
       PRINT #7:"Co-ordinate values AFTER transformation."
    END IF
  END IF
  PRINT
  PRINT "Co-ordinate values AFTER transformation"
  PRINT                                  .
  IF anss$ = "Y" or anss$ = "y" then
    IF qp$ = "y" or qp$ = "Y" then
       PRINT #7, using "                                  ############################## >#######":"TEST
OF PRECISION using file:",NA9$;
       PRINT #7:".txt"
       PRINT #7, using "                                    ####################################":"Dx
Dy       Dz"
    END IF
  END IF

  LET j=1
  LET sx=0
  LET sy=0
  LET sz=0
  FOR I = 1 to n
     LET xl1(i)=xl1(i)+x2
     LET yl1(i)=yl1(i)+y2
     LET zl1(i)=zl1(i)+z2
     PRINT  nnp(I), xl1(I), yl1(I), zl1(I)
     IF qp$ = "y" or qp$ = "Y" then
       IF anss$ = "Y" or anss$ = "y" then
        IF j <= s then
          CALL INCR
          IF nnp(I) = np(m) then
!            PRINT #7:"nnp(I)",nnp(I),"np(m)",np(m)
           PRINT #7, using "  ##   ####.##   ####.##   ####.##     ###.###   ###.###   ###.###
##":nnp(I),xl1(I),yl1(I),zl1(I),xp(m)-xl1(I),yp(m)-yl1(I),zp(m)-zl1(I),nnp(I)
            LET sx=sx+(xp(j)-xl1(I))^2
            LET sy=sy+(yp(j)-yl1(I))^2
            LET sz=sz+(zp(j)-zl1(I))^2
            LET j=m+1
          else
            PRINT #7, using "  ##   ####.##   ####.##   ####.##
##":nnp(I),xl1(I),yl1(I),zl1(I),nnp(I)
          END IF
        else
         PRINT #7, using "  ##   ####.##   ####.##   ####.##":nnp(I),xl1(I),yl1(I),zl1(I)
        END IF
       ELSE
          PRINT #7, using "  ##   ####.##   ####.##   ####.##":nnp(I),xl1(I),yl1(I),zl1(I)
       END IF
     END IF
     IF ans$ = "Y" or ans$ = "y" then
       PRINT #4, using "%%% -%%%.## -%%%.## -%%%.##":nnp(i),xl1(i),yl1(i),zl1(i)
     END IF
  NEXT I
  IF qp$ = "y" or qp$ = "Y" then
   PRINT #7:
   IF s = 1 then
   PRINT #7, using "                                                    #####
##.#":"Vec.=",(sx+sy+sz)^0.5
   PRINT #7:
   else
   PRINT #7: "                                 Est Pop Standard Deviations"
   PRINT #7:
   PRINT #7, using "                                      #### ##.# #### ##.# #### ##.# #####
##.#":"SDx=",(sx/(s-1))^0.5,"SDy=",(sy/(s-1))^0.5,"SDz=",(sz/(s-1))^0.5,"Vec.=",((sx+sy+sz)/(s-
1))^0.5
   PRINT #7:
   END IF
  END IF

  CLOSE #4
  PRINT
  PRINT "Press any key to continue"
```

```
   GET KEY trash
END IF
 IF qp$ = "y" or qp$ = "Y" then
    PRINT #7:chr$ (12)
    CLOSE #7
 END IF
!SET MODE "HISTORY"
CLEAR

USE
   PRINT "Error: "; ExText$
   LET Err1 = 1
   CLOSE #1
   CLOSE #4
   CLOSE #5
   CLOSE #7
 INPUT PROMPT " Press any letter/number key when error corrected":junk$
 END WHEN
LOOP UNTIL Err1 = 0

NEXT ii

SUB INCR
    FOR m = j to i
    IF m = s then EXIT SUB
    IF np(m) = nnp(i) then EXIT SUB
    NEXT m
END SUB

END
```

APPENDIX B - Program RAN.TRU

This program investigates the effect of marker parameters on the precision of locating the tumour.

```
REM This is program "RAN.TRU"
LIBRARY "c:\true\shell.tru"
LIBRARY "c:\true\fntdlib.trc"
OPTION BASE 1
declare DEF COT, SEC, CSC, ASIN, ACOS, ACOT, ASEC, ACSC

DIM x(1),y(1),z(1),na(1)
DIM x1(1),y1(1),z1(1),nb(1)
DIM xl(1),yl(1),zl(1)
DIM xl1(1),yl1(1),zl1(1),nnp(1)
DIM xp(1),yp(1),zp(1),np(1)
DIM r(3,3)
DIM x6(1),y6(1),z6(1),x7(1),y7(1),z7(1)
DIM x4(1),y4(1),z4(1),x5(1),y5(1),z5(1),d(1,1),f(1,1),g(1,1)
DIM a(1,1),l(1,1),b(1,1),c(3,3)

CLEAR

PRINT "              ********************************************************"
PRINT "              *    Calculating Hypothetical marker positions, and    *"
PRINT "              *                    then Rodrigues Parameters         *"
PRINT "              *            and Test of Precision for an              *"
PRINT "              *         (un)scaled 3D transformation.                *"
PRINT "              *                                                      *"
PRINT "              *    A second set of marker positions with randomly    *"
PRINT "              *           generated errors is rotated into the       *"
PRINT "              *             original co-ordinate system.             *"
PRINT "              ********************************************************"
PRINT

RANDOMIZE

LET mr  = 0   !mean of sample residuals
LET msr = 0   !mean of sample of vector residuals for the tumour - working variable
LET ssr = 0   !std dev of tumour vector residuals
LET msv = 0   !mean of sample of vector residuals of markers - working variable

rem FOR ii = 1 to 20
DO
 LET Err1 = 0
 WHEN ERROR IN


DO
  INPUT PROMPT " No. of marker points =  ":NMP$
  LET nmp = val(NMP$)

!set the marker positions
  LET phi = 2*Pi/nmp/4
! distribute mrkers evenly over the first quadrant only
  LET the = Pi/2  ! no z-axis
LOOP UNTIL nmp > 3
PRINT

INPUT PROMPT " Minimum resolution of CT scanner (mm) =  ":D$
  LET res = val(D$)
  LET DD$ = STR$ (res * 10)   !for the file label
PRINT

INPUT PROMPT " No of trials =  ":NT$
  LET int = val(NT$)
PRINT

rem INPUT PROMPT " Distance of markers from tumour (mm) =  ":R$ !for entry of distances
rem LET ir = val(R$)
rem PRINT


!OPEN FILE AND WRITE HEADINGS
    OPEN #4: NAME NT$ & "_" & DD$ & "_" & NMP$ & "x.txt", ACCESS OUTIN, CREATE NEWOLD,organization
text
```

```
rem OPEN #4: NAME NMP$ & "_" & DD$ & "_" & R$ & "r.txt", ACCESS OUTIN, CREATE NEWOLD,organization
text
SET #4: POINTER BEGIN
IF int = 1 THEN
   PRINT #4:  "int   nmp   ir     res           dx          dy          dz      dRVect Transf resid
vect "
ELSE
   PRINT #4:  "int  nmp ir   res    MuResidual MudRVect  SigdRVect MuTr.res.vec"
END IF

 FOR ir = 4 to 30 STEP 2       !automatically increase marker distances from 4 to 30 mm

!STEP THROUGH THE NUMBER OF TRIALS
 FOR irc = 1 to int

! Calculate "Ideal" marker positions.

PRINT
MAT REDIM x(nmp),y(nmp),z(nmp),na(nmp)
FOR I = 1 to nmp
    LET na(i)= I
    LET x(i)=ir*sin(the)*sin((I-1)*phi)
    LET y(i)=ir*sin(the)*cos((I-1)*phi)
    LET z(i)=ir*cos(the)
rem    PRINT  na(I),x(I), y(I), z(I)
NEXT I
 rem  PRINT "Press any key to continue"
 rem  GET KEY trash
 PRINT

! Calculate "random" marker positions.
MAT REDIM x1(nmp),y1(nmp),z1(nmp),nb(nmp)
FOR I = 1 to nmp
    LET rphi = 2*Pi*rnd  !random angle between 0 & 360deg
    LET rthe = Pi*rnd    !not used
    LET nb(i)=I
    LET x1(i)=x(i) + res*sin(rthe)*sin(rphi)
    LET y1(i)=y(i) + res*sin(rthe)*cos(rphi)
    LET z1(i)=z(i) + res*cos(the)              ! no error in z direction!
rem    PRINT  rphi*360/(2*Pi), nb(I), x1(I), y1(I), z1(I)
NEXT I
   CLEAR

!Order the points

LET j = 1
FOR i = 1 to nmp
 IF j <= nmp then
  IF na(i) = nb(j) then
   LET x(j)=x(i)
   LET y(j)=y(i)
   LET z(j)=z(i)
   LET j=j+1
  END IF
 END IF
NEXT i

MAT REDIM x6(nmp),y6(nmp),z6(nmp),x7(nmp),y7(nmp),z7(nmp)
MAT REDIM x4(nmp),y4(nmp),z4(nmp),x5(nmp),y5(nmp),z5(nmp)
MAT reDIM a(3*nmp,3),l(3*nmp,1),b(3,3*nmp),c(3,3),d(3,3),f(3,3*nmp),g(3,1)

!Deriving centroid coordinates
LET x2=0
LET y2=0
LET z2=0
LET x3=0
LET y3=0
LET z3=0
FOR i = 1 to nmp
    LET x2=x(i)+x2
    LET y2=y(i)+y2
    LET z2=z(i)+z2
    LET x3=x1(i)+x3
    LET y3=y1(i)+y3
    LET z3=z1(i)+z3
NEXT i
LET x2=x2/nmp
LET y2=y2/nmp
LET z2=z2/nmp
```

```
LET x3=x3/nmp
LET y3=y3/nmp
LET z3=z3/nmp

FOR i= 1 to nmp
    LET x(i)=x(i)-x2
    LET y(i)=y(i)-y2
    LET z(i)=z(i)-z2
    LET x1(i)=x1(i)-x3
    LET y1(i)=y1(i)-y3
    LET z1(i)=z1(i)-z3
NEXT i

LET total = 0
!FOR I = 1 to s-1
FOR I = 1 to nmp-1
!    FOR J = I+1 to s
    FOR J = I+1 to nmp
        LET ddd=sqr( (x(J)-x(I))^2 + (y(J)-y(I))^2 + (z(J)-z(I))^2 )
        LET total=total+ddd
    NEXT J
NEXT I

LET total1 = 0
FOR I = 1 to nmp-1
    FOR J = I+1 to nmp
        LET ddd=sqr( (x1(J)-x1(I))^2 + (y1(J)-y1(I))^2 + (z1(J)-z1(I))^2 )
        LET total1=total1+ddd
    NEXT J
NEXT I

LET scale = total /total1

FOR i = 1 to nmp
    LET x4(i)=x1(i)+x(i)
    LET y4(i)=y1(i)+y(i)
    LET z4(i)=z1(i)+z(i)
    LET x5(i)=2*(x1(i)-x(i))
    LET y5(i)=2*(y1(i)-y(i))
    LET z5(i)=2*(z1(i)-z(i))
NEXT i

! solving Lambda , Mu and Nu

FOR i = 1 to nmp
    LET a(3*i-2,1)=0
    LET a(3*i-2,2)=-z4(i)
    LET a(3*i-2,3)=y4(i)
    LET a(3*i-1,1)=z4(i)
    LET a(3*i-1,2)=0
    LET a(3*i-1,3)=-x4(i)
    LET a(3*i,1)=-y4(i)
    LET a(3*i,2)=x4(i)
    LET a(3*i,3)=0
    LET l(3*i-2,1)=x5(i)
    LET l(3*i-1,1)=y5(i)
    LET l(3*i,1)=z5(i)
NEXT i
MAT b=trn(a)
MAT c=b*a
MAT d= inv(c)
MAT f=d*b
MAT g= f*l
LET l1=g(1,1)
LET m1=g(2,1)
LET n1=g(3,1)
! forming rotation matrix
LET d1=1+(l1^2+m1^2+n1^2)/4
LET d2= 2-d1
LET r(1,1)=(l1^2/2+d2)/d1
LET r(1,2)=(l1*m1/2-n1)/d1
LET r(1,3)=(l1*n1/2+m1)/d1
LET r(2,1)=(l1*m1/2+n1)/d1
LET r(2,2)=(m1^2/2+d2)/d1
LET r(2,3)=(m1*n1/2-l1)/d1
LET r(3,1)=(l1*n1/2-m1)/d1
LET r(3,2)=(m1*n1/2+l1)/d1
LET r(3,3)=(n1^2/2+d2)/d1
! to test precision of the transformation
```

```
FOR i = 1 to nmp
    LET x6(i)=x1(i)*r(1,1)+y1(i)*r(1,2)+z1(i)*r(1,3)
    LET y6(i)=x1(i)*r(2,1)+y1(i)*r(2,2)+z1(i)*r(2,3)
    LET z6(i)=x1(i)*r(3,1)+y1(i)*r(3,2)+z1(i)*r(3,3)
    LET x7(i)=x(i)-x6(i)
    LET y7(i)=y(i)-y6(i)
    LET z7(i)=z(i)-z6(i)
NEXT i
CLEAR

LET sx=0
LET sy=0
LET sz=0
FOR i = 1 to nmp
    LET sx=sx+x7(i)^2  !sum of squares of residuals of markers
    LET sy=sy+y7(i)^2
    LET sz=sz+z7(i)^2
NEXT i

LET Vec = ((sx+sy+sz)/(nmp-1))^0.5  !vector of sample standard deviations of markers

rem   PRINT "Co-ordinate value BEFORE transformation"

! Tumour point origin
       LET nnp(1)=1
       LET xl(1)=0
       LET yl(1)=0
       LET zl(1)=0

rem       PRINT  ir, xl(1), yl(1), zl(1)

       LET xl(1)=xl(1)-x3
       LET yl(1)=yl(1)-y3
       LET zl(1)=zl(1)-z3
   FOR I = 1 to 1
       LET xll(i)=xl(i)*r(1,1)+yl(i)*r(1,2)+zl(i)*r(1,3)
       LET yll(i)=xl(i)*r(2,1)+yl(i)*r(2,2)+zl(i)*r(2,3)
       LET zll(i)=xl(i)*r(3,1)+yl(i)*r(3,2)+zl(i)*r(3,3)
   NEXT I
rem   PRINT

      FOR I = 1 to 1
          LET np(i)=1
          LET xp(i)=0
          LET yp(i)=0
          LET zp(i)=0
      NEXT I

rem   PRINT
rem   PRINT "Co-ordinate values AFTER transformation"
rem   PRINT

   LET j=1
   LET rx=0
   LET ry=0
   LET rz=0
   LET sx=0
   LET sy=0
   LET sz=0
   FOR I = 1 to 1   !only one tumour point
       LET xll(i)=xll(i)+x2
       LET yll(i)=yll(i)+y2
       LET zll(i)=zll(i)+z2
       LET rx=rx+(xp(j)-xll(I))    !(sum of) residuals of tumour point
       LET ry=ry+(yp(j)-yll(I))
       LET rz=rz+(zp(j)-zll(I))
       LET sx=sx+(xp(j)-xll(I))^2  !(sum of) squares of residuals of tumour point
       LET sy=sy+(yp(j)-yll(I))^2
       LET sz=sz+(zp(j)-zll(I))^2
IF int = 1 THEN
 PRINT #4, using "%%% %%% %%%.## -%%%.## -%%%.## -%%%.## -%%%.## -%%%.##":nmp,ir,res,xp(i)-
xll(i),yp(i)-yll(i),zp(i)-zll(i),(sx+sy+sz)^0.5,Vec
ELSE
 LET mr  = mr  + (rx+ry+rz)     !sum of tumour residuals
 LET msr = msr + (sx+sy+sz)^.5  !sum of tumour residual vectors (SigVi)
 LET ssr = ssr + (sx + sy + sz) !sum of sq of tumour residuals  Sig(Vi^2)
 LET msv = msv + Vec   !sum of vector of marker residuals
END IF
```

```
    PRINT        "irc  nmp ir  res    dx      dy      dz      mr    dRVect   Transf resid vect "
    PRINT  using "###  ### ### ##.## ###.### ###.### ###.### ###.## ###.###
###.###":irc,nmp,ir,res,xp(I)-xl1(I),yp(I)-yl1(I),zp(I)-zl1(I),mr,(sx+sy+sz)^0.5,Vec

   NEXT I
     PRINT

  IF strash <> 103 THEN
     PRINT "Press key 'g' to continue to end"
     GET KEY strash
  END IF


CLEAR

NEXT irc

IF int <> 1 then
! calculate means
  LET mr  = mr/int   !mean res of tumour
  LET msr = msr/int  !mean res vector of tumour
  LET ssr = ((ssr)/int - msr*msr)^0.5  !st dev of mean res vector of tumour
  LET msv = msv/int !mean of vectors of res marker positions

PRINT #4, using "%%%  %%% %%% %%%.## -%%%.####  -%%%.#### -%%%.#### -%%%.#### -
%%%.####":int,nmp,ir,res,mr,msr,ssr,msv

   LET ssx=0
   LET ssy=0
   LET ssz=0
   LET mr =0
   LET msr=0
   LET msv=0
   LET ssr = 0
END IF

NEXT ir

CLOSE #4

USE
   PRINT "Error: "; ExText$
   LET Err1 = 1
   CLOSE #1
   CLOSE #4
   CLOSE #5
   CLOSE #7
 INPUT PROMPT " Press any letter/number key when error corrected":junk$
 END WHEN
LOOP UNTIL Err1 = 0

rem NEXT ii

SET MODE "HISTORY"
END
```

REFERENCES

Adams LP, B Gutschow, A Tregidga, and M Klein. Near real time biostereometric studies of regional body surface motion in respiration, in Gruen/Baltsavias (eds): **1990**, pp 762-767.

Adams LP and H Rüther. A Stereophotogrammetric System using Multiple Digital Cameras for the Accurate placement of a Proton Beam, in Gruen, A and Kahmen, H (eds): *Optical 3-D Measurement techniques*. Herbert Wichmann, Vienna, Austria, **1989**, pp 164-172.

Adler JR and JG Depp. Image-image correlation: A promising technique for frameless stereotaxis. *Neurological Society* ; **1992**.

Altman DG and JM Bland. Measurement in Medicine: the Analysis of Method Comparison Studies. *The Statistician* 32:307-317; **1983**.

Balter JM, KL Lam, HM Sandler, and RK Ten Haken. Automated localisation of the prostate at the time of treatment using implanted radiopaque markers: technical feasibility. *International Journal of Radiation Oncology, Biology and Physics* 33:1281-1286; **1995**.

Baroni G, G Ferrigno, and A Pedotti. Optoelectronic techniques for patient repositioning in radiotherapy. *Technology and Health Care* 3:251-262; **1996**.

Baroni G, G Ferrigno, A Pedotti, PW Cattaneo, D Scannicchio, F Corbella, and F Gerardi. New methods for patient alignment, in Amaldi, Ugo, Larsson, Börje, and Lemoigne, Yves (eds): *Advances in Hadrontherapy*. Elsevier Science B.V., Amsterdam, **1997**, pp 278-283.

Baroni G, G Ferrigno, and A Pelizzari. Implementation and application of a real-time motion analysis based on passive markers. *Medical and Biological Engineering Computing* 36:693-703; **1998**.

Bel A, M van Herk, and H Bartolink. A verification procedure to improve patient setup accuracy using portal images. *Radiotherapy and Oncology* 29:253-260; **1993**.

Bennett KF, H Rüther, G van der Vlugt, and ADB Yates. Patient positioning for proton therapy at the National Accelerator Centre. *South African Journal of Science* 90:370-371; **1994**.

Betti OO, B Munari, and R Rosler. Stereotactic radiosurgery with the linear accelerator: treatment of arteriovenous malformations. *Neurosurgery* 24:311-321; **1989**.

Boxwala AA, EL Chaney, DS Fritsch, S Raghavan, C Coffey, S Major, and K Muller. Comparison of computer workstation with light box for detecting setup errors from portal images. *International Journal of Radiation Oncology, Biology and Physics* 44:711-716; **1999**.

Brown RA. A computerized tomography-computer graphics approach to stereotaxic localization. *Journal of Neurosurgery* 50:720; **1979**.

Delannes M, NJ Daly, J Bonnet, J Sabatier, and M Tremoulet. Fractionated radiotherapy of small inoperable lesions of the brain using a noninvasive stereotactic frame. *International Journal of Radiation Oncology, Biology and Physics* 21:749-755; **1991**.

Dunbar SF, NJ Tarbell, HM Kooy, and JS Loeffler. Stereotactic Radiotherapy for pediatric and adult brain tumors: Preliminary report. *International Journal of Radiation Oncology, Biology and Physics* 30:531-539; **1994**.

el-Gayed A, A Bel, and R Vijlbrief. Time trend of patient setup deviations during pelvic irradiation using electronic portal imaging. *Radiotherapy and Oncology* 26:162-171; **1993**.

Friedman WA and FJ Bova. The University of Florida radiosurgery system. *Surgical Neurology* 17:229-237; **1989**.

Gall KP, LJ Verhey, and M Wagner. Computer-assisted positioning of radiotherapy patients using implanted radiopaque fiducials. *Medical Physics* 20:1153-1157; **1993**.

Gill SS, DGT Thomas, AP Warrington, and M Brada. Relocatable frame for stereotactic external beam radiotherapy. *International Journal of Radiation Oncology, Biology and Physics* 20:599-603; **1991**.

Goitein M, M Abrahms, and D Rowell. Multi-dimensional treatment planning. II Beam's eye-view, back projection and projection through CT sections. *International Journal of Radiation Oncology, Biology and Physics* 9:789-797; **1983**.

Graham JD, AP Warrington, SS Gill, and M Brada. A non-invasive, relocatable stereotactic frame for fractionated radiotherapy and multiple imaging. *Radiotherapy and Oncology* 21:60-62; **1991**.

Hamilton RJ, FT Kuchnir, CA Pelizzari, PJ Sweeney, and SJ Rubin. Repositioning accuracy of a non-invasive head fixation system for stereotactic radiotherapy. *Medical Physics* 23:1909-1917; **1996**.

Hariz MI, R Henriksson, PO Löfroth, LV Laitinen, and NE Säterborg. A non-invasive method for fractionated stereotactic irradiation of brain tumors with linear accelerator. *Radiotherapy and Oncology* 17:57-72; **1990**.

Hartmann GH. Focussed X-radiation - The Linear Accelerator Arc Method. In: *Physical Aspects of Stereotactic Radiosurgery*, edited by M.H.Phillips. Plenum Medical Book Company, pp 129-187; **1993.**

Hartmann GH, B Bauer-Kirpes, CF Serago, and WJ Lorenz. Precision and accuracy of stereotactic convergent beam irradiations from a linear accelerator. *International Journal of Radiation Oncology, Biology and Physics* 28:481-492; **1993**.

Heilbrun MP, TS Roberts, MLJ Apuzzo, and TH Wells. Preliminary experience with Brown-Roberts-wells (BRW) computerized tomography stereotaxic guidance system. *Journal of Neurosurgery* 59:217-222; **1983**.

Houdek PV, JG Schwade, CF Serago, HJ Landy, VJ Pisciotta, Wu Xiaodong, AM Markoe, and AA Lewin. Computer controlled stereotaxic radiotherapy system. *International Journal of Radiation Oncology, Biology and Physics* 22:175-180; **1991**.

ICRU Report 50: Prescribing, Recording, and Reporting Photon Beam Therapy. Bethesda, MD, International Commission on Radiation Units and Measurements, **1993**.

Jones D, DA Christopherson, and JT Washington. A frameless method for stereotactic radiotherapy. *British Journal of Radiology* 66:1142-1150; **1993**.

Jones DTL. NAC - The Only Proton Therapy Facility in the Southern Hemisphere. In: *Ion Beams in Tumor Therapy*, edited by U.Linz. Weinheim, Germany: Chapman & Hall GmbH, pp 350-359; **1995.**

Jones DTL, AN Schreuder, JE Symons, EA de Kock, FJA Vernimmen, CE Stannard, J Wilson, and G Schmitt. Status Report of the NAC Particle Therapy Programme. *Strahlentherapie und Onkologie* 175:30-32; **1999**.

Jones DTL, AN Schreuder, JE Symons, H Rüther, G van der Vlugt, KF Bennett, and ADB Yates. Use of stereophotogrammetry in proton radiation therapy, in *International FIG Symposium, Commission 6, Photogrammetry in Engineering Surveying*. International Federation of Surveyors, Washington, DC, **1995**, pp 138-153.

Kooy HM, SF Dunbar, NJ Tarbell, E Mannarino, N Ferarro, S Shusterman, M Bellerive, CV McDonough, and JS Loeffler. Adaptation and verification of the relocatable Gill-Thomas-Cosman frame in stereotactic radiotherapy. *International Journal of Radiation Oncology, Biology and Physics* 30:685-691; **1994**.

Kutcher GJ, L Coia, and M Gillin. Comprehensive QA for radiation oncology: Report of AAPM Radiation Therapy Committee Task Group 40. *Medical Physics* 21:581-618; **1994**.

Kutcher GJ, GS Mageras, and SA Leibel. Control, Correction, and Modeling of Setup Errors and Organ Motion. *Seminars in Radiation Oncology* 5:134-145; **1995**.

Laitinen LV. Noninvasive multipurpose stereoadapter. *Neurological Research* 9:137-141; **1987**.

Laitinen LV, B Liliequist, M Fagerland, and AT Erikson. An adapter for computer tomography-guided stereotaxis. *Surgical Neurology* 23:559-566; **1985**.

Leksell L. A stereotaxic apparatus for intracerebral surgery. *Acta Chirurg Scandanavia* 99:229-233; **1949**.

Leksell L. Stereotaxis and radiosurgery. An operative system. *Acta Chirurg Scandanavia* ; **1971**.

Leksell L. Stereotactic radiosurgery. *Journal of Necrology, Neurosurgery & Psychiatry* 46:797-803; **1983**.

Levin CV, JK Hough, LP Adams, D Boonzaier, H Rüther, and S Wynchank. Determining locations of intracranial lesions for proton therapy. *Physics in Medicine and Biology* 38:1393-1401; **1993**.

Li S, JF Jackson, LT Myers, NA Detorie, and JF Dicello. A simple and accurate coordinate transformation for a stereotactic radiotherapy system. *Medical Physics* 26:581-523; **1999**.

Lutz W, KR Winston, and N Maleki. A system for stereotactic radiosurgery with a linear accelerator. *International Journal of Radiation Oncology, Biology and Physics* 14:373-381; **1988**.

Lyman JT, MH Phillips, KA Frankel, and JI Fabrikant. Stereotactic frame for neuroradiology and charged particle Bragg peak radiosurgery on intracranial disorders. *International Journal of Radiation Oncology, Biology and Physics* 16:1615-1621; **1989**.

Marks JE and AG Haus. The effect of immobilisation on localisation error in the radiotherapy of head and neck cancer. *Clinical Radiology* 27:175-177; **1976**.

Menke M, T Mack, and W Schlegel. Modification of Planned 3D Dose distributions by patient set-up errors and an approach of evaluation., in Minet, P (eds): European Association of Radiology, Liège, Belgium, **1993**, pp 323-334.

Mijnheer B, J Batterman, and A Wambersie. What degree of accuracy is required and can be achieved in photon and neutron therapy? *Radiotherapy and Oncology* 8:237-252; **1987**.

Mitine C, G Leunens, and J Verstraete. Is it necessary to repeat quality control procedures for head and neck patients? *Radiotherapy and Oncology* 21:201-210; **1991**.

Mundinger F and CB Ostertag. Treatment of small cerebral gliomas with CT-aided stereotaxic curietherapy. *Neuroradialogy* 16:564-567; **1978**.

Phillips MH. Stereotactic Radiosurgery - Introduction to Physical Principles. In: *Physical Aspects of Stereotactic Radiosurgery*, edited by M.H.Phillips. New York: Plenum Medical Book Company, pp 1-44; **1993.**

Podgorsak E, G Pike, M Pla, A Oliver, and l Souhami. Radiosurgery with photon beams: physical aspects and adequacy of linear accelerators. *Radiotherapy and Oncology* 17:349-358; **1990**.

Podgorsak E, l Souhami, J-L Caron, M Pla, B Clark, C Pla, and P Cadman. A technique for fractionated stereotactic radiotherapy in the treatment of intracranial tumors. *International Journal of Radiation Oncology, Biology and Physics* 27:1225-1230; **1993**.

Rabinowitz I, J Broomberg, M Goitein, K McCarthy, and J Leong. Accuracy of radiation field alignment in clinical practice. *International Journal of Radiation Oncology, Biology and Physics* 11:1857-1867; **1985**.

Riechert T and F Mundinger. Beschreibung und Anwendung eines Zielgerätes für stereotaktische Hirnoperationen. *Acta Neurochirurg (Wien)* Suppl. 3:308-337; **1955**.

Rogus RD, RL Stern, and HD Kubo. Accuracy of a photogrammetry-based patient positioning and monitoring system for radiation therapy. *Medical Physics* 26:721-728; **1999**.

Rosenthal SA, LM Galvin, JW Goldwein, AR Smith, and JE Bond. Improved methods for determination of variability in patient positioning for radiation therapy using simulation and serial portal film measurements. *International Journal of Radiation Oncology, Biology and Physics* 23:621-625; **1992**.

Rosenthal SJ, KP Gall, M Jackson, and AF Thornton. A precision cranial immobilization system for conformal stereotactic fractionated radiation therapy. *International Journal of Radiation Oncology, Biology and Physics* 33:1239-1245; **1995.**

Schlegel W, O Pastyr, T Bortfeld, G Becker, L Schad, G Gademann, and WJ Lorenz. Computer systems and mechanical tools for stereotactically guided conformation therapy with linear accelerators. *International Journal of Radiation Oncology, Biology and Physics* 24:781-787; **1992.**

Schreuder AN, DTL Jones, JE Symons, EA de Kock, FJA Vernimmen, J Wilson, LP Adams, and JK Hough. Three years' experience with the NAC protontherapy patient postioning system, in Amaldi, Ugo, Larsson, Börje, and Lemoigne, Yves (eds): *Advances in Hadrontherapy*. Elsevier Science B.V., Amsterdam, **1997**, pp 251-260.

Schwade JG, PV Houdek, HJ Landy, JL Bujnoski, AA Lewin, AA Abitbol, CF Serago, and VJ Pisciotta. Small field stereotactic external beam radiation therapy of intracranial lesions: Fractionated treatment with a fixed halo immobilization device. *Radiology* 176:563-565; **1990.**

Scott PJ. The Reflex Plotters: Measurements without Photographs. *Photogrammetric Record* 10:435-446; **1981.**

Serago CF, AA Lewin, PV Houdek, S Gonzalez-Arias, GH Hartmann, AA Abitbol, and JG Schwade. Stereotactic target point verification of an X ray and CT localizer. *International Journal of Radiation Oncology, Biology and Physics* 20:517-523; **1991.**

Serago CF, MM Urie, PG Okunieff, KP Gall, SJ Rosenthal, and ME Serago. Measurement of intracranial motion and implications for precision radiation therapy and radiosurgery. *Radiology* 185:273; **1992.**

Shalev S and G Gluhchev. When and how to correct a patient setup, in Hounsell, AR, Wilkinson, JM, and Williams, PC (eds): *Proceedings of the 11th International Conference on the Use of Computers in Radiation Therapy*. North Western Medical Physics Department, Christie Hospital, Manchester, UK, **1994**, pp 274-275.

Siddon RL and NH Barth. Stereotactic localisation of intracranial targets. *International Journal of Radiation Oncology, Biology and Physics* 13:1241-1246; **1987.**

Simon,J.L. and P.Bruce. *THE NEW BIOSTATISTICS OF RESAMPLING.* http://www.inform.umd.edu/EdRes/Topic/Statistics/Resampling_Statistics/Introductory_Text/, **1993.**

Tatsuzaki H and MM Urie. Importance of precise positioning for proton beam therapy in the base of skull and cervical spine. *International Journal of Radiation Oncology, Biology and Physics* 21:757-765; **1991.**

Thompson,E.H. *An introduction to the algebra of matrices with some applications*. London: Adam Hilger, **1969.**

Thornton AF, RK Ten Haken, A Gerhadsson, and M Correll. Three-dimensional motion analysis of an improved head immobilization system for simulation, CT, MRI, and PET imaging. *Radiotherapy and Oncology* 20:224-228; **1991.**

Urie MM. Treatment planning for proton beams. In: *Ion Beams in Tumor Therapy*, edited by U.Linz. Weinheim, Germany: Chapmann & Hall, **1995.**

van de Steene J, F van den Heuvel, A Bel, D Verellen, J de Mey, M Noppen, M de Beukeleer, and G Storme. Electronic portal imaging with on-line correction of setup error in thoracic irradiation: clinical evaluation. *International Journal of Radiation Oncology, Biology and Physics* 40:967-976; **1998.**

van der Vlugt, G. The development of a real-time photogrammetric system for patient positioning in proton therapy . *Master of Science in Engineering* degree at University of Cape Town, **1991.**

van der Vlugt G and H Rüther. A real-time photogrammetric system for patient positioning in proton therapy. *International Archives of Photogrammetry and Remote Sensing* 29:880-885; **1992.**

Vaughan CL. Personal Communication. **1999.**

Verhey LJ. Immobilizing and Positioning Patients for Radiotherapy. *Seminars in Radiation Oncology* 5:100-114; **1995.**

Verhey LJ, M Goitein, P McNulty, JE Munzenrider, and HD Suit. Precise positioning of patients for radiation therapy. *International Journal of Radiation Oncology, Biology and Physics* 8:289-294; **1982**.

Yan D, J Wong, and Gustafson. Implementation of "accept or reject" strategies in megavoltage treatment verification, in Hounsell, AR, Wilkinson, JM, and Williams, PC (eds): *Proceedings of the 11th International Conference on the Use of Computers in Radiation Therapy*. North Western Medical Physics Department, Christie Hospital, Manchester, UK, **1994**

Yue N, Z Chen, JE Bond, YH Son, and R Nath. Combined use of transverse and scout computed tomography scans to localize radioactive seeds in an interstitial brachytherapy implant. *Medical Physics* 26:502-505; **1999**.